Progetto di ricerca co-finanziato finanziato dall'Unione europea nel quadro del Programma PON R&I 2014- 2020 risorse FSE REACT-EU Azione IV.4 "Dottorati su tematiche INNOVAZIONE"

DIPARTIMENTO DI MEDICINA MOLECOLARE E TRASLAZIONALE

DOTTORATO DI RICERCA IN

PRECISION MEDICINE

Coordinatrice: Prof.ssa Stefania Mitola

MED/04 - Patologia generale

CICLO XXXVII

DEVELOPMENT OF ADVANCED MODELS OF HUMAN AIRWAY EPITHELIUM TO STUDY CHRONIC OBSTRUCTIVE PULMONARY DISEASE (COPD)

DOTTORANDA

GIULIA RIPARI

RELATORE: Prof.ssa Annalisa Del Prete

CORRELATORE: Prof.ssa Daniela Bosisio

TUTOR: Dr. Fabrizio Facchinetti (Chiesi Farmaceutici)

CO-TUTOR: Dr.ssa Gessica Marchini (Chiesi Farmaceutici)

ABSTRACT

L'ampia diffusione e il peso sostanziale delle malattie polmonari sulla salute umana, di cui la broncopneumopatia cronica ostruttiva (BPCO), sottolineano la necessità di migliorare i modelli di ricerca per comprendere meglio la fisiopatologia polmonare e accelerare lo sviluppo di strategie terapeutiche innovative e più specifiche. I modelli di interfaccia aria-liquido (ALI) si distinguono come potenti strumenti per mimare il microambiente delle vie aeree, replicando le caratteristiche essenziali della barriera in vivo e rispecchiando il fenotipo dei tessuti delle vie aeree umane. In questo progetto, abbiamo cercato di creare le condizioni per la coltura e la manipolazione in-house di un modello ALI di epitelio delle vie aeree umane, con l'obiettivo generale di ottenere un modello 3D avanzato per lo studio della BPCO. Le colture di MucilAir ALI sono state coltivate in terreno proprietario standard (monocolture) o in terreno arricchito con l'1% di FBS (co-colture) e valutate per le funzioni di barriera mediante la resistenza elettrica transepiteliale (TEER), per la vitalità mediante il rilascio di lattato deidrogenasi (LDH) e per la morfologia mediante l'istologia. L'induzione dell'iperplasia delle cellule di goblet (GCH) è stata valutata mediante analisi istologica in termini di accumulo di granuli secretori PAS-positivi e mediante immunofluorescenza con colorazione per Muc5AC e FoxJ1 in condizioni statiche e dinamiche. Le cellule mononucleate del sangue periferico (PBMC) congelate sono state scongelate in RPMI 10% FBS, lasciate recuperare per 2 ore e poi risospese in terreno ALI integrato con 1% FBS per la co-coltura. La vitalità è stata valutata mediante il rilascio di LDH e le proprietà funzionali mediante il confronto del rilascio di TNFα rispetto alle PBMC fresche e al terreno standard. LPS è stato utilizzato come stimolo infiammatorio prototipico. L'espressione genica e la secrezione proteica sono state valutate rispettivamente analisi PCR sull'mRNA totale e con l'ELISA sui supernatanti. Quando possibile, a causa della disponibilità dei campioni e dei vincoli di tempo, abbiamo confrontato il comportamento di colture di ALI provenienti da donatori sani e BPCO o da produttori diversi, come MucilAir ed EpiAirway. In primo luogo, abbiamo riprodotto un fenotipo iperplastico delle cellule goblet nelle cellule epiteliali delle vie aeree umane coltivate in condizioni di ALI in seguito a stimolazione con IL-13. L'inibitore dell'IL-13, un anticorpo monoclonale, ha revertito questo fenotipo in modo dose-dipendente e anche la modulazione dei geni legati alla mucina. In secondo luogo, abbiamo cercato di indurre l'infiammazione nel modello ALI. In questo contesto, abbiamo confermato la refrattarietà delle cellule epiteliali alla stimolazione con LPS e abbiamo allestito una co-cultura epiteliale/immunitaria, utilizzando PBMC congelate come

componente immunitaria, in cui l'attivazione epiteliale è indirettamente indotta dalle cellule immunitarie attivate. In terzo luogo, abbiamo ottenuto la prova di concetto che il nostro modello di ALI in co-cultura infiammata può essere utilizzato per studiare gli effetti di farmaci antinfiammatori, come l'inibitore della PDE4 Tanimilast, di proprietà di Chiesi Farmaceutici. Come progetto collaterale, abbiamo studiato se l'attivazione delle cellule dendritiche umane indotta da TSLP, un'allarmina coinvolta nell'attivazione Th2 nella sindrome da sovrapposizione asma-COPD (ACOS), potesse essere influenzata dal trattamento con Tanimilast. Abbiamo caratterizzato modelli avanzati di cellule epiteliali primarie delle vie aeree umane in ALI che assomigliano più da vicino a ciò che accade in vivo e abbiamo ottenuto la prova di concetto che il modello di co-cultura epiteliale/immune ALI è fattibile e applicabile allo studio dell'infiammazione e dei farmaci antinfiammatori in vitro.

ABSTRACT

Background

The widespread prevalence and substantial burden of lung diseases on human health, of which Chronic Obstructive Pulmonary Disease (COPD) is a prototypical example, emphasize the need for improved research models to better understand lung pathophysiology and to speed up the development of innovative and more specific therapeutic strategies. *In vitro* models are of particular relevance in terms of efficacy, cost reduction and also adherence to the principles of the 3Rs (Replacement, Reduction, Refinement) aiming at a more humane animal research. Among these, Air-Liquid Interface (ALI) models stand out as powerful tools for mimicking the airway microenvironment by replicating essential *in vivo* barrier characteristics and closing mirroring the phenotype of human airway tissues.

Aim

In this project, we aimed at setting up the conditions for in house culturing and manipulation of an ALI model of human airway epithelium, with the overarching goal to achieve an advanced 3D model for the study of COPD and possibly of other inflammatory diseases of the respiratory tract.

Methods

MucilAir ALI cultures were grown in standard proprietary medium (mono-cultures) or medium enriched with 1% FBS (co-cultures) and assessed for barrier functions by transepithelial electrical resistance (TEER), for vitality by the release of lactate dehydrogenase (LDH) and for morphology by histology. Induction of Goblet Cell Hyperplasia (GCH) was assessed by histological analysis in terms of accumulation of PAS-positive secretory granules and by immunofluorescence by staining for Muc5AC and FoxJ1 in both static and dynamic conditions. Frozen peripheral blood mononuclear cells (PBMCs) were thawed in RPMI 10% FBS, left to recover for 2 hours and then resuspended in ALI medium supplemented with 1% FBS for co-culture. Vitality was assessed by LDH release and functional properties by comparison of TNFα release in respect to fresh PBMCs and standard medium. LPS was used as a prototypical inflammatory stimulus. Gene expression and protein secretion were assessed by real-time PCR on total mRNA and ELISA on cell-free-supernatants respectively. When possible, due to sample availability and time constraints, we compared the

behaviour of ALI cultures from healthy and COPD donors or from different producers such as MucilAir and EpiAirway.

Results

First, we reproduced a goblet hyperplastic phenotype in human airway epithelial cells cultured under ALI conditions following IL-13 stimulation. IL-13 inhibitor, a fully monoclonal antibody against a common IL-4/IL-13 receptor chain, reverted this phenotype in a dose dependent manner and also reverted the modulation of mucin-related genes. Second, we aimed at inducing inflammation in the ALI model. In this context, we confirmed the refractoriness of epithelial cells to LPS stimulation and set up an epithelial/immune co-culture, using frozen PBMCs as the immune component, in which epithelial activation is indirectly induced by activated immune cells. Third, we obtained the proof of concept that our inflamed co-culture ALI model can be used to study the effects of anti-inflammatory drugs, such as Chiesi Farmaceutici's proprietary PDE4 inhibitor Tanimilast. As a side project, we investigated whether human dendritic cell activation induced by TSLP, an alarmin involved in Th2 activation in Asthma-COPD Overlap Syndrome (ACOS) could be influenced by the treatment with Tanimilast.

Conclusions

We characterized advanced models of human primary airway epithelial cells at ALI that more closely resembles what happens *in vivo* and gained proof of concept that the epithelial/immune co-culture ALI model is feasible and applicable to the study of inflammation and anti-inflammatory drugs in *in vitro* settings. All in all, our work represents a privileged starting point for future developments of this technique, paving the way to a more efficient, fast, and less expensive drug discovery to treat inflammatory diseases of the respiratory tract.

INDEX

INTRODUCTION

1. Chronic Obstructive Pulmonary Disease (COPD)

1.1 Overview of COPD pathology

COPD is an irreversible and heterogeneous lung pathology characterized by persistent airflow obstruction and chronic respiratory symptoms, due to abnormalities of the airways (bronchitis) and/or alveoli (emphysema) [1]. It is the third leading cause of death and disability worldwide, after ischemic heart disease and neoplasms. COPD prevalence in 2017, among females and males, was estimated to be 10.6% worldwide, translating to 480 million cases. The number of affected individuals is projected to increase of 23.3% until 2050, highlighting its relevance as a pressing healthcare issue [2]. Unfortunately, COPD is often not diagnosed, and poorly treated by current therapies as it has proved difficult to treat the underlying inflammation, widely corticosteroid-resistant in most patients [3].

The broad range of clinical manifestations and differences in response to therapy suggest that the disease may express different subtypes or endotypes, which may require precision medicine tailored to individual patient profiles [4]. The global impact of COPD continues to provide impetus to find inflammatory mechanisms or pathways that can be targeted therapeutically.

Although cigarette smoke is the major risk factor for the development of COPD, there are several other factors that can cause or exacerbate the pathology, including air pollution, allergens, occupational exposure to particulate matter, gases and toxic particles, and alpha-1 antitrypsin deficiency [5].

1.2 Pathogenesis of COPD

COPD is characterized by two primary conditions: emphysema and chronic bronchitis (Figure 1) [6]. Emphysema is characterized by abnormal permanent enlargement of lung air spaces with a progressive destruction of their walls, leading to reduced surface area for gas exchange.

Chronic bronchitis is long-term inflammation of the bronchial tubes, resulting in mucus hypersecretion and outflow obstruction. The pathologic correlate is goblet cell hyperplasia (GCH), which consists in an increase in the number and size of mucus producing goblet cells [7].

The persistent chronic airflow limitation in COPD, due to a remodeling and narrowing of small airways and consequent loss of the alveolar attachments, results in diminished lung recoil, higher

resistance to flow and closure of small airways at higher lung volumes during expiration, with air trapping in the lung. This leads to pulmonary hyperinflation, which gives rise to dyspnea and decreased exercise tolerance. Both the small-airway remodeling and narrowing and loss of lung elasticity, due to lung parenchymal destruction, are the results of chronic inflammation in the lung periphery [8].

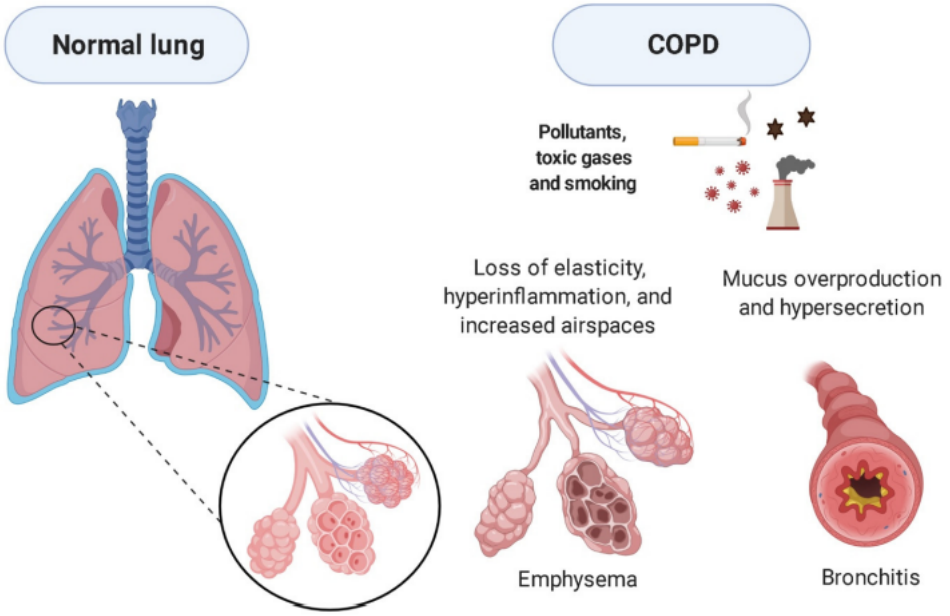

Figure 1. COPD phenotypes and morphological differences between a normal lung and a lung with COPD [6].

1.3 Immunopathology of COPD

A pivotal feature in the pathogenesis of COPD is inflammation, causing a chain of immune responses within the respiratory tract. Chronic exposure of the airway epithelium to toxic substances such as tobacco smoke and inhaled pollutants triggers the activation of immune cells, including neutrophils, macrophages, B and T lymphocytes, and dendritic cells (Figure 2) [9].

Neutrophils are recruited in large numbers in the airways of COPD patients under oxidative stress and secrete several serine proteases, including matrix metalloproteinases (MMPs) and neutrophil elastase (NE), as well as myeloperoxidase (MPO), all of which contribute to alveolar destruction. MMPs are a family of zinc-dependent proteases commonly classified according to the substrates they degrade. Most studies have shown increased MMPs in bronchoalveolar lavage fluid (BALF) and plasma of emphysema patients and contribute to airway obstruction by destroying the structural components of extracellular matrix (ECM) [10].

NE is a neutrophil-derived serine which, similarly to MMPs, causes tissue damage by degrading ECM. In addition to matrix destruction, NE can also promote mucus secretion from submucosal glands and goblet cells, which are involved in airway obstruction [11].

MPO is a heme-containing peroxidase highly expressed in neutrophils and released from secondary granules following neutrophil activation. It is an inflammatory mediator upregulated during the inflammatory response and associated to reactive chloride species-3-Chlorotyrosine expression, which is increased in sputum of COPD patients [11].

Macrophages are the most highly represented immune cells in the respiratory tract and exert a key role in COPD by directly surveying airways, removing cellular debris, and resolving inflammation. They are able to adopt phenotypical changes based on the stimuli they receive from the surrounding tissues. Depending on the stimulus they are described as M1/M2 macrophage, and this polarization is characterized by the expression of different surface markers and the production of specific factors [12]. M1 macrophages express various pro-inflammatory mediators such as tumor necrosis factor α (TNFα), interleukin-1 (IL-1), interleukin-6 (IL-6), interleukin-12 (IL-12), interleukin-23 (IL-23), and reactive nitrogen and oxygen intermediates. In contrast to M1 macrophages, M2 phenotype exert their role in tuning inflammation, scavenging debris, and tissue remodelling [12].

Several studies demonstrate that the surrounding pulmonary environment in COPD may generate a specific phenotype that is permanently pro-inflammatory (M1) [13].

Furthermore, epithelial and bronchial smooth muscle cells, as well as alveolar macrophages, also recruit adaptive immune cells, $CD8^+$ cytotoxic lymphocytes, and $CD4^+$ T cells through the activation of CXC chemokine receptor-3 (CXCR3) mediated by the chemokines CXCL9, CXCL10, and CXCL11. Activated airway dendritic cells (DCs) initiate adaptive immune responses by inducing cytotoxic $CD8^+$ T cells and by steering the differentiation of $CD4^+$ T cells [14].

Cell-mediated adaptive immune responses can drive inflammation towards one of four major polarized responses: type 1 (T1; interferon driven, generally as response to viruses); type 2 (T2; IL-4, IL-5, and IL-13 driven, considered a response to helminths or allergens); type 17 (T17; IL-17 and IL-22 driven, a response to extracellular bacteria); and T regulatory (regulatory T cell, anti-inflammatory). Markers of T17-driven inflammation in the airway are upregulated with emphysema, neutrophilic inflammation, and corticosteroid-resistance, while the T2-signature is a major component underlying asthma-COPD overlap entity. Indeed, there is a potential overlap in various inflammatory mechanisms driving COPD via the alarmins IL-33 and thymic stromal lymphopoietin (TSLP) [15].

TSLP is an epithelium-derived cytokine, mainly expressed by bronchial epithelial cells, that plays a key role in both COPD and allergic asthma pathobiology by orchestrating T2 inflammatory cascade

through DCs. TSLP release from airway smooth muscle cells in COPD patients appears to be triggered by TNFα, indicating that TSLP is an upstream pathway for airway inflammation [16].

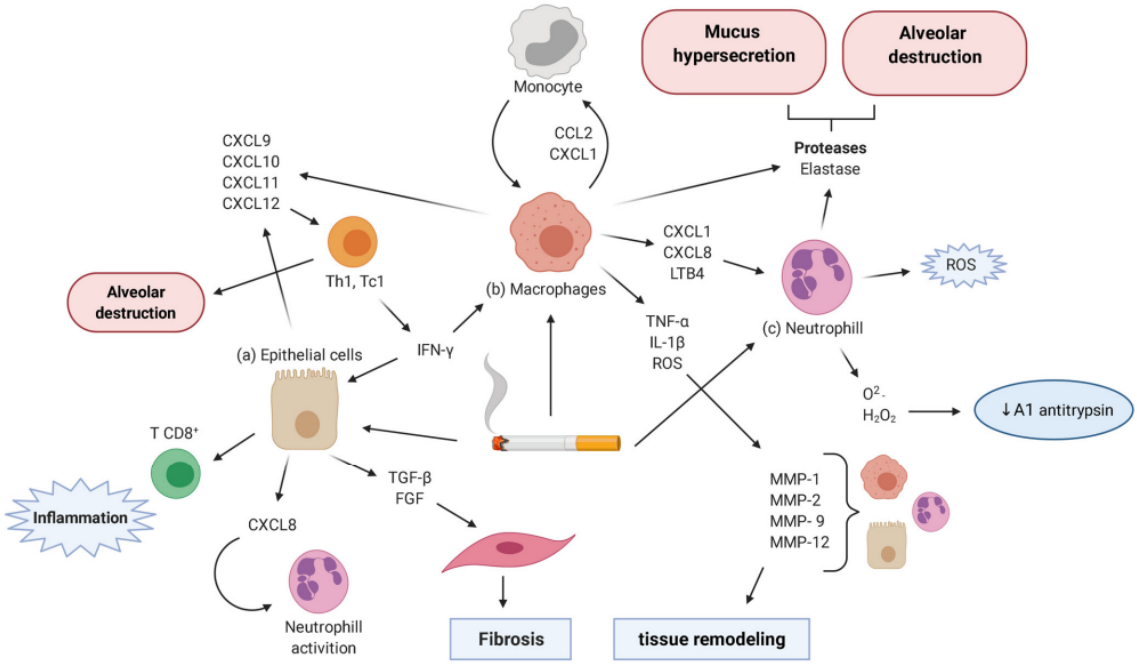

Figure 2. COPD pathophysiology. Cigarette smoke activates macrophages and epithelial cells to release chemotactic factors which attract neutrophils. These cells release factors that activate fibroblasts, resulting in tissue remodeling and abnormal repair processes. An imbalance between proteases released from neutrophils and macrophages leads to emphysema and mucus hypersecretion [6].

2. Peripheral Blood Mononuclear Cells (PBMCs)

2.1 Overview of PBMCs

PBMCs are a heterogeneous specialized population of blood cells originating from hematopoietic stem cells (HSCs) that reside in the bone marrow. HSCs give rise to all blood cells of the immune system through a process called hematopoiesis and generate the myeloid (monocytes, macrophages, granulocytes, megakaryocytes, dendritic cells, erythrocytes) and lymphoid (B cells, T cells, NK cells) lineages (Figure 3). The specific cellular sub-type composition of PBMC depends on the individual and is related to health status. Usually in humans, lymphocytes are most abundant, ranging from 70 to 90%; monocytes 10-20%; and other cells, such as DCs, are only 1-2%. The proportions of cell types within the lymphocyte population include 70-85 % $CD3^+$ T cells, 5-10 % B cells, and 5-20 % NK cells. The $CD3^+$ lymphocytes are composed of $CD4^+$ and $CD8^+$ T cells, in approximately a 2:1 ratio. After activation, the $CD4^+$ T cell subset may develop into different effector/regulatory cell

subsets. All of these blood cells belong to the innate and adaptive immune systems and contain protein signatures corresponding to essential immunological interplay and undergo characteristic changes in various disease states [17].

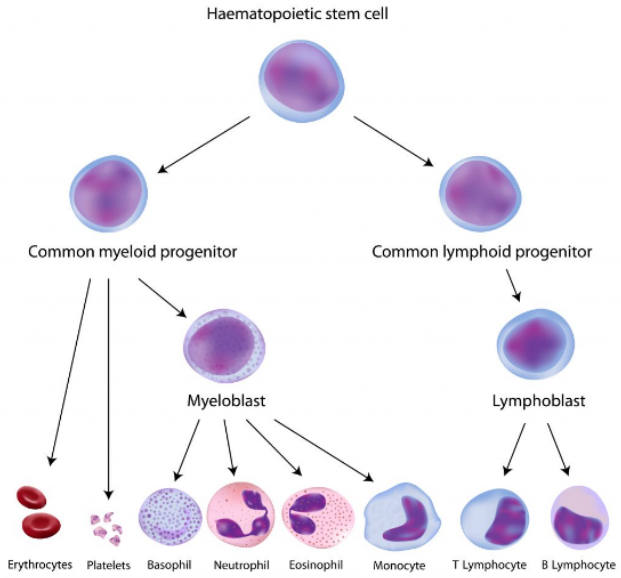

Figure 3. Overview of the different blood cells that arise from hematopoiesis (adapted from https://cgt.global/peripheral-blood-mononuclear-cells/).

2.2 Features and mechanisms

Most PBMCs are naïve or resting cells without effector functions. In the absence of an ongoing immune response, T cells, the largest fraction of PBMCs, are mainly present as naïve or memory T cells. The naïve T cells have not yet encountered an antigen and are commonly characterized by the absence of activation markers such as CD25, CD44 or CD69, and of the memory marker CD450RO isoform [17]. The initiation of an adaptive immune response is effectively dependent on the presentation of the antigen by cells of the innate immune system (especially DCs) that have encountered clear and unequivocal evidence of infection in the form of pathogen-associated molecular patterns (PAMPs). T- or B -cell once a specific antigen bind to the respective receptor are activated and a cascade of signal transduction events started within the responding lymphocyte. Activated T-cells must differentiate into distinct types of effector T-cells: T-helper (Th) cells, cytotoxic T-cells (CTLs), and regulatory T-cells (Treg). $CD4^+$ T-cells coordinate the immune response by differentiating into distinct T-helper subsets that tailor the immune response towards a particular infectious agent. T-helper cells achieve this by releasing powerful inflammatory cytokines, which direct the subsequent responses of $CD8^+$ T-cells, B-lymphocytes, and cells of the innate

immune system, such as macrophages. Activated B cells undergo rounds of mutation and selection to generate high-affinity memory B cells and plasma cells that secrete their antigen-specific receptor in the form of antibodies [19].

2.3 The relevance of PBMCs in COPD

COPD is a systemic disease and PBMCs contribute toward modulation of inflammatory responses. Several studies have demonstrated a link between PBMCs and the pathogenesis of COPD. Xiaoyan Qu et al. evaluated the long noncoding RNA (lncRNA) and mRNA expression profile of PBMCs from healthy non-smokers, smokers without airflow limitation, and COPD patients, and demonstrated that the regulation profile of lncRNA and miRNA on target genes was different in PBMCs of COPD patients compared to healthy and non-smokers [19]. Moreover, Keddache et al. characterized inflammatory and immune profiles from PBMCs in a group of patients with mild-to-moderate COPD secondary to organic dust exposure (OD-COPD), tobacco smoking (T-COPD), or both, revealing that inflammatory responses were different between all groups [20]. Because PBMCs are important in both defending against infection and in modulating immune responses in the lung, their role as mediators of lung injury was investigated following exposure to bacteria-derived materials. Different modulation of specific cytokines and chemokines was observed in cocultures depending on the stimulating agents [21].

Changes in PBMCs are easily identified and may serve as useful indicators in diagnostic approaches. It is increasingly recognised that biomarkers of systemic inflammation, such as soluble tumour necrosis factor receptor (sTNFR), are augmented in COPD patients. The systemic inflammation in chronic diseases also influences PBMC function: T lymphocytes have been reported to have impaired function in COPD, and monocytes isolated from COPD patients produce more MMP-9 and IL-6 compared to control monocytes, with indicators of NF-kB activation [22]. Indeed, infiltration of cytotoxic $CD8^+$ T cells into the airways of diseased patients may promote destruction of lung tissue. In addition, increased number of IL-17-producing cells in the bronchial submucosa and alveolar wall may induce neutrophilic airway inflammation characteristic of COPD [23].

3. Dendritic cells (DCs)

3.1 Overview of DCs

The discovery of DCs dates to 1973 by two scientists named Ralph Steinman and Zanvil Cohn, who examined spleen adherent cells by phase contrast microscopy and found a small population of cells with stellate shape (Figure 4) [24]. DCs represent a specialized population of antigen presenting cells

(APC), serving as sentinels of innate immunity and key initiators of adaptive immune responses. They are widely distributed in every part of the body, including peripheral blood, the skin, mucosal surfaces, interstitial tissues lymphoid, and non-lymphoid tissue areas, with a powerful role in the immune system owing to their capability to present antigens to T-cells. In addition, they are involved in regulating immune tolerance by maintaining steady-state immune homeostasis through the continuous presentation of tissue-derived self-antigens to $CD4^+$ and $CD8^+$ T cells [24].

DCs originate from pluripotent hematopoietic stem cells (HSCs) in the bone marrow, which are derived from either lymphoid or myeloid progenitors. The phenotypic features and anatomical locations of these two precursors differ, but both the myeloid and lymphoid DCs expressed high level of CD11c, major histocompatibility complex-II (MHC-II), and costimulatory molecules CD40, CD80, CD83, and CD86. Myeloid DCs are primarily located in the spleen marginal zone, whereas the lymphoid DCs are found in the T-cell area of the spleen and lymph nodes. DC subsets play different roles in the regulation of B-cell activation and the differentiation of T-cells, and in terms of the expression of surface markers [25].

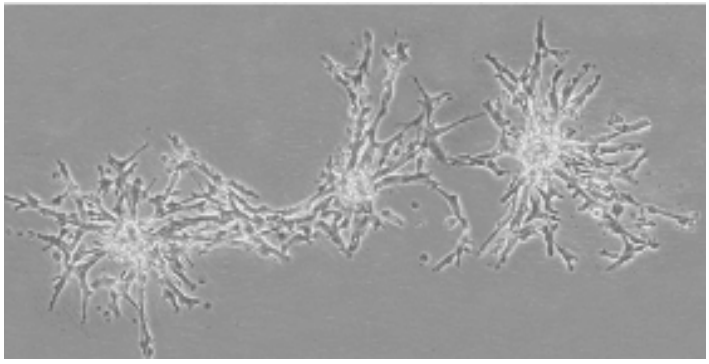

Figure 4. Morphological characteristics of DCs alignment in rows after culturing for 10 days, observed under phase-contrast microscope (adapted from https://www.semanticscholar.org/paper/Isolation-of-chicken-follicular-dendritic-cells.-Cacho-Gallego) [26].

DC subsets

DCs can be divided into two major populations: conventional DCs (cDCs) and non-Conventional DCs (Table 1) [27]. Based on their ontogeny, cDCs subsets consist of two groups generally classified as conventional DC1 (cDC1) and conventional DC2 (cDC2). Both subsets present exogenous and endogenous antigens to T cells and regulate T cell proliferation, survival, and effector function. More specifically, cDC1 cells efficiently cross-present antigens to $CD8^+$ T cells and produce high levels of IL-12p70, thus promoting cytotoxic T cells and Th1 cells, while cDC2 cells are more efficient in presenting antigens on MHC class II, supporting Th1, Th2, and Th17 polarization [28].

cDC1 cells depend on the transcription factors BATF3, IRF8, and ID2 for their development and selectively express the membrane markers CD141/Thrombomodulin/BDCA-3 and Clec9A. In contrast, the development of cDC2 depends on the transcription factors RELB, IRF4, and ZEB2 and they are commonly distinguished from cDC1 by their preferential expression of CD11b and CD172a [29].

Non-conventional DCs include plasmacytoid DCs (pDCs) and monocyte-derived DCs (moDCs). pDC differentiation is dependent on the transcription factors TCF4, IRF8 and Ikaros family zinc finger (IKZF1) and can be identified by the phenotypic markers BDCA-2/CD303, BDCA-4/CD304, ILT7, and the receptor for IL-7. Finally, moDCs, also known as "inflammatory DCs", arise from blood circulating monocytes recruited into tissues upon stimulation and activation as a consequence to inflammatory stimuli [30].

Unified classification	Differential TFs	Conventional markers	Extended markers	Notes
Plasmacytoid DC	E2-2 ZEB2 **IRF8** **IRF4**	CD123, CD303/CLEC4C/BDCA-2 CD304/NRP1/BDCA-4	FCER1 ILT3, ILT7 DR6	DC6 [9]
Myeloid cDC1	ID2 **IRF8** BATF3	CD141/BDCA-1	CLEC9A CADM1 XCR1 BTLA CD26 DNAM-1/CD226	DC1 [9] No antibody for XCR1 in human
Myeloid cDC2	ID2 ZEB2 **IRF4** Notch2/KLF4	CD1c/BDCA-1 CD11c CD11b	CD2 FCER1 SIRPA ILT1 DCIR/CLEC4A CLEC10A	DC2/DC3 [9] DCIR clone specific [26]
Langerhans cell	ID2 RUNX3	CD207 CD1a E-Cadherin	EpCAM TROP2	
Pre-DC	ZEB2 **IRF4** KLF4	CD123, CD303	AXL SIGLEC 6 CX3CR1 CD169 (SIGLEC 1) CD22 (SIGLEC 2) CD33 (SIGLEC 3)	DC5 'AS' DC [9]
Mo-DC	MAFB KLF4	CD11c CD1c/BDCA-1 CD1a	SIRPA S100A8/A9 CD206 DC-SIGN/CD209	
Non-classical monocyte		CD16 CX3CR1 +/-SLAN		DC4 [9] SLAN DC?

cDC, conventional DC; DC, dendritic cell; Mo-DC, monocyte-derived DC; pDC, plasmacytoid DC; TF, transcription factor. IRF4 and IRF8 are highlighted in bold.

Table 1. Human dendritic cells subset characterization [27].

3.2 DCs activation and functions

Under homeostatic conditions, DCs are in an immature or semi-mature state in the periphery, so they express low levels of co-stimulatory molecules such as CD80, CD86, MHC I-II and secrete low levels of pro-inflammatory cytokines such as IL-6 and TNF-α. Upon receiving activating signals from various inputs such as PAMPs or inflammatory cytokines, DCs undergo a maturation process

characterized by phenotypical and functional alterations: 1) upregulation of cell surface MHC gene products and co-stimulatory molecules (CD40, CD80, CD83 and CD86); 2) release of relevant chemokine receptors that improve DC migration to secondary lymphoid tissue, where they present antigen (Ag) to Ag-specific T cells and subsequently induce T cell responses against specific pathogens [31]. Notably, the mobilization of DCs is mediated by the chemokine receptor CCR7 which is upregulated during maturation process. At the lymph nodes, mature DCs present their processed Ag-peptides to $CD4^+$ and $CD8^+$ T cells via MHC-II and I molecules, respectively (Figure 5) [32].

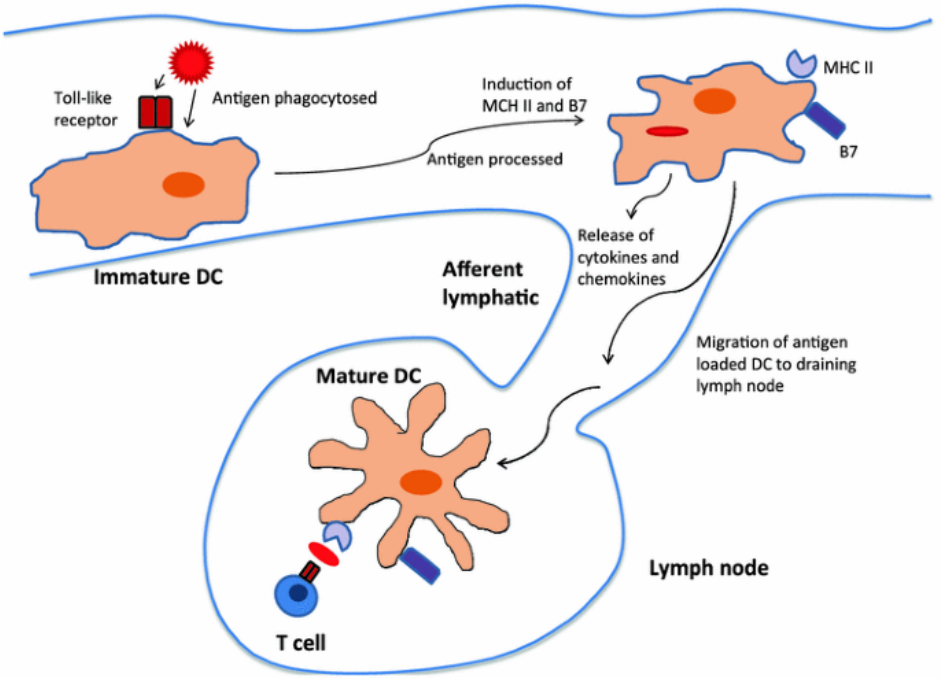

Figure 5. Dendritic cell activation of T cells [33].

Naïve T cells typically require two signals for proper activation: one derived from T-cell receptor ligation (TCR) and the other provided by simultaneous engagement of CD28 on the T-cell by CD80 or CD86 on the DCs. Although TCR/CD28 stimulation provides signals to initiate and sustain T-cell proliferation, DC-delivered cytokines represent the third signal responsible for $CD4^+$ T-cell different orientation towards distinct effector lineages such as Th1, Th2 and Th17 (Figure 6) [34].

Differentiation of Th1 cells, a subset that confers protection against intracellular pathogens and tumors, is initiated by IL-12. T-cells activated in the presence of IL-4 develop into Th2 cells which release type 2 cytokines (IL-4, IL-5 and IL-13) against helminths. Th17 cells direct the immune response against extracellular bacteria and fungi and are activated by IL-6 and TGFβ (33, 34). Th17-

derived polarizing cytokines (IL-17, IL-21 and IL-22) are considered as a hallmark of autoimmune diseases and tissue inflammation [35].

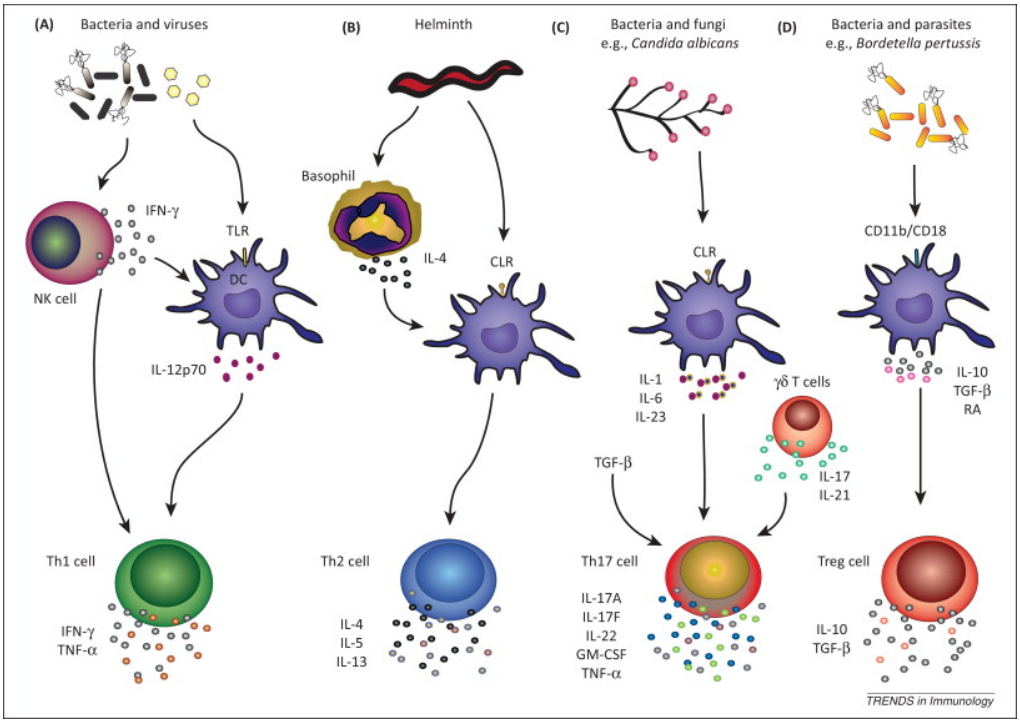

Figure 6. CD4$^+$ T cells development and their functional subsets in immunity (adapted from *https://www.biorender.com)*.

CD8$^+$ T-cells, when activated, differentiate into cytotoxic T-cells (CTLs) after MHC binding in the presence of a wide spectrum of cytokines including IL-2, IL-12, IFN**γ**, IL-27, and IL-23. The combined action of TCR/co-receptor triggering, together with these cytokines, promotes the proliferation, differentiation, and survival of CTLs and the expression of the cytotoxic molecule as perforin and granzymes, which CTLs use to rapidly kill virus-infected or tumorigenic cells. Once the infection has been eradicated, the CTL population is reduced by apoptosis, but a small number survive to differentiate into CD8$^+$ memory T cells, providing immunological memory [35].

3.3 Role of DCs in COPD

DC accumulation and activation in the airways has been postulated to be a driver of COPD pathogenesis. Data obtained from a mouse model of COPD describe a strong increase of DCs in the lung in response to cigarette smoke (CS), suggesting that DCs actively participate in disease progression [36]. Moreover, the number of DCs infiltrating the small airways of patients with COPD rise along with disease severity [37]. CS may impair the differentiation of DC precursors, leading to an altered composition of the DC population in the lungs of smokers and COPD patients [38].

In vitro studies suggest that CS reduces DC maturation ability (decreased CD83 expression), altering and suppressing their normal function (either directly or indirectly through increased alveolar macrophages and/or suppression of epithelial cytokine cell release and inhibition of costimulatory molecule expression), and increasing susceptibility to microbial infections in smokers/smoking COPD patients, perpetuating damaging inflammation [38]. Stoll et al. observed an imbalance of DC co-stimulatory molecules OX40L/PD-L1 caused by a decreased capability of APCs to control inflammation, correlated with the severity of pulmonary emphysema in enrolled COPD donors [39]. In addition, the reduced expression of CCR7 combined with increased expression of maturation markers on BAL DCs of smokers suggest that activated DCs could be retained in the airway mucosa and present their Ags locally, inducing lymphocyte proliferation and lymphoid neogenesis in the lung, and contributing to the ongoing inflammation [38][40]. Abnormal DC responses will contribute to an increase in the frequency of exacerbations and are concurrent with the altered pattern of inflammation associated with acute worsening of COPD. Indeed, CS-induced impairment in DC maturation may enhance $CD8^+$ T-cell proliferation via increased cross-presentation of foreign and self-Ags [41].

4. Breakthrough COPD treatments

4.1 Phosphodiesterase (PDE) enzymes and inhibitors

4.1.1 Overview of PDE family and PDE4 enzymes cAMP signaling pathway

Cyclic adenosine monophosphate (cAMP) is a ubiquitous second messenger that modulates several intracellular signaling pathways, thus playing a pivotal role in the regulation of different physiological processes, including apoptosis, cell proliferation, inflammation, immune response, and bone remodeling [42]. cAMP is synthesized from adenosine triphosphate (ATP) and adenylate cyclase (AC) and is inactivated by hydrolysis to its inactive form AMP, by a variety of phosphodiesterases (PDEs), which are spatially organized alongside cAMP effectors. In this way, cAMP is generated in distinct intracellular pools in a precise manner, allowing for distinct microdomains of cAMP signaling cascades across different cell types [43]. A normal concentration of cAMP suppresses key inflammatory responses. However, augmented level of PDEs hydrolyses leads to the decline in cAMP, activating down-stream inflammatory signaling pathways (43). Therefore, it has been shown that cAMP signaling pathways lead to a combination of pro- and anti- inflammatory processes (Figure 7), explained by the existence of distinct cAMP microdomains [43].

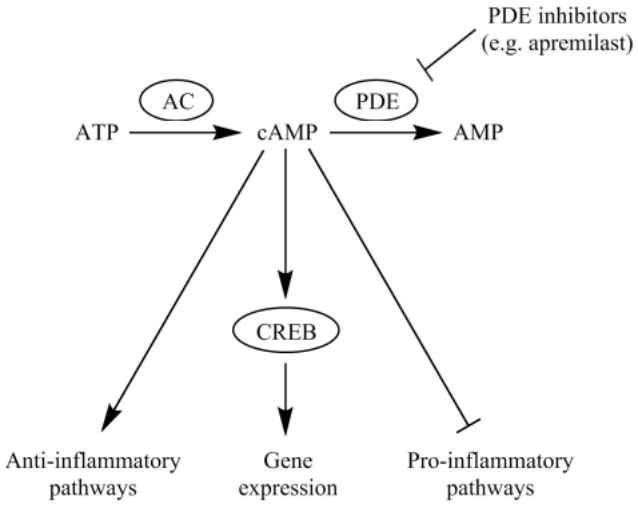

Figure 7. Homeostasis and down-stream effects of cAMP signaling [43].

PDE family

PDEs are a superfamily composed of 11 families with a distinct substrate specificity, molecular structure, and subcellular localization, responsible for the hydrolysis of cAMP and thereby controlling cAMP gradients and compartmentalization (Table 2). All PDEs contain a conserved catalytic domain and a variable N-terminal domain that determine regulation and localization of the enzyme. In general, PDEs are divided into three groups according to the substrate specificity: the cAMP-specific PDEs (PDE4, PDE7 and PDE8), the cGMP-specific PDEs (PDE5, PDE6, and PDE9), and dual cAMP/cGMP specific PDEs (PDE1, PDE2, PDE3, PDE10, and PDE11) [44][45]. Previous studies showed that some dual-specific PDEs play vital roles in the cross-talk between cAMP and cGMP. For instance, in PDE3 isoform, cGMP acts as a competitive inhibitor of cAMP hydrolysis, because of the higher affinity and lower catalytic hydrolysis rate for cGMP as compared to cAMP [45].

PDE Family	Cyclic Nucleotide Substrates	Inhibitors (K_i)
PDE1: Ca^{2+}/CAM stimulated PDE	cAMP and cGMP	Vinpocetine (14 μM), W-7 (300 μM)
PDE2: cGMP-stimulated PDE	cAMP and cGMP	EHNA (1 μM)
PDE3: cGMP-inhibited PDE	cAMP > cGMP	Cilostamide (20 nM), milrinone (150 nM), zardaverine (IC_{50} 0.5–2 μM)
PDE4: High affinity, Rolipram-sensitive cAMP-specific PDE	cAMP	Rolipram (1 μM), Ro 20-1724 (5 μM), piclamilast (1 nM), zardaverine (IC_{50} 0.8–4 μM)
PDE5: cGMP-specific PDE	cGMP	Zaprinast (130 nM), sildenafil (10 nM), vardenafil (1 nM), tadalafil (10 nM)
PDE6: Photoreceptor cGMP-specific PDE	cGMP	Zaprinast (400 nM), dipyridamole (125 nM), sildenafil (50 nM)
PDE7: High-affinity, Rolipram-insensitive cAMP-specific PDE	cAMP	IBMX (4 μM), dipyridamole (600 nM)
PDE8: High-affinity and IBMX-insensitive cAMP-specific PDE	cAMP	Dipyridamole (9 μM)
PDE9: High-affinity cGMP-specific PDE	cGMP	Zaprinast (35 μM)
PDE10: cAMP-Inhibited cGMP PDE	cAMP < cGMP	Dipyridamole (1 μM),
PDE11: Dual specificity cGMP-binding PDE	cAMP and cGMP	Zaprinast (12 μM), dipyridamole (0.4 μM), tadalafil (60 μM)

Table 2. Cyclic nucleotide phosphodiesterase families [46].

PDE4

The Phosphodiesterase-4 (PDE4) family is recognized as the major responsible for cAMP-hydrolysis, widely expressed in inflammatory and immune cells (eosinophils, neutrophils, monocytes, macrophages, T- and B- lymphocytes), and acting as an intracellular non-receptor enzyme that regulates inflammation, antibody IgE release, and generation of lipid mediators [47].

The PDE4 subfamily includes four isoforms highly specific for cAMP degradation (PDE4A, PDE4B, PDE4C, and PDE4D) and is the largest among the 11 PDE families. Surprisingly, unlike other PDE4 subfamilies that are detected in several different human cells and tissues, PDE4C is absent in inflammatory cells [44].

Targeting PDE4 has been demonstrated to be an effective therapeutic strategy for inflammatory conditions, such as asthma, COPD, psoriasis, atopic dermatitis, lupus, and neuroinflammation. Many studies has shown that PDE4 inhibition represses the release of a variety of pro-inflammatory mediators from neutrophils, such as MMP-9, leukotriene B4, neutrophil elastase and ROS. Likewise, several research groups have shown that PDE4 inhibition was able to block eosinophils infiltration into the lung and reduce their survival, and suppress eosinophil chemotaxis, CD11b expression, and L-selectin shedding [44].

4.1.2 PDE4 inhibition in inflammatory cells

PDE4 inhibition results in the accumulation of intracellular cAMP and subsequently activates protein kinase A (PKA), cyclic nucleotide-gated ion channels, and the exchange protein 1/2 (Epac1/2). All these molecules are involved in the regulation of pro-inflammatory and anti-inflammatory cytokines synthesis, activation of T cells, neutrophil degranulation, performance of antigen-presentation, and epithelial integrity via initiation of multiple downstream elements (Figure 8) [48]. The consequent release of the catalytic subunit from the regulatory subunit following PKA activation could potentiate the phosphorylation of cAMP-responsive element binding protein (CREB), activating transcription factor 1 (ATF-1) and cAMP responsive element modulator (CREM) and recruiting the CREB binding protein (CBP) or the homologous protein p300, leading to a decrease of inflammatory cytokines and an increase of anti-inflammatory cytokines. Therefore, rising levels of intracellular cAMP following PDE4 inhibition is closely associated with the suppression of the overactivity of immune responses or intermediates [49].

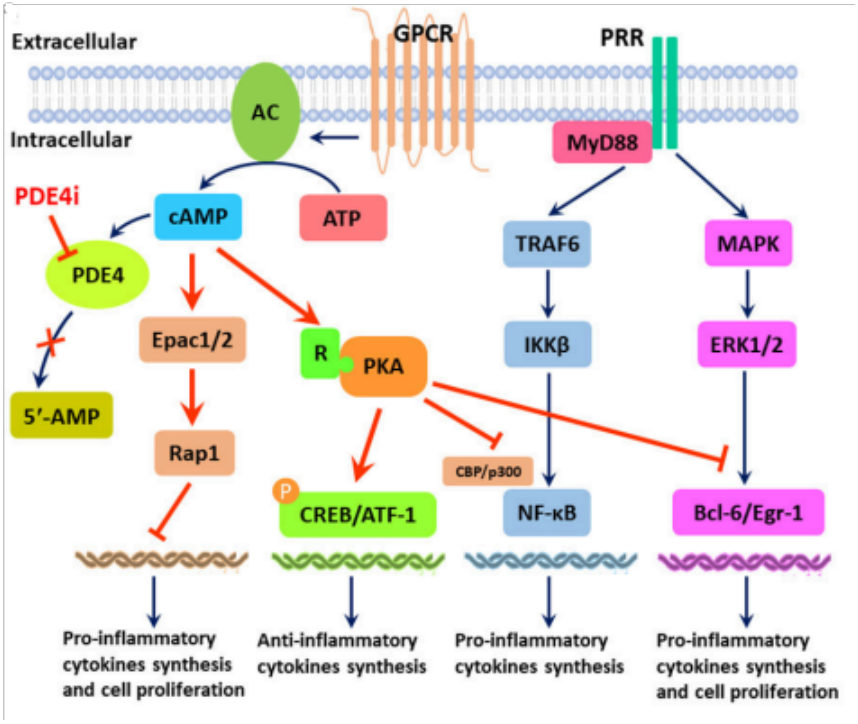

Figure 8. Mechanisms of PDE4 inhibition in inflammatory responses [48].

It has been shown that PDE4 inhibition could modulate both innate and adaptive responses. Blocking PDE4 showed an increase in regulatory activities in macrophages, monocytes, and dendritic cells [48]. PDE4 inhibitors abrogate several T-lymphocyte functions and intercept T-cell activation and downstream signaling events. Effects on T-cell receptor (TCR)-induced activation of T cells, with

consequent reduction of cytokines and chemokines released from T helper-1 (Th1), Th2, and Th17 cells, have also been reported [50][51]. In human peripheral $CD4^+$ T cells it has been shown that PDE4 inhibition reduced the release of interleukin IL-2, IL-5 and IFN-γ [52]. *In vitro* studies revealed that immature DCs showed reduced ability to produce IL-12 and TNFα upon LPS or CD40 ligand (CD40L) stimulation in the presence of PDE4 inhibitors [53]. Inhibition of PDE4 not only reduced NF-kB mediated TNFα expression, but also increased the release of an anti-inflammatory cytokine, IL-10, through PKA activation [50]. In addition, Bopp et al. demonstrated that rolipram was able to strongly block Th2 response both *in vitro*, by co-culture with natural regulatory T cells (nTreg), and *in vivo* using two different mouse models of Th2-dependent airway inflammation and hyperresponsiveness, thus highlighting the potential relevance of using PDE4 inhibitors in human inflammatory diseases [54]. Owning to the distribution of PDE4 in the human body, inhibitor proprieties are also extended to other cell types in the respiratory tract (Figure 9). For instance, reduction of PDE4 activities was shown to promote the barrier function of epithelial cells by suppressing inflammatory mediator production, decreasing mucus secretion [55].

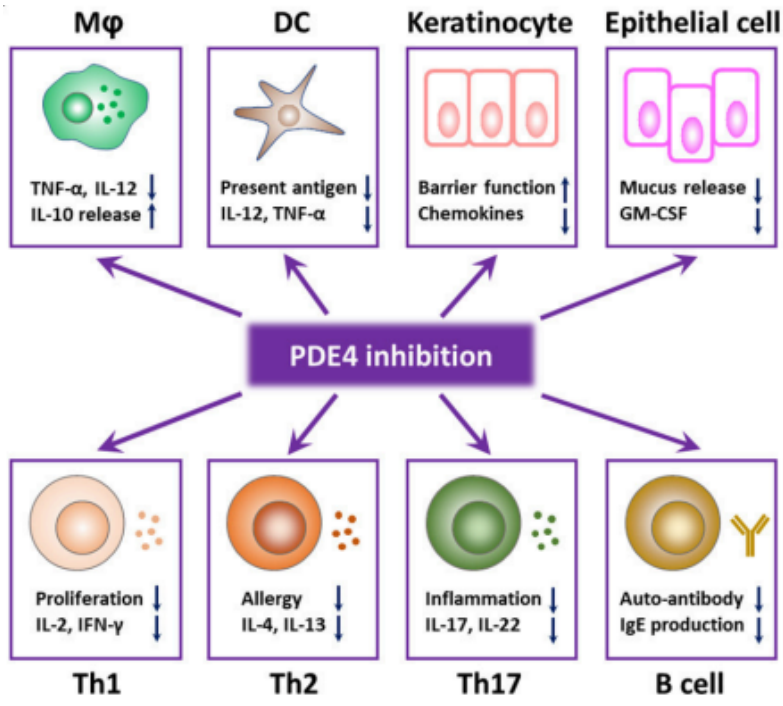

Figure 9. PDE4 inhibition has a wide spectrum of anti-inflammatory effects [48].

4.1.3 PDE4 inhibition as a therapeutic state in respiratory disorders

The prominent immune-modulatory proprieties of PDE4 inhibition in various inflammatory and immune cells has demonstrated its therapeutic potential in lung inflammatory diseases, such as COPD

and asthma. Currently, roflumilast is the only PDE4 inhibitor approved by FDA for the treatment of COPD. The attenuation of airway inflammation in COPD patients taking oral roflumilast was demonstrated by a reduction in sputum cell counts including neutrophils, eosinophils, and macrophages. This finding emphasized the role of aPDE4 inhibitor on mitigating neutrophilic airway inflammation in COPD [56]. Schmid et al. showed that roflumilast can rescue smoke-induced mucociliary disfunction by reversing the decrease in cystic fibrosis transmembrane conductance regulator (CFTR) activity [57]. Restoration of CFTR, a cAMP-regulated transporter expressed on the apical surface of lung epithelial cells, is a promising way to manage chronic bronchitis and further preventing COPD progression [57]. Additionally, the add-on roflumilast to inhaled tiotropium bromide (LAMA) or inhaled salmeterol (LABA) revealed lung function improvement in COPD patient as compared to placebo [58]. A study with cilomilast showed a significant reduction in $CD8^+$ T lymphocytes and $CD68^+$ monocytes/macrophages, two critical components of COPD pathogenesis, in bronchial biopsies of COPD patients [59].

However, the therapeutic utility of PDE4 inhibitors has also been demonstrated in various animal models of asthma and in clinical trials. In particular, repeated studies have documented the ability of PDE4 inhibitors to stop eosinophil recruitment to the airways and bronchial hyperresponsiveness [60]. Roflumilast was found able to improve lung function of asthmatic patients when combined with inhaled corticosteroids [60]. A systematic review and meta-analysis of major databases concluded that in patients with mild asthma, oral PDE4 inhibitor can be considered as an alternative treatment to regular bronchodilators and inhaled controllers [61]. Further, roflumilast has been shown to block inflammatory cell influx through inhibition of P and E-selectin expression on endothelial cells, CD11b expression on neutrophils, and the release of various inflammatory mediators including TNFα and Th2 cytokines. Mild asthmatic patients with active treatment displayed attenuated allergen-induced airway inflammation, along with lower accumulation of inflammatory cells and cytokines [62]. This evidence may also provide rationale for future investigation of the use of PDE4 inhibitors in asthma COPD overlap syndrome (ACOS), which is associated with poor outcomes [56].

4.1.4 The new inhaled PDE4 inhibitor Tanimilast

Tanimilast (international non-proprietary name of CHF6001) is a novel and potent selective inhaled PDE4 inhibitor developed for the treatment of COPD and asthma. The compound is able to inhibit all of the four isoforms (A-D) with equal potency and especially being 10- and 900-fold more potent than the oral roflumilast and cilomilast, respectively [63].

Tanimilast has been developed as an extra fine formulation with mass median aerodynamic diameter ≤ 2 μm to limit systemic exposure and achieve high retention in the lung, by-passing adverse events (including diarrhoea, nausea, weight loss and abdominal pain) reported with oral formulations [64].
When tested in *in vitro* and *in vivo* models, Tanimilast proved to be a highly potent inhibitor of the release of a wide range of inflammatory mediators from different human cell types including DCs, neutrophils, eosinophils, macrophages, lymphocytes and airway bronchial epithelial cells [65]. Indeed, the anti-inflammatory effects were highlighted by its ability to inhibit the release of TNFα from PBMCs, different macrophagic cell lines, as well as DCs. Moreover, neutrophilic-endothelium adhesion, cytokine production, degranulation, apoptosis, and NET formation were efficiently inhibited, as shown in a recent study [65]. In mice exposed to 11 days of CS, once daily, intranasal, Tanimilast reduced neutrophil infiltration, even in mice resistant to corticosteroids [63].
Interestingly, Tanimilast was able to modulate inflammation by down-regulating DC-derived pro-inflammatory mediators, particularly Th1/Th17 effector cells, and $CD8^+$ T cell activation, fine tuning the activity of the master inflammatory transcription factor NF-kB [66]. Again, it showed inhibitory effects on rhinovirus (RV1B)-induced cytokine (CXCL8, IP-10 and RANTES) production in *in vitro* human bronchial epithelial cells (BEAS-2B) culture [63].
In patients with chronic bronchitis, Tanimilast administered in addition to inhaled corticosteroids (ICS), a LABA and a LAMA, massively reduced inflammatory, remodeling, and lung integrity-related mediators, providing rationale for its use in symptomatic patients despite not being a part of standard-of-care therapy [64]. Moreover, recent data highlighted the role of Tanimilast in a Th2-oriented skewing of the immune response, in LPS-stimulated DCs co-cultured with $CD4^+$ T cells, and in the regulation of a broad panel of genes involved in T-cell immunosuppression, including IDO1, VEGF-A, AREG, TSP-1, IRF-8 [66].
Several clinical trials are ongoing and Tanimilast has reached phase IIA for asthma and phase III for COPD by showing promising pharmacodynamic results associated with good tolerability and a good safety profile.

4.2 Monoclonal antibodies (mAbs)

4.2.1 Monoclonal antibody therapy

The improved understanding of airway inflammatory process has prompted the use of therapeutic antibodies, which act by modulating the function of certain inflammatory mediators such as TNFα, Th2 cytokines, alarmins (IL-23, IL-33, TSLP), and transforming growth factor (TGF)-β, in order to achieve a more selective anti-inflammatory response [67].

All currently clinically used monoclonal antibodies (mAbs) are immunoglobulin G (IgG) and are characterized by the same basic structure: they are large heterodimeric protein molecules with a high molecular weight (150 kDa) consisting of four polypeptide chains, two with equal heavy chains (50 kDa) and two with equal light chains (25 kDa). The heavy and light chains are held together by disulfide bonds to form a Y-shape consisting of constant domains (CH and CL) and variable domains (VH and VL) (Figure 10). The two variable regions and the CH1 domains of the heavy chains comprise the antigen binding fragment (Fab) with each variable domain containing the complementarity determining region, which is highly specific for the target antigen [68].

The IgG antibody family consists of four subclasses: IgG1, IgG2, IgG3, and IgG4, distinguished by small differences in the constant region of the heavy chain [69]. These four IgG subclasses distinctly differ in their effector functions via interactions with Fc gamma receptors (FcyRs) and complement C1q. Currently, marketed mAbs are predominantly IgG1, with a proportionately small number of IgG2, IgG4 and murine IgG2a isotypes. The preference of this subclass is dependent on the presence of different effector functions, such as antibody-dependent cell cytotoxicity (ADCC) or complement-dependent cytotoxicity (CDC), required for the mAb activity [70].

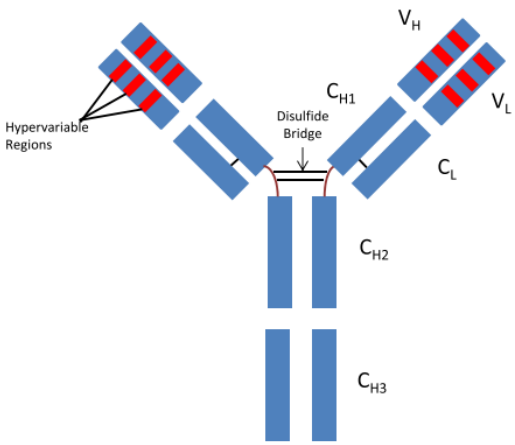

Figure 10. Antibody structure [68].

Several monoclonal antibody treatments have indication for severe type 2 asthma, including anti-IgE omalizumab, anti-IL-5 mepolizumab/reslizumab, anti-IL-5R benralizumab and anti-IL-4Ralpha IL-13 inhibitor (Table 3), demonstrating improvement in lung function and a reduction in exacerbation rates.

Although biologics targeting Th2-cytokines have proven effective in asthma, their possible role in type 2 eosinophilic inflammation in COPD is still under investigation [71].

Therapeutic	Mechanism of action	Effects on asthma exacerbation frequency	Effects on lung function
Omalizumab	Blocks IgE from binding FcεRI	25% reduction	Minimal
Mepolizumab	Binds IL-5 ligand, blocking IL-5-IL-5R interactions	50% reduction	Inconsistent
Reslizumab	Binds IL-5 ligand, blocking IL-5-IL-5R interactions	50-60% reduction	Significant improvement
Benralizumab	Binds IL-5Rα, blocking IL-5-IL-5R interactions and leading to eosinophil, basophil apoptosis	25-60% reduction	Significant improvement
Dupilumab	Binds IL-4Rα, blocking IL-4 and IL-13 signalling	50-70% reduction	Significant improvement

Table 3. Anti-IL biologics currently approved by the US FDA for the treatment of type-2 asthma [72].

4.2.2 IL-13 inhibitor for COPD Type 2 Inflammation

IL-13 inhibitor, a human IgG4 monoclonal antibody, targets IL-4 subunit alpha (IL-4Rα) inducing a dual blockade on IL-4 and IL-13 signaling through type 1 and 2 receptors. The type 1 receptor, expressed in B and T-cells, monocytes, eosinophils, and fibroblasts, is a heterodimeric receptor complex consisting of IL-4Rα and common γ chain subunits. The type 2 receptor, present in monocytes, fibroblasts, eosinophils, activated B cells, epithelial cells, goblet cells, and smooth muscle cells, is a heterodimeric receptor complex composed of IL-4Rα and IL-13Rα1 subunits. IL-4 binds to type 1 and type 2 receptors, while IL-13 binds to the type 2 receptor. IL-13 inhibitor binding to IL-4Rα of type 1 and 2 receptors, mitigates type 2 cascade by inhibiting IL-4/IL-13 axis [73].

IL-4 is an essential factor that drives Th2 differentiation and expansion, B cell growth, isotype class switching to IgE, and eosinophil trafficking, whereas IL-13 not only promotes several of those functions, but also causes GCH in epithelial cells and proliferation of smooth muscle cells. Additionally, IL-4 and IL-13 activate other hematopoietic/immune cells such as mast cells, basophils, and macrophages (Figure 11) [74]. Thus, due to their redundant functions, simultaneous signal blocking via IL-4Rα binding is an indispensable requirement for the inhibition of type 2 inflammatory pathways, such as Th2 cell-induced antigen-presentation cell activation, eosinophil infiltration of the lungs, and expression of pro-inflammatory cytokines and chemokines in the airways [75].

The FDA initially approved IL-13 inhibitor in 2017 for adult patients with moderate-to-severe atopic dermatitis (AD). Subsequent approvals for IL-13 inhibitor included patients with moderate-to-severe asthma, chronic rhinosinusitis with nasal polyposis (CRSwNP), eosinophilic esophagitis (EoE), and prurigo nodularis (PN) [73]. IL-13 inhibitor demonstrated clinically meaningful efficacy with a good safety profile across type 2 inflammatory diseases in adults and paediatrics patients.

Several randomized clinical trials are currently investigating the efficacy of IL-13 inhibitor in eosinophilic COPD. In the BOREAS multi-center randomized trial (52-week, phase III, double-blind), COPD patients (939 enrolled in total) who received IL-13 inhibitor had fewer exacerbations,

better lung function, and less severe respiratory symptoms than those who received placebo within 2 to 4 weeks after initiation of the treatment [76]. Hence, IL-13 inhibitor could represent a potential step forward in the therapeutical resources for COPD patients already receiving maximal inhaler therapy.

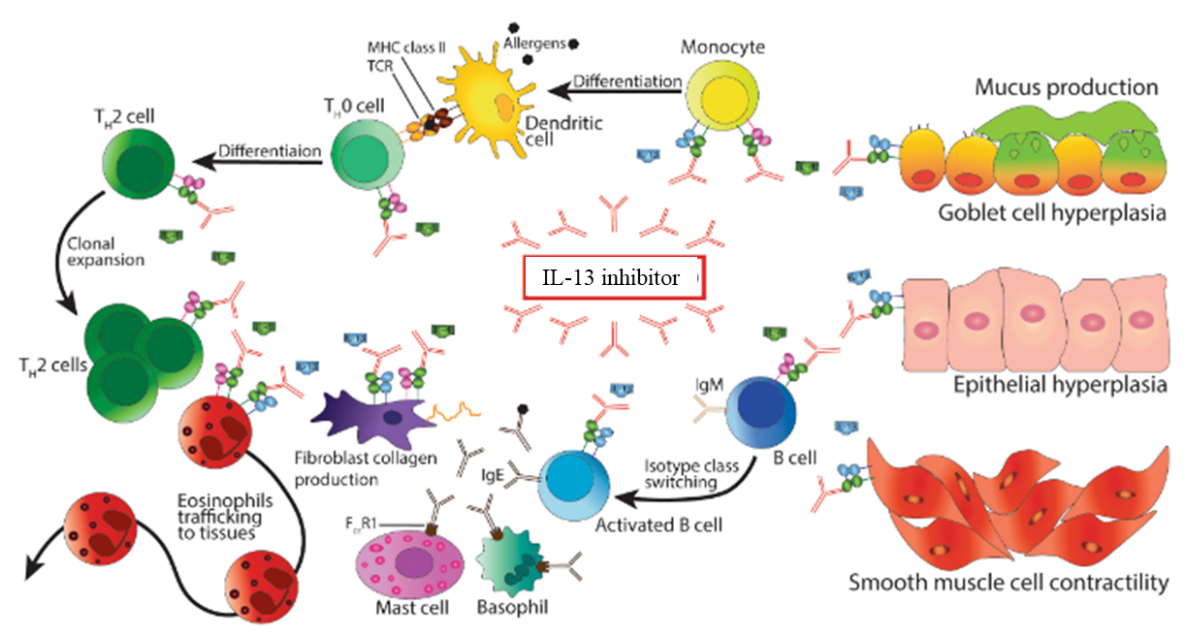

Figure 11. IL-13 inhibitor mechanism of action within the type 2 inflammatory cascade [73].

5. Current *in vitro* advances in cell culture systems

5.1 Overview of 3D *In Vitro* Models

Over the past few years, advances in cell culture techniques have revolutionized *in vitro* culture tools for biomedical research by creating powerful three-dimensional (3D) models for improving our understanding of cell biology and the molecular mechanisms underlying disease. This methodology refine drug development and testing, driving forward advanced in regenerative medicine and tissue engineering [77]. Research has focused on fine-tuning new technological approaches to novel 3D *in vitro* models also in agreement with the 3Rs (Replacement, Reduction, Refinement) principles of the European Union. For years, two-dimensional (2D) cell culture systems have been widely used and have represented the primary methods of *in vitro* research. Traditional cell isolation techniques and culture methods for adherence-dependent cells typically involve submersion cultures of cell monolayers on two-dimensional plastic substrates. These methods were developed to promote survival and proliferation of cells, and generally lead to loss of differentiated cellular functions. Moreover, 2D cultures are a poor representation of human or animal physiology, limiting cell-cell and cell-extracellular matrix (ECM) interactions or the correct oxygen and nutrient gradients

responsible for the activation of specific cellular and molecular events. Recognition of the limitations of 2D culture environments has motivated efforts to develop 3D cell culture conditions that better replicate *in vivo* tissue architectures and provide more physiologically relevant "organotypic" *in vitro* tissue models [78]. In a 3D space composed of an ECM (scaffold), nutrients, oxygen, and drugs are supplied to the cells through a diffusion gradient, allowing permeation more biologically similar to an *in vivo*-like milieu. Cell-cell and/or cell-ECM connections and paracrine signaling by diffusion of cell secretions, that do not exist in conventional 2D cell culture, are the cornerstone features of the 3D cell culture model [79]. Spheroids and organoids represent the two most prominent models where cells are cultured in three dimensions (Figure 12). The first are a type of scaffold-free 3D cell culture model composed of a spherical aggregation of cells, formed via cell-to cell adhesion and derived from cell lines, primary cells or tumor biopsies. The second, organoids, are highly complex self-organized 3D structures, composed of tissue-derived cells (TDCs) or induced pluripotent stem cells (iPSCs), reflecting the *in vivo* organs in both architecture and function to a high degree. Spheroids and organoid culture models have distinct and overlapping purposes and they differ in terms of cell sources, protocol for culture, and time required for establishment [80]. Advances in the development of spheroids and organoids and their application in various fields of research have been also enabled by the rise of new high-throughput technological approaches, such as microfluidic techniques and 3D bioprinting.

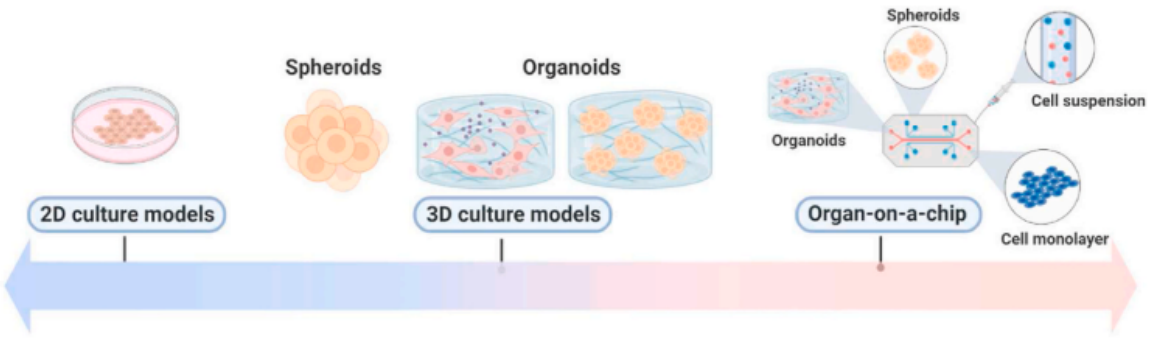

Figure 12. Three-dimensional (3D) in vitro models [81].

5.1.1 Reproducibility of in vivo-like static condition

5.1.1.1 3D reconstructed human airway: Air-Liquid Interface (ALI) model

The establishment and improvement of appropriate research models is fundamental to investigate the mechanisms of human lung development and pathophysiology, and for developing new therapies.

An ideal lung model should realistically reproduce both morphological and functional characteristics. This key consideration has driven the development of alternative *in vitro* cell culture methods aimed to mimic the respiratory tree, consisting of the airways coated by epithelium, which appears as a pseudostratified, ciliated layer across the trachea, and the bronchi, mainly composed of basal cells and ciliated columnar cells interspersed with mucus producing goblet cells (Figure 13) [82].

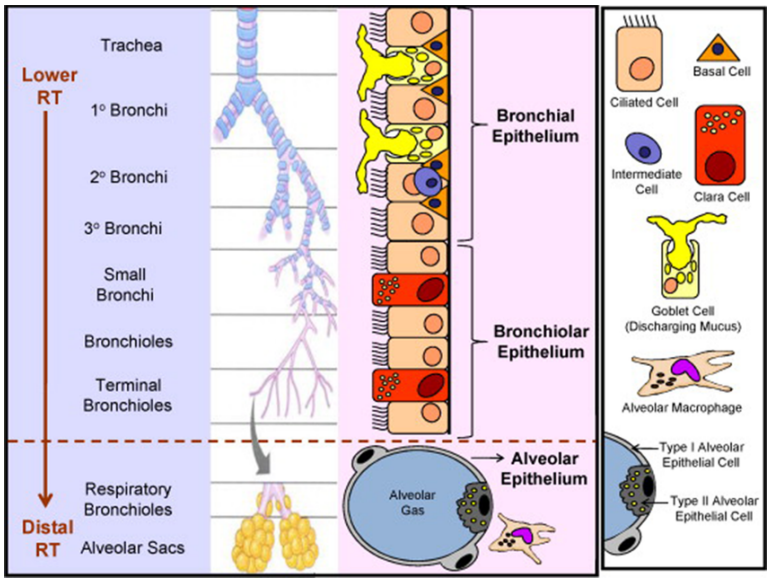

Figure 13. Principle cell types alongside the human respiratory tract [84].

The *in vitro* lung models range from simple cell-free biochemical assays to monolayer media-submerged systems, in which cells of the same type are cultured on a dish or a membrane and exposed to media on both the apical and basal sides, to the most recent and advanced multi-cell-type cultures grown at air-liquid interface (ALI) [83]. Unlike the submerged model, the ALI aims to mimic the airway microenvironment by seeding airway epithelial cells on a permeable membrane of a transwell insert. The system is initially supplied with culture medium to both the apical and basal compartments, and once cell confluence is reached, the apical surface will be in contact with the atmosphere (air) and the basal side exposed to culture medium (liquid) (Figure 14). This configuration allows cell differentiation, over the course of 21 days, towards a mucociliary phenotype, simulating *in vivo* conditions better than in conventional cell culture. Hence, primary differentiated polarized human airway epithelium cultures at ALI represent a relevant *in vitro* tool for study mechanisms of most respiratory diseases [84].

ALI models can be established with a variety of cell types, including primary cells from animals or human donors and immortalized cell lines. Primary cells can be isolated from explanted human tissue,

obtained commercially as frozen stocks, or purchased fully differentiated and ready-to-use, from suppliers such as MucilAir (Epithelix, Geneva, Switzerland) or EpiAirway (MatTec, Ashland, MA, USA).

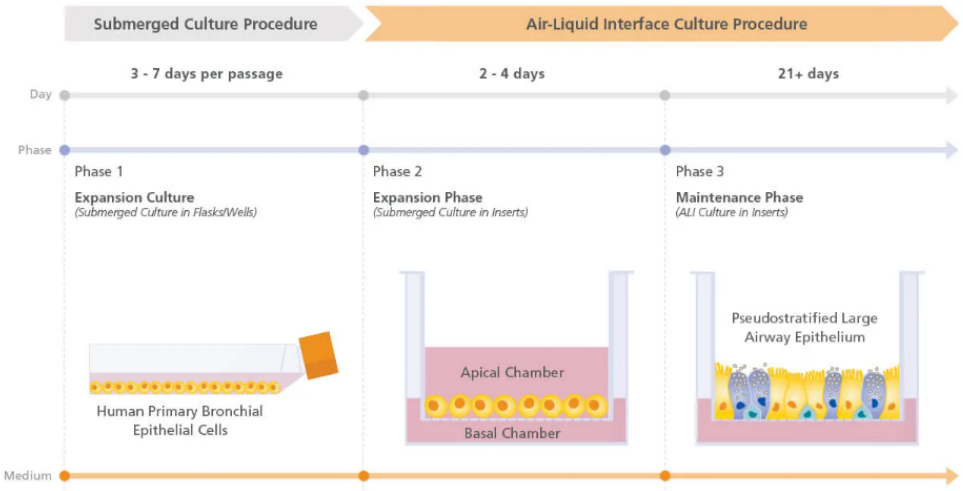

Figure 14. Air-Liquid interface culture schematic (adapted from https://www.stemcell.com).

5.1.1.2 ALI Model in Health and Disease state

Considering the central role played by epithelial cells in COPD pathogenesis, ALI models can grant a deeper understanding of the disease-driving mechanisms as well as identification of novel therapeutic options. Modelling airway disease at ALI is a significant challenge for many researchers. Several studies have shown that after growing and differentiating cells at ALI, they can be exposed to CS to achieve an *in vitro* system incorporating most of the effects observed also *in vivo*. Shamberger et al. demonstrated that CS exposure of healthy human primary bronchial epithelial cells (pHBEC) impaired the cellular composition of the airway epithelium by affecting basal cell differentiation and mucus-secreting cell numbers along with mucociliary clearance. These changes contribute to a mucus-rich lung environment due to the increasing number of goblet cells [85]. Indeed, Gindele et al. studies showed that smoking induces changes in secretory cell populations leading to hyperplasia of mucous-producing goblet cells and a reduction of club cells, which are associated with epithelial defense mechanisms [86].

The research conducted by Ji et al. described the successful development of both healthy and chronic-bronchitis-like ALI models using pHBEC treated with IL-13 [87]. According to previous studies, treatment of epithelial cells with IL-13 induced an increase in mucus-producing cells, metaplasia or hyperplasia, as well as an increase in the expression and production of MUC5AC. Finally, Thai et al. have developed ALI-models using both human and mouse primary epithelial cells to study IL-13

driven effects on mucin-related genes expression [84]. All these *in vitro* modelling approaches contribute to the improvement of the translatability of ALI-based systems in COPD research.

5.1.1.3 ALI co-culture system

Co-culture models allow to create a reliable *in vitro* system, significantly impacting the outcome of ALI experiments. In COPD research, several studies have used co-culture models to study the cellular networks involved in the disease. Luukkainen et al. established an *in vitro* co-culture model involving H3N2-infection of human nasal epithelium with PBMC to investigate the early crosstalk between the infected epithelial layer and the cellular components of the innate arm of the immune response [88]. In another study, Ladjemi et al. developed a co-culture characterized by primary epithelial cells from COPD donors and B-cells. They exploited this system to highlight how the bronchial epithelium influenced the humoral response in the lung. Their findings showed that COPD epithelium induced B-cell immunoglobulin-A (IgA) upregulation via IL-6/IL-6 receptor (IL-6R) [89]. Gras et al. investigated epithelial-dendritic crosstalk in normal and diseased conditions and showed that epithelial phenotype alters dendritic cell responses [90]. An additional co-culture model of respiratory epithelial cells and lung fibroblasts was established to understand the mechanisms behind airway remodeling and inflammation in COPD. The authors observed a stronger interleukin-1 α (IL-1 α)-mediated inflammation in co-cultures exposed to CS, confirming the link between smoke and inflammation [91]. Additionally, several groups have performed triple co-culture models. Rothen-Rutishauser and colleagues generated a triple co-culture models with DCs, macrophages, and primary airway epithelial cells (pAECs) and observed significant upregulation of inflammatory cytokines compared to mono-culture. This three-dimensional model has been used to investigate particle uptake and translocation by the three cell types and their possible interplay during this process [92]. Similarly, Costa et al. utilized triple culture models to evaluate nanocarrier transport through the blood-air barrier and noticed that macrophages were critical in driving inflammatory response [84]. Paplinska-Goryca used a triple-cell co-culture model combining nasal epithelial cells, monocyte derived macrophages, and monocyte derived DCs to define different patterns of TSLP and IL-33 expression in the airway epithelium of healthy donors, donors with asthma and donors with COPD. The study demonstrated that communication between immunological cells and bronchial epithelium is a dynamic process: crosstalk affects their function in unstimulated as well as in inflammatory conditions [93]. Taken together, these data support the idea that triple co-culture represent an important step toward the realization of a more representative model of COPD disease. Therefore, co-culturing different cell or tissue types is essential to constructing *in vitro* models that are

representative of the *in vivo* biological context, as cells communicate to induce and modulate a wide range of functions and metabolic states throughout the body.

5.1.2 Reproducibility of in vivo-like dynamic condition

5.1.2.1 3D dynamic cell culture systems

The current advances in 3D cell culture approaches have gradually prompted the development of 3D dynamic cell cultures, to provide a more reliable cell growth environment *in vitro.* Different researchers have successfully demonstrated the ability to create dynamic cultures, enabling the exposure of cells to heterogenous environments. These systems can be mainly categorized as (a) microcarrier and bioreactor-based systems, which implement nutrient exchange, homogenous oxygen gradient, and cell proliferation and differentiation, and (b) organ-on-chip (OOC), a system combining multiple cell types linked by microfluidics devices, aiming to mimic organ structure and function [94]. Interestingly, OOC have been developed in recent years and allow continuous cell culture medium pumping through the cell-growing carrier, therefore generating shear stress which may contribute to changes in cell behaviour and physiology. Currently, there are OOC under both physiological and pathological conditions for nearly every single organ, including the lung [95]. The advantages of these sophisticated platforms have enabled researchers to develop more biomimetic systems that recreate both biochemical and mechanical aspects of cellular microenvironments in the human body. The versatility of fluidic systems can be leveraged to model a wide broad of physiological lung conditions, in both healthy and diseased states, at different levels within the hierarchical lung structure. For instance, Benam et al. developed a small-airway-on-a-chip device to model lung inflammatory disease and identified new anti-inflammatory therapies [96]. This system mimicked the effect of epithelial-endothelial crosstalk on lung inflammation in a microfluidic device, as a platform for obtaining organ-level responses to pathological processes.
In summary, increased use of dynamic cell culture systems may provide novel insights into cellular processes that were not previously accessible with static culture methods.

5.1.2.2 MIVO Organ-On-a-Chip Technology

The Multi *In Vitro* Organ (MIVO) (Figure 15) device is a cell culture chamber able to host living tissues (e.g. cellular monolayers, 3D reconstructed tissues, tissue biopsies) or artificial membranes under physiological conditions, providing a multiple fluidic circulation system that mimics the human circulatory system with the vascularization of the tissue of interest. It works assembled to a pumping

system and provides a controlled and reproducible fluid flow in terms of direction, speed, and induced shear stresses, enabling the mimicry of different physiological flows and *in vivo* tissue complexity. A three-way valve placed in the fluidic circuit allows sampling of the media over time without affecting the sterility environment and the tissue. It is well-established that fluids represent a crucial component of every tissue, represented by immune cells' ability to flow through the body and extravasate into tissues to interact with other cells, vascular endothelial cells, and epithelial cells of the lung. Hence, the introduction of a fluid flow within cell cultures is expected to improve the resemblance of *in vivo* contexts, to facilitate both nutrient transport and the wash-out of catabolic products, and provide optimal conditions to observe cell behaviour.

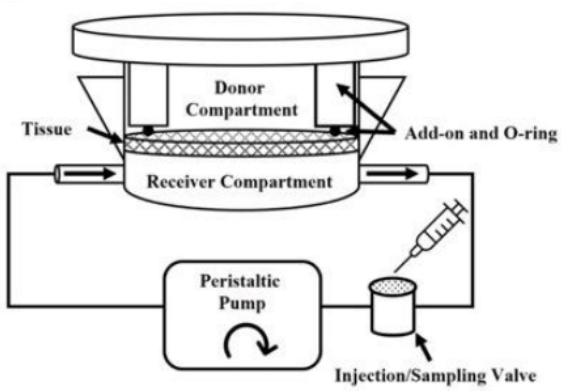

Figure 15. MIVO fluidic chamber (adapted from https://www.react4life.com/platforms/)

Several studies have recently adopted this platform for recapitulating the systemic administration of anticancer drugs and for carrying out efficacy assays in comparison with static traditional conditions, demonstrating the high predictability of this *in vitro* 3R approach [97]. For example, Marzagalli et al. were able to recapitulate the infiltration and the cytotoxic activity of circulating NK cells under physiological fluid flow within 3D tumor model [98]. A comparative analysis between static and dynamic conditions has been performed on different cell lines (3T3 fibroblast and HepG2 hepatoma cells), by culturing the cells into MIVO device and applying a constant and controlled physiological capillary flow. Importantly, the fluidic condition increased the proliferation rate of HepG2 cells and induced a two-fold significant increase of 3T3 cell viability. Similarly, a comparison between the static culture and the MIVO based fluid-dynamic conditions was conducted culturing human ovarian cells (SKOV-3) and testing the efficacy of cisplatin. Interestingly, cancer cells cultured in the MIVO displayed a more significant change in viability in response to the drug, indicating that the *in vivo*-

like dynamic environment allowed better modelling of the 3D tumor environment and potentially better prediction of *in vivo* drug efficacy than a static model [99].

Regarding ALI, innovative research recently published elucidated the absorption mechanisms of different sugars (mannitol and lactulose) in healthy and pathological conditions by combining the Epi-Intestinal tissue (Mattek) with MIVO, confirming its ability to better mimic physiological stimuli of the intestinal environment [100][101].

Therefore, the experimental approach combining 3D culture and fluid-dynamic conditions represents an effective approach to meet the challenge of faithfully recapitulating complex human pathophysiology.

AIM OF THE THESIS

The global prevalence and major burden of lung diseases on human health highlights the importance of improving study models to better understand lung pathophysiology and to accelerate the discovery of new therapeutic strategies. Despite conventional *in vitro* and *in vivo* animal models allowed to acquire a vast understanding of the pathophysiology of respiratory diseases, they only partially reflect the human airway setting. In particular, the improvement of *in vitro* models is of particular relevance in terms of efficacy, by speeding up basic research as well as drug discovery, cost reduction and also adherence to the principles of the 3Rs (Replacement, Reduction, Refinement) aiming at a more humane animal research.

As compared to the two-dimensional (2D) monolayer media-submerged model, three-dimensional (3D) *in vitro* models reproduce a microenvironment mimicking the *in vivo* architecture and functional features of tissues. Cells seeded into 3D models recreate in vivo barrier features, including cellular morphology, functional tight junctions and mucus production [102]. In ALI models, cells are grown on a porous filter that physically separates the lung epithelial tissue from the underlying media, allowing the surface of the cells to communicate with the surrounding air, while the basal surface draws on nutrients via diffusion through the porous membrane. When human bronchial epithelial cells are grown at ALI, ciliated and mucus-producing cells polarize and gain the proper apical-basal morphology [103]. 3D *in vitro* models, which potentially enable a more physiological cell response to both pathological stimuli and drugs and may also allow to study the interactions among different tissues and immune cells, range in the complexity and accuracy in mimicking the airway microenvironment. In addition, they are only starting to be widely employed and literature is often scarce both concerning culture conditions and experimental behaviour.

Taking advantage of the partnership with Chiesi Farmaceutici, the main goal of my work was to set up a 3D ALI model that could be easily cultured and manipulated in house to perform studies on the pathophysiology and pharmacology of COPD and possibly other inflammatory diseases. To this end, we also had to implement technologies (such as TEER measurement) and strategies (such as LDH measurement and histological stains) to assess the integrity of the epithelial barriers upon the different treatments. When possible, due to sample availability and time constraints, we compared the behaviour of ALI cultures from healthy and COPD donors or from different producers such as MucilAir and EpiAirway.

I also had the chance to conduct a side project that allowed me to practice with human dendritic cells, which represent a very interesting immune cell type to be used in ALI co-cultures because of their dual nature of proinflammatory sentinels and regulators of the immune response [94]. In this project, we investigated whether human dendritic cell activation induced by TSLP, an alarmin involved in Th2 activation in Asthma-COPD Overlap Syndrome (ACOS) [104][105][106] could be influenced by the treatment with the Chiesi Farmaceutici's proprietary PDE4 inhibitor Tanimilast.

METHODS

1. 2D experiments

1.1 Dendritic cell preparation and culture

Peripheral blood mononuclear cells (PBMCs) were isolated from buffy coats of healthy blood donors (through the courtesy of the Centro Trasfusionale, Spedali Civili di Brescia, Brescia, Italy) by Ficoll gradient (Ficoll-Paque^{TM} Plus, GE Healthcare, Israel).
Monocytes were enriched from PBMCs using CD14 Microbeads (Miltenyi Biotec) and subsequently cultured in RPMI 1640 complemented with 10% FBS for 6 days with IL-4 (20 ng/ml) and GM-CSF (50 ng/ml) at 8 x 10^5/ml to generate immature monocyte-derived DCs (moDCs). The maturation of moDCs was induced by incubation with pro-inflammatory stimulus: 100 ng/ml TSLP (R&D System) and or 100 ng/ml LPS (Escherichia coli 055:B5, Sigma-Aldrich) for 24 hours.
CD1c (BDCA-1)$^+$ mDCs were obtained from PBMCs by immunomagnetic separation using the CD1c (BDCA-1)$^+$ Dendritic Cell Isolation Kit (Miltenyi Biotec, Germany) and stimulated with TSLP 20 ng/ml (R&D Systems, Minneapolis, MN, USA), for 24 hours. Where indicated, cells were pretreated for 1 hour with tanimilast 10^{-7} M or budesonide at 10^{-7} M (Chiesi Pharmaceuticals, Italy). mDCs were cultured in RPMI 1640 medium supplemented with 2% heat-inactivated fetal calf serum (FCS).

1.2 Analysis of cell membrane markers of activation

Dendritic cell activation was determined by analysing cell membrane markers by flow cytometry. After a 24-hour stimulation, moDCs were stained with the following antibodies: PE-Vio770-conjugated anti-human CD80 and Vioblue-conjugated anti-human CD86 (Miltenyi Biotec) while mDC were stained Vioblue-conjugated anti-human CD86 (Miltenyi Biotec) and PE-conjugated anti-Ox40L (BD Science, Franklin Lakes, NJ, USA). Live/Dead Fixable Dead Cell Stain Kit was used to assess cell viability (Invitrogen, Carlsbad, CA, USA). Following the staining, cells were passed on a MACSQuant16 flow cytometer and data were analyzed with FlowJo 10.

1.3 Allogenic naïve CD4$^+$ T cell preparation and Mixed Leucocyte Reaction (MLR)

DCs stimulated with TSLP in the absence or in the presence of tanimilast or budesonide at 10^{-7} M, or with the only vehicle, were co-cultured with allogenic naïve T cells at different DC:T ratio. Allogenic

naïve $CD4^+$ T cells were purified from PBMCs by immunomagnetic separation using the Naïve $CD4^+$ T Cell Isolation Kit II (Miltenyi Biotec). The co-culture was conducted in RPMI 1640 medium containing 10% heat-inactivated FCS for 6 days. Where indicated, co-cultures at day six were re-stimulated with 125 ng/ml PMA and 1 ug/ml Ionomycin (Sigma-Aldrich, Germany) for 4.5 or 24 hours.

1.4 Proliferation assay

CFSE fluorescence was used as a readout for T cell proliferation. Allogenic naïve $CD4^+$ T cells were labeled with CFSE (CellTrace-CFSE, Thermo Fisher Scientific, Waltham, MA, USA) and then cultured with matured mDCs. After 6 days, alloreactive T cell proliferation was assessed by measuring the loss of the dye CFSE upon cell division using flow cytometry. Data were then analysed with FlowJo 10.

1.5 DC polarizing functions

At day six of co-culture, T cell polarization was investigated by assessing the relevant cytokine production by intracellular staining with the Inside staining kit (Miltenyi Biotec) according to the manufacturer's instructions. Cells were re-stimulated for 4.5 hours with PMA/Ionomycin and 5 ug/ml Brefeldin A (Sigma-Aldrich) was added for the last 2 hours of treatment. Then, cells were harvested, fixed and stained for 10 minutes at room temperature with the following antibodies: APC-conjugated anti-IL-13 (Biolegend), FITC-conjugated anti-IFNγ and PE-conjugated anti-TNFα (Miltenyi Biotec). Live/Dead Fixable Dead Cell Stain Kit was used to assess cell viability (Invitrogen). Following the staining, cells were passed on the flow cytometer and data were analyzed with FlowJo 10.

1.6 Analysis of cytokine secretion

Prism 7 (Graph-Pad Software) was used to prepare graphics and perform statistical analyses. Normally distributed data were expressed as the mean ± SEM (n=3-10) and statistical analysis was performed by one-way ANOVA with Dunnett's post-hoc test or One-sample T test as opportune. *$P < 0.05$ versus vehicle-treated cells (-). $^{\#}P < 0.05$ versus TSLP-stimulated cells.

1.7 Statistical analysis

Prism 7 (Graph-Pad Software) was used to prepare graphics and perform statistical analyses. Normally distributed data ware expressed as the mean ± SEM (n=3-10) and statistical analysis was

performed by one-way ANOVA with Dunnett's post-hoc test. *P < 0.05 versus untreated cells (-). #P < 0.05 versus TSLP stimulated cells.

2. 3D lung system

2.1 Epithelix

MucilAir-Bronchial tissue (Epithelix Sarl, Geneve, Switzerland) is an organotypic 3D airway tissue model, solely reconstituted using human primary cells at low passage (P1), isolated from human biological samples, in which cells are cultured at ALI and capable of differentiating to form a pseudostratified cell layer containing the three main representative cellular types of the upper airway: basal, goblet and ciliated cells. The tissues used in all experiments consisted of bronchial epithelial cells from Healthy and COPD donors, as described in the Certificate of Analysis provided by Epithelix Sarl. Immediately after arrival in the laboratory, the MucilAir tissues were rapidly transferred to a 24-well plate previously filled with 0.7 mL of the specific MucilAir maintenance medium (Epithelix, Sarl) at room temperature. The wells were placed in an incubator at 37° C, 5% CO_2. Prior to the start of the experiments, the MucilAir tissues were first acclimatized by incubation for at least 24 hours.

2.2 Mattek

A commercially available *in vitro* organotypic model of human mucociliary airway epithelium (EpiAirway™) was used for these studies (AIR-100; Mattek Corporation, Ashland, MA). As Epithelix, the EpiAirway model is cultured under submerged conditions until the epithelial cells formed a confluent monolayer, followed by culture at the ALI for up to 21 days to produce the fully differentiated airway models. The tissues used in all experiments consisted of human-derived tracheal/bronchial epithelial cells from Healthy and COPD donors, as described in the Certificate of Analysis provided by Mattek Corporation. Immediately after arrival in the laboratory, the EpiAirway tissues were rapidly transferred to a 12-well plate previously filled with 6 mL of the specific EpiAirway maintenance medium (Mattek Corporation) at room temperature. The wells were placed in an incubator at 37° C, 5% CO_2. Prior to the start of the experiments, the EpiAirway tissues were first acclimatized by incubation for at least 24 hours.

2.3 MIVO platform

Single-Flow MIVO® device (React4Life, Genoa, Italy) was adopted to perform in vitro dynamic cultures. Briefly, ALI inserts were placed within the MIVO® chamber, producing two fluidically independent compartments: (1) the tissue culture chamber and (2) the circulatory one, connected to a closed-loop fluidic circuit. The whole system is connected to a peristaltic pump that circulated the culture medium through a series of tubes. The culture medium was placed in the circuit, with or without the stimulus, at 0.4 mL/min flow (2 rpm with 2 mm diameter tubes).

3. Immune cell preparation

3.1 Thawing the PBMCs

The cryopreserved PBMCs vials from 2 Healthy Donors provided by BioIvt, LLC were placed in a 37° C water bath for rapid thawing, and then transferred into a 15 mL conical centrifuge tube filled with pre-warmed RPMI 1640 supplemented with 10% heat-inactivated, endotoxin free FBS, 2 mM L-glutamine, penicillin and streptomycin (from Gibco, Thermo Fisher Scientific). The cells were washed at 400 rcf for 8 min, resuspended in culture medium, and added basolaterally in ALI system.

3.2 PBMCs purification

Whole blood from blood donation of anonymous healthy donors were obtained and preserved by the Servizio Sanitario Aziendale, Chiesi Farmaceutici S.p.a. according to the Italian low concerning blood component preparation and analysis. PBMCs were obtained by density gradient centrifugation and resuspended in complete medium (RPMI 1640 supplemented with 10% heat-inactivated, endotoxin free FBS, 2 mM L-glutamine, penicillin and streptomycin (from Gibco, Thermo Fisher Scientific). Where indicated cells were cultured at ALI via the basolateral compartment and treated with LPS during 24 hours.

4. ALI culture stimulation

Part of the experiments involved tissues being cultured with 0.7 mL/well of exposure medium containing different concentrations of IL-13 (from Gibco, Thermo Fisher Scientific) and IL-13 inhibitor, with medium replacement every 2 days, during a period of 14 days. However, in other experiments tissues were cultured with 0.7 mL/well of exposure medium added with LPS (from Sigma-Aldrich) and $1x10^5$ cryopreserved PBMCs (from BioIvt, LLC, UK) for 24 hours, or with 1 ml/well of exposure medium added with LPS (from Sigma-Aldrich) and $2x10^5$ cryopreserved PBMCs

(from BioIvt, LLC, UK) for 24 hours. Where indicated, cells were pretreated for 1 hour with Tanimilast (from Chiesi Farmaceutici).

5. Measurement of transepithelial electrical resistance (TEER)

TEER was performed using Millicell ERS-2 Voltohmmeter (Merck Millipore, Burlington, MA, USA) according to the manufacturer's protocol. Two hundred microliters of phosphate-buffered saline (PBS) were added in the upper compartment of ALI cell culture systems. The long stem of the electrode was inserted through the gap of the Transwell to be in contact with the basolateral medium and the short stem of the electrode was placed above the apical surface to be in contact with the apical PBS. The measured resistance was multiplied by the surface area of the epithelium to obtain TEER ($\Omega^* cm^2$).

6. LDH toxicity assay

Viability was determined by measuring lactate dehydrogenase (LDH) into the culture medium using a commercially available colorimetric assay kit (from Promega) according to the manufacturer's instructions.

7. Quantitative polymerase chain reaction (qPCR)

RNA was extracted using TRIzol reagent, treated with DNAse according to the manufacturer's instructions and reverse transcription performed using SuperScript VILO Master Mix (from Invitrogen). The TaqMan Gene Expression Master Mix (from Applied Biosystems) for quantitative real-time PCR was used according to the manufacturer's instructions. Reactions were run in triplicate on a QuantStudio™ 7 Flex System (from Applied Biosystems) and analysed by QuantStudio Software v1.3. Gene expression was normalized based on 28s mRNA content.

8. Cytokine detection

TNF-α, IL-6 and CXCL8 were measured by sandwich Elisa according to the manufacturer's instructions (DuoSet® ELISA Development System, R&D Systems). All assays were performed on cell free supernatants according to the manufacturer's protocol.

9. Histochemical analysis

MucilAir cultures were fixed in 10% neutral buffered formalin (overnight, room temperature), paraffin embedded, and sectioned prior to staining with hematoxylin and eosin (H&E) and periodic

Acid-Schiff-Alcian Blue (PAS-AB). Thick (5 µm) histological cross sections were used to observed the pseudostratified epithelial morphology by image analysis on Aperio VERSA scanner.

10. Immunohistochemical analysis

Formalin fixed paraffin embedded MucilAir tissue sections were stained with anti Muc5AC and FoxJ1 antibodies and performed on a Leica BOND RX automated stainer (Polymer Refine kit and Polymer HRP Plex Refine kit). The section was pre-treated using heat mediated antigen retrieval with EDTA buffer (pH9, epitope retrieval solution 2) for 30 mins at 98°C and then incubated with ab235445 (FoxJ1) at 1/2000 dilution, for 60 mins at room temperature and detected using an HRP conjugated compact polymer system, DAB was used as the chromogen. Afterwards, incubation with ab3649 (Muc5AC) at 1:1000 dilution for 60 min at RT was performed and then was detected using an HRP conjugated compact polymer system, GREEN was used as the chromogen. The section was then counterstained with hematoxylin, dehydrated, cleared and mounted with CV ULTRA (Leica). Cytoplasm staining of Muc5AC (green) and FoxJ1 (brown) labelling granules stored in goblet cells and ciliated cells nuclei, respectively.

11. Statistical analysis

Statistical significance among the experimental groups was determined using one-way ANOVA with Dunnet's post-hoc test (GraphPad Prism 9, GraphPad Software) as indicated in each figure legend. P-value < 0.05 was considered significant.

RESULTS

PART I

A. GCH induction in MucilAir Tissues by IL-13

1. Results

Previous *in vitro* studies found that a two-week exposure of ALI to IL-13 could induce an increase in size and number of mucin-laden goblet cells which closely resembles the morphological features of GCH observed *in vivo* [107]. In this part of the work, we aimed at reproducing these findings with human primary airway epithelial cells (hAECs) at ALI culture (MucilAir™). MucilAir tissues from one healthy donor and one COPD patient were treated with increasing concentrations of IL-13 via the basolateral culture medium in the presence or absence of an IL-13 inhibitor. Further, we reproduced this model also in a dynamic setting taking advantage of the MIVO platform.
To assess GCH induction the following aspects were considered:

- Tissue barrier integrity, evaluated by resistance measurements (TEER)
- Morphological and phenotypic organization, assessed by histological staining
- Gene expression changes, examined by RT-PCR

1.1 Assessment of barrier integrity of ALI cultures in the presence of IL-13 and an IL-13 inhibitor

As all epithelial cells, bronchial epithelial cells form a barrier that is maintained by the formation of tight junctions. *In vitro*, barrier integrity can be assessed by measuring the transepithelial electrical resistance (TEER). A value > 100 $\Omega \cdot cm^2$ is generally accepted to indicate a tight barrier for MucilAir, according to the manufacturer's specifications.
Figure 1 shows the effects of IL-13 on epithelia integrity as assessed by TEER measurement, recorded at various time-points from two days to two weeks post-seeding. Both in the healthy (Figure 1. A) and in the COPD (Figure 1. B) donors, all TEER values were above the minimal acceptable value of 100 $\Omega \cdot cm^2$, indicating that the exposure to IL-13 had no negative impact on tissue barrier integrity. Despite no statistically significant differences could be detected, we noticed that TEER values in unstimulated ALI were lower in the COPD donor, where IL-13 appeared to improve TEER levels.

A. B.

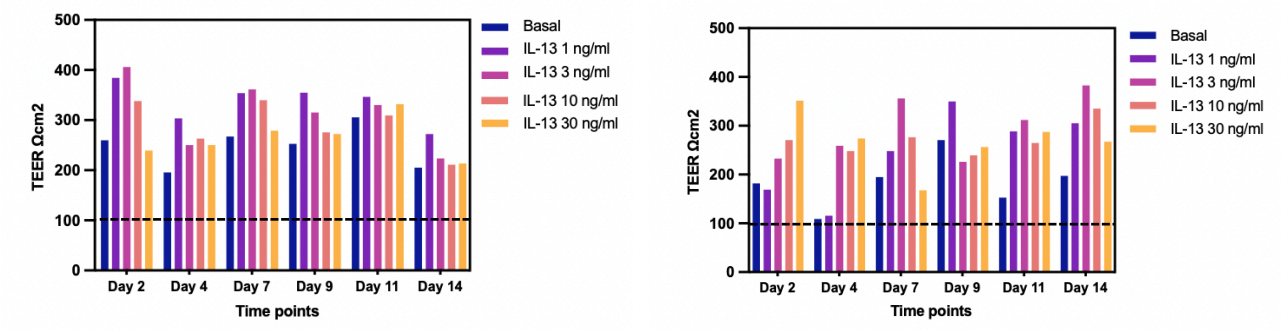

Figure 1. Assessment of barrier integrity in bronchial MucilAir tissues. MucilAir tissues from one healthy donor (A) and one COPD patient (B) were exposed to 1-3-10-30 ng/ml of IL-13 for 14 days. Each point was performed in triplicate and TEER values are shown as the mean of the three. TEER was measured at different time points by using a voltohmmeter and is expressed as $\Omega \cdot cm^2$. All values remained above the threshold of 100 $\Omega \cdot cm^2$, indicating a substantial barrier integrity in all conditions. Despite fluctuations, no difference reached statistical significance.

The same experimental setting was used to test the effect of an anti-IL-13 monoclonal antibody (IL-13 inhibitor) on barrier integrity. Similar to previous experiments, both in the healthy (Figure 2. A) and in the COPD (Figure 2. B) donors, all TEER values were above the minimal acceptable value of 100 $\Omega \cdot cm^2$, indicating that the inhibitor did not negatively impact on tissue barrier integrity.

A. B.

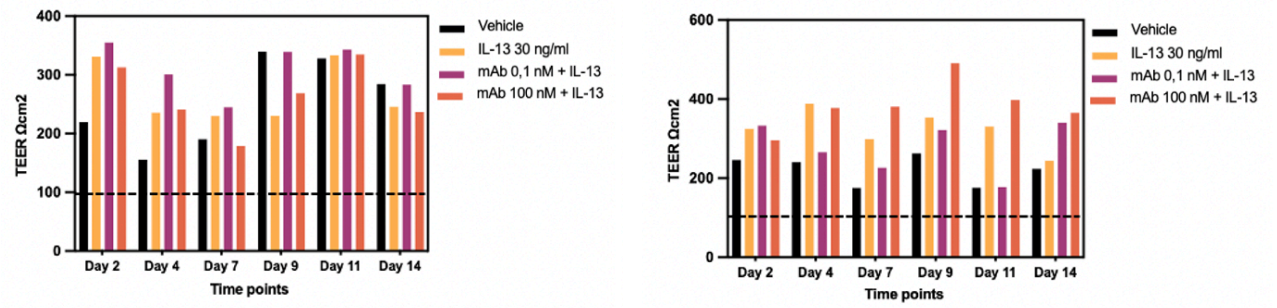

Figure 2. Change in transepithelial electrical resistance of bronchial MucilAir tissues. MucilAir tissues were treated with either IL-13 and a IL-13 inhibitor (0.1 – 100 nM) or a vehicle control for 14 days. Each point was performed in triplicate and TEER values are shown as the mean of the three. TEER was measured at different time points by using a voltohmmeter and is expressed as $\Omega \cdot cm^2$. All values remained above the threshold of 100 $\Omega \cdot cm^2$, indicating a substantial barrier integrity in all conditions. Despite fluctuations, no difference reached statistical significance.

1.2 Assessment of ALI morphological and phenotypic organization upon IL-13 treatment

At the end of the 14-day treatment with IL-13, morphological and phenotypical indicators of GCH were investigated by cross-sectional analysis in healthy and COPD donors (Figure 3. A and B, respectively), in the presence or absence of the IL-13 inhibitor.

Tissue morphology was assessed by H&E (not shown) and PAS-AB (Figure 3). Stained paraffin-embedded sections confirmed that untreated epithelial cells adopt a polarized pseudostratified epithelial morphology with ciliated cells facing the apical side. Exposure to IL-13 resulted in an increase in the number and volume of goblet cells when compared to control, in a dose-dependent manner (Figure 3. A1, B1). In contrast, a reduction in epithelial thickness and in goblet cell volume was prominent in tissues exposed to IL-13 inhibitor (Figure 3. A2, B2). As the IL-13 inhibitor dose increased, the typical goblet cup-like shape appeared smaller, indicating a reversion towards the basal condition.

A.

1.

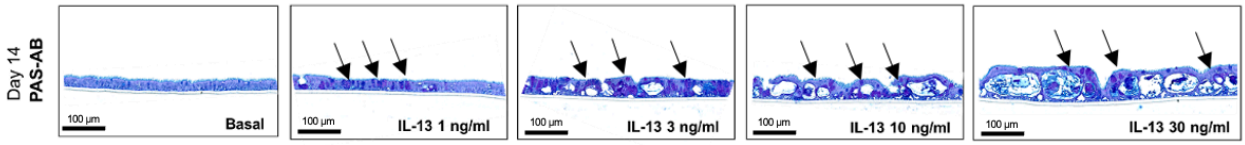

2.

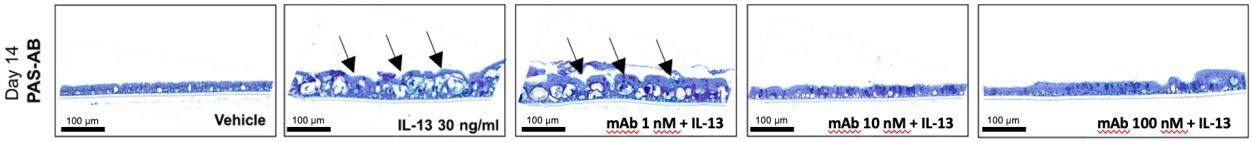

B.

1.

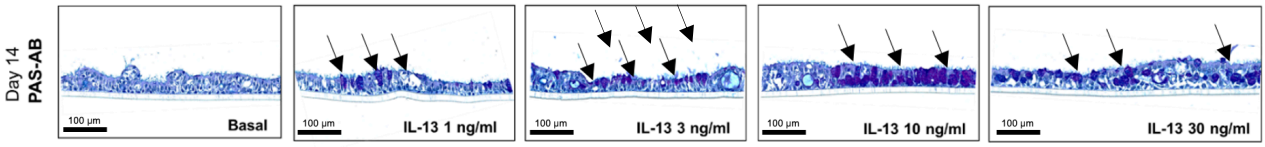

2.

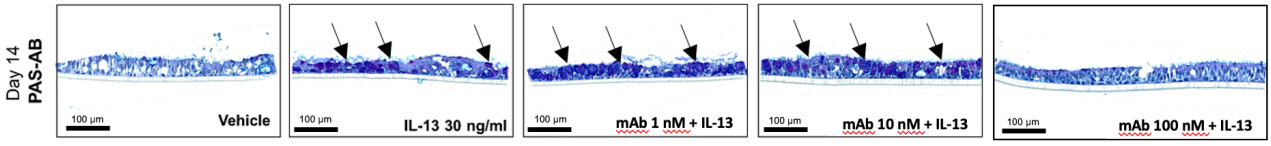

Figure 3. Representative images of Periodic Acid-Schiff (PAS)-Alcian blue (AB) staining of formalin-fixed paraffin-embedded sections of MucilAir tissues (5 µm) from a healthy (A) and COPD donor (B) collected at day 14 of growth in the presence of IL-13 (1-3-10-30 ng/ml, A.1 and B.1) or IL-13 30 ng/ml + increasing concentrations of IL-13 inhibitor (1-10-100 nM A.2 and B.2). All cross-sectional images are oriented with the basolateral surface of the culture at the bottom of the image and the apical surface at the top of the image. Arrows show goblet cells with secretory granules which stain in dark blu with PAS-AB. Scale bars = 100 µm.

To further confirm the increase in goblet cells, formalin-fixed paraffin-embedded slices from ALI cultures were subjected to immunohistoflurescence (IF) evaluation. Figure 4 shows IF staining for MUC5AC and forkhead box J1 protein (FOXJ1) indicating that IL-13 promoted significant remodeling of the pseudostratified epithelium, from ciliated to goblet cells, in both the healthy (A) and COPD (B) donor and that inhibitor reduced this phenotypic transformation in a dose-dependent manner.

A.

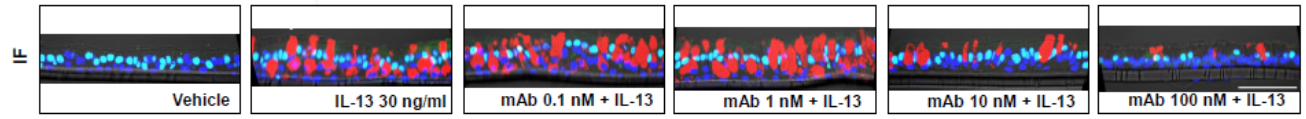

B.

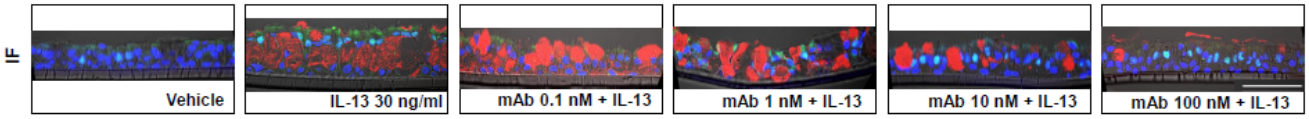

Figure 4. Immunohistochemical images of formalin-fixed paraffin-embedded sections of MucilAir tissues (5 µm) grown with IL-13 (30 ng/ml) in the presence of IL-13 inhibitor (0.1-1-10-100 nM), collected at day 14, from a healthy (A) and a COPD donor (B). IF staining for Muc5AC (ab3649, red) and FoxJ1 (ab235445, green), labelling granules stored in goblet cells and ciliated cells nuclei, respectively.

1.3 Gene expression changes induced by IL-13 in ALI cultures

Aberrant mucin secretion and accumulation in the airway lumen are clinical hallmarks associated to COPD. Gene targeting and expression studies demonstrated important roles for transcription factors in controlling goblet cell differentiation.

Among 20 genes associated with IL-13-induced goblet cell differentiation and mucus hypersecretion, 6 have been verified in IL-13 stimulated MucilAir tissues, with or without pharmacological treatment, at the mRNA level. In particular, arachidonate 15-lipoxygenase (ALOX15), SAM-pointed domain-containing ETS transcription factor (SPDEF) and calcium-activated chloride channel regulator

(CLCA1) have been described as highly inducible IL-13 target genes in mice and humans, implicated in the pathogenesis of mucus hypersecretory-associated respiratory diseases [107][108]. MUC5B and club cell protein 16 (CC16) have demonstrated protective capacity in GCH models. CC16 is reported to limit airway epithelial cell production of CXCL8, a key pro-inflammatory molecule that accumulates in COPD lungs [107][109]. MUC5B is able to interfere with the STAT6-SPDEF pathway by affecting airway mucus production [110]. Finally, for ciliated cell lineage tagging, the expression of ciliary regulating protein forkhead box J1 protein (FOXJ1) on airway epithelium is an important indicator of airway cilia function. Low expression of FOXJ1 modulated by inflammatory factors, e.g. IL-13, may impair cilia architecture and cause cilia loss [111].

Figure 5 shows that IL-13 significantly induced the up-regulation of the hyperplasia-related genes ALOX15, CLCA1 and SPDEF in a dose-dependent manner both in the healthy (Figure 5. A1) and in the COPD donors (Figure 5. B1). As we expected, IL-13 inhibitor reduced the induction of these genes, especially CLCA1 and SPDEF, as the concentration increased (Figure 5. A2 and B2), thus reinforcing the idea that IL-13 inhibition can to prevent the dysregulation of epithelial function by counteracting the IL-13 signalling.

By contrast, in COPD tissues IL-13 reduced the expression of MUC5AB, FOXJ1 and CC16 but not in healthy tissues (not shown) in a dose dependent manner (Figure 5. C1), which were partially restored by IL-13 inhibition (Figure 5. C2).

A.

1.

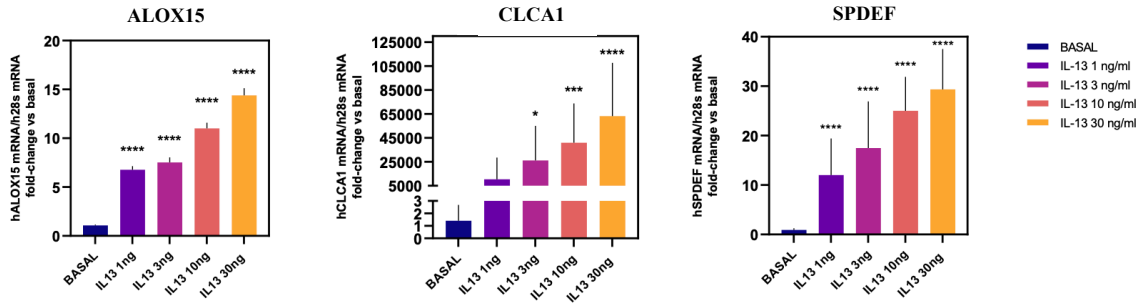

2.

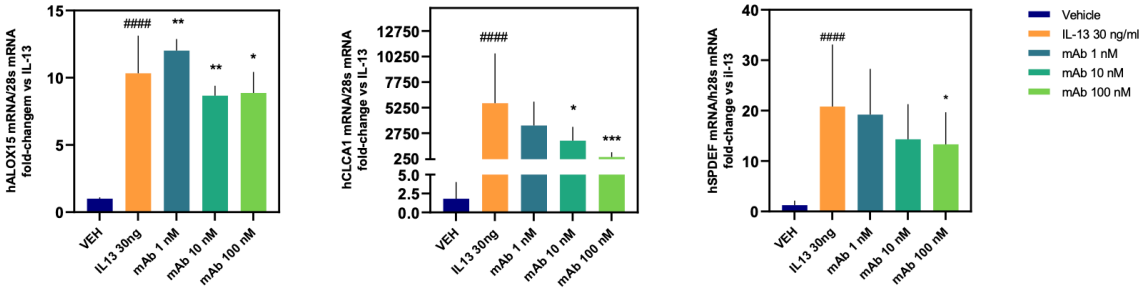

B.

1.

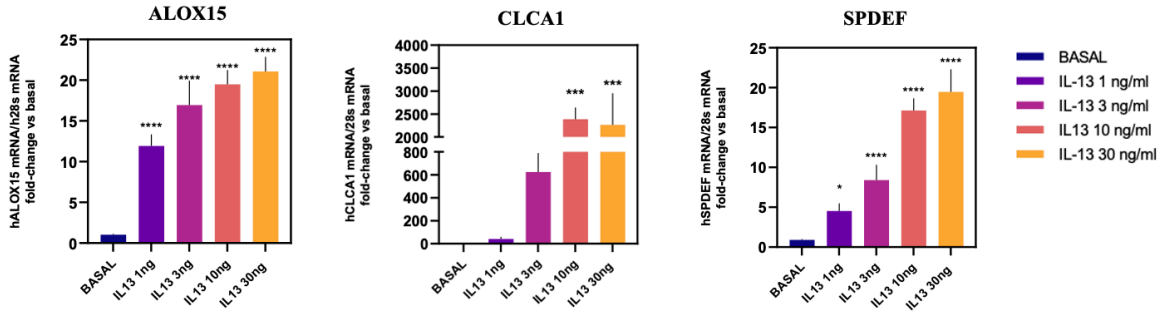

2.

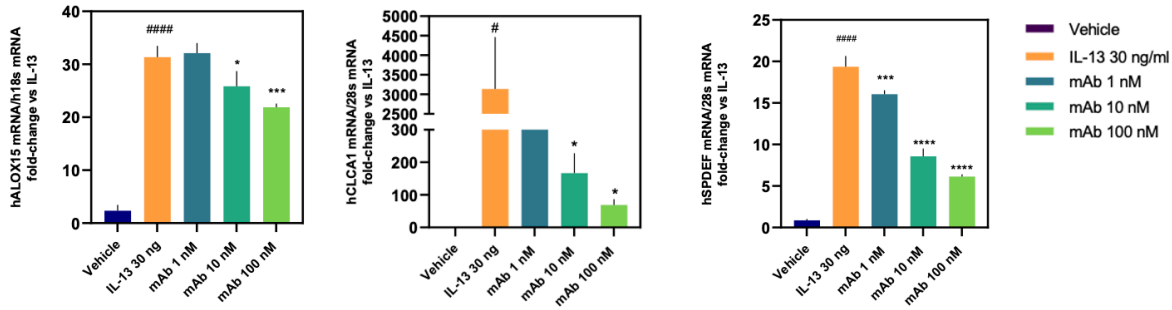

C.

1.

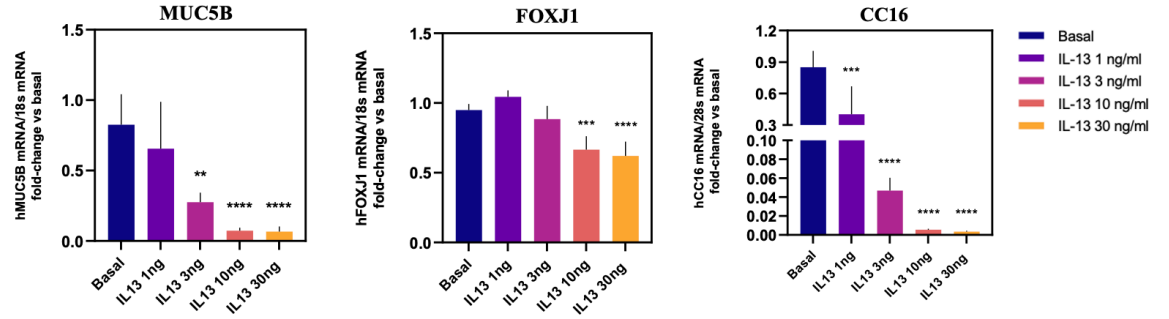

2.

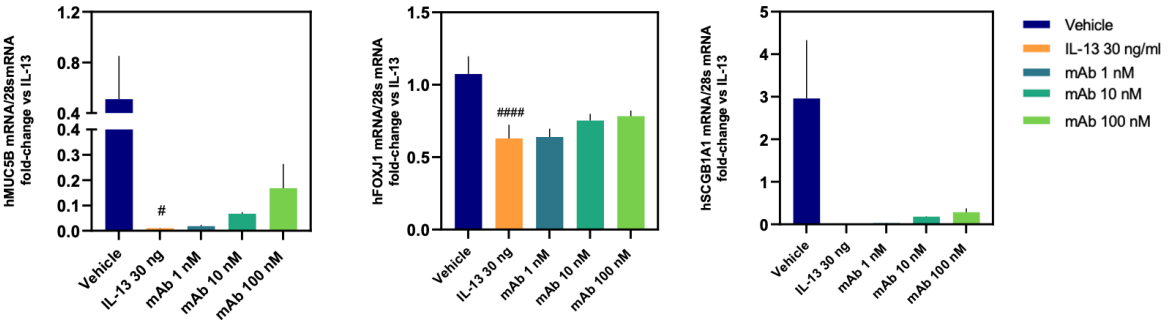

Figure 5. IL-13 exposure alters the expression of hyperplasia-related genes. Quantitative RT-PCR analysis of MucilAir tissues was performed at day 14, from one healthy (A) and one COPD donor (B, C). Exposure to IL-13 led to a significant change in mRNA expression of genes related to aspects of epithelium and goblet cell differentiation: MUC5B, SPDEF, CLCA1, CC16, ALOX15 and FOXJ1. Data expressed as mean ± SD, are the average of n=3 technical replicates run for

each RNA sample. The 28s housekeeping gene was used as normalization control for each sample. Significance is indicated as * for p value: **** $p < 0.0001$, *** $p < 0.001$, ** $p < 0.01$, * $p < 0.05$ versus basal or IL-13 30 ng/ml; #### $p < 0.0001$, ### $p < 0.001$, ## $p < 0.01$, # $p < 0.05$ versus vehicle, by one-way ANOVA Dunnett's test.

1.4 Reproducibility of GCH in MIVO technology

1.4.1 Evaluation of ALI tissue barrier integrity upon IL-13 stimulation

First, we assessed the modulation of TEER in a dynamic system as compared to the static ALI setup (Figure 6). Both systems followed the same 14-day protocol to induce GCH through IL-13 stimulation (30 ng/ml). In an initial pilot experiment using MucilAir ALI tissues from a healthy donor, we set a basolateral flow rate of 0.8 ml/min to MIVO pump. TEER values were measured every two days before each medium replacement. Since a marked decrease in tissue barrier integrity was detected in the MIVO system within the first 48 hours, the flow rate was reduced to 0.4 ml/min thus allowing the stabilization of TEER values from day 4 onward. Despite the presence of IL-13 clearly reduced TEER values, differences were not statistically significant between static and dynamic conditions and values always remained above 100 $\Omega \cdot cm^2$. This indicated that, once the flow rate was optimized, the dynamic environment did not negatively impact on tissue barrier integrity.

A. B.

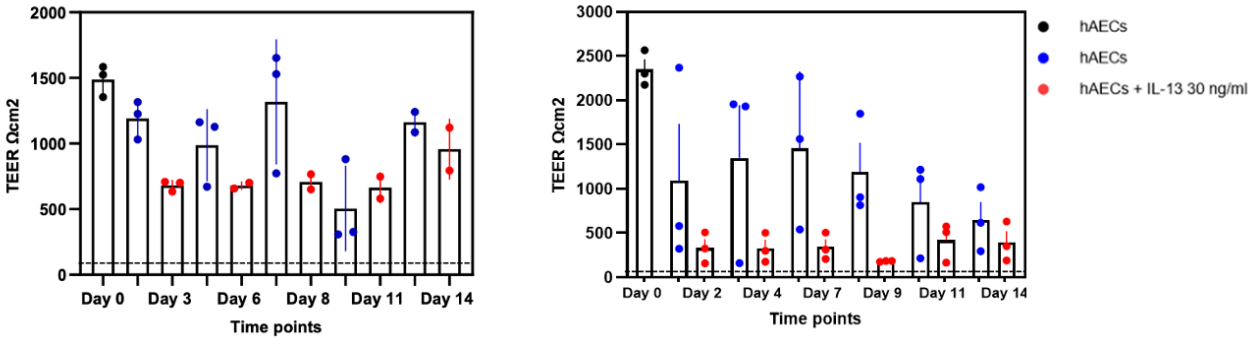

Figure 6. TEER measurements in static (A) and dynamic (B) systems. MucilAir tissues from a healthy donor were exposed to 30 ng/ml of IL-13 for 14 days. Each point was performed in triplicate: bars of TEER values represent both individual triplicates and the mean +/-SE. TEER was measured at different time points by using a voltohmmeter and is represented as $\Omega \cdot cm^2$. Differences did not reach statistical significance and all values stayed above the threshold of 100 $\Omega \cdot cm^2$.

1.4.2 Comparison of morphological and phenotypic changes between static and dynamic ALI model

Next, we examined the morphological and phenotypic changes induced by a 14-day IL-13 stimulation in the two systems by PAS-AB and H&E staining. As expected, stained paraffin-embedded sections of the static model revealed that untreated epithelial cells maintained their optimal morphology and that IL-13 induced hyperplasia of goblet cells (Figure 7. A). By contrast, in the dynamic condition, the epithelium appeared thinned at baseline and did not maintain a good structural integrity, nor IL-13 induced the expected modification (Figure 7. B). We hypothesize that the initial high flow rate likely compromised the tissue from the outset, therefore suggesting that stimulation could be repeated.

A.

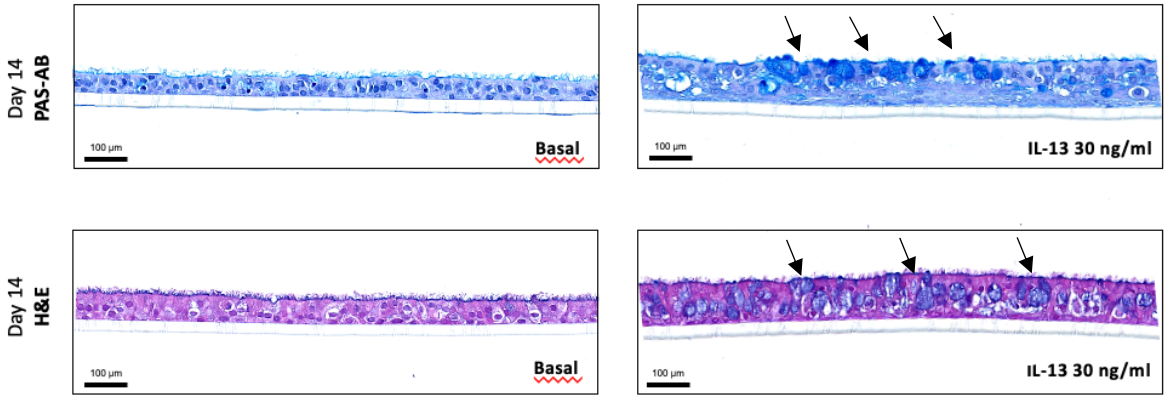

B.

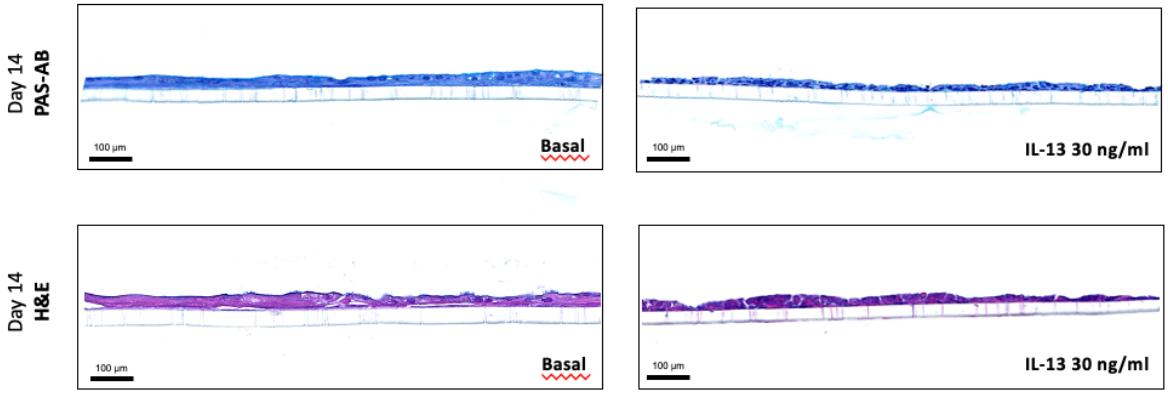

Figure 7. Representative images of Periodic Acid-Schiff (PAS)-Alcian blue and H&E staining of formalin-fixed paraffin-embedded sections of MucilAir tissues (5 µm) grown with IL-13 30 ng/ml, collected at day 14, in static (A) and dynamic condition (B). All cross-sectional images are oriented with the basolateral surface of the culture at the bottom of the image

and the apical surface at the top of the image. Arrows show goblet cells with secretory granules which stain in dark blu with PAS-AB or purple with H&E. Scale bars = 100 µm.

1.4.3 Evaluation of a new experimental setup in MIVO fluidic system

Based on previous results, we set the initial flow rate at 0.4 ml/min. In addition, because of the possibility that a dynamic system might accelerate the onset of hyperplasia [112], we reduced the stimulation duration to 11 days (while retaining the 14-day treatment protocol for the static model). As shown in figure 8, TEER values remained comparable in the two conditions and closer to the starting ALI culture, confirming that a constant flow rate of 0.4 ml/min could grant epithelial resistance and possibly ensure tissue integrity.

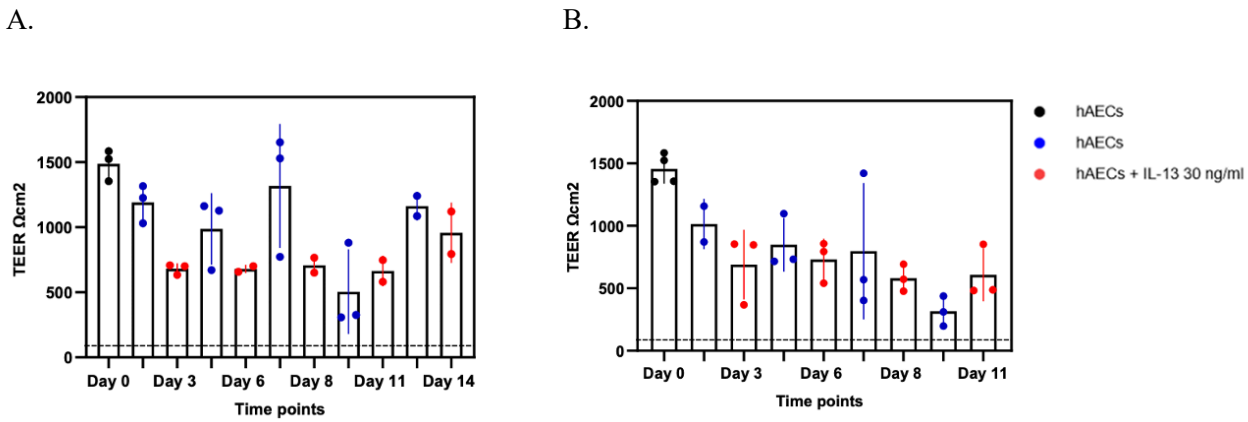

Figure 8. Assessment of tissue barrier integrity in static (A) and dynamic (B) systems. MucilAir tissues were exposed to 30 ng/ml of IL-13 for 14 days (static configuration) or 11 days (dynamic configuration). Each point was performed in triplicate: bars of TEER values represent both individual triplicates and the mean +/-SE. TEER was measured at different time points by using a voltohmmeter and is represented as $\Omega \cdot cm^2$. Differences did not reach significance and all values stayed above the threshold of 100 $\Omega \cdot cm^2$.

At the end of the culture, we analysed the inserts PAS-AB and H&E staining. Figure 24 shows that the untreated sections of the dynamic model (Figure 9. B) now retains the characteristic morphology of the pseudostratified epithelium, albeit with a thinner epithelial layer in respect to the static model (Figure 9. A). After 14 days, IL-13 stimulation in the static model induced hyperplasia of goblet cells, accompanied by an increased presence of mucus granules, with epithelium appearing globally thicker as compared to control (Figure 9. A) and a similar effect was achieved in MIVO model (Figure 9. B).

A.

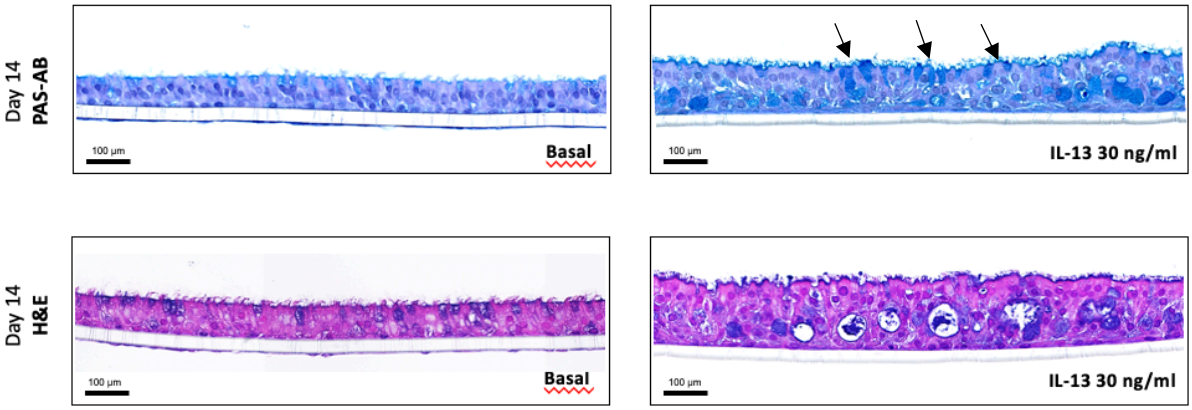

B.

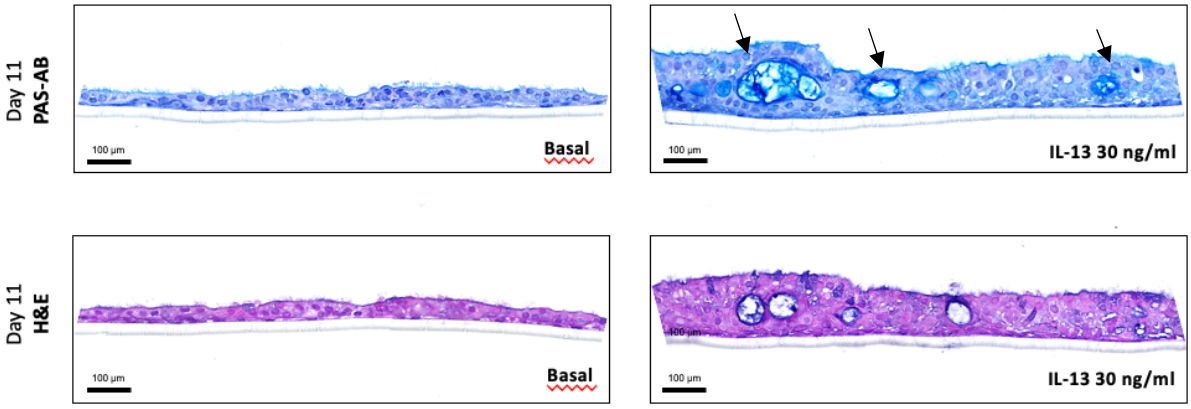

Figure 9. Stained sections of MucilAir tissues (5 µm) grown with IL-13 30 ng/ml, collected at day 14 in static (A) and at day 11 in dynamic condition (B). All cross-sectional images are oriented with the basolateral surface of the culture at the bottom of the image and the apical surface at the top of the image. Arrows show goblet cells with secretory granules. Scale bars = 100 µm.

2. Discussion

GCH is a common clinical feature affecting the bronchial epithelium of COPD patients that can be initiated or exacerbated by exposure to different stimuli including infections, air pollution and tobacco smoke. Long-term mucus overproduction following GCH contributes to airway narrowing and occlusion leading to loss of lung functions and recurrent airway infection. The resulting vicious circle is difficult to manage from a clinical and pharmacological point of view.

Several *in vitro* and *in vivo* studies demonstrated that Th2 cytokines, especially IL-13, can induce the mucus hypersecretory phenotype by increasing expression of goblet cell markers and contributing to the remodelling of the epithelium [107]. Mitsuko et al. reported that IL-13 induced elevated goblet cell differentiation along with inhibition of ciliated cell differentiation in primary airway epithelial cells from guinea pigs cultured at ALI [111]. Likewise, expression of the receptor for IL-13 was shown in well-differentiated cultures of human airway epithelial cells, which responded to IL-13 switching to a goblet-cell dependent, hypersecretory phenotype [107]. Activation of the IL-13 receptor α_1 led to MUC5AC production via the JAK-STAT6 pathway, possibly followed by the activation of SPDEF and CLCA1 [113]. Additionally, IL-13 also indices epidermal growth factor receptor (EGFR), which increases transcription of MUC5AC via extracellular signal-regulated kinase (ERK1/2) signaling as well as NF-kB pathways [114]. Tyner et al. demonstrated that epithelial remodelling toward the GCH phenotype occurred upon both EGFR survival and IL-13 trans-differentiation signals. Finally, activation of phosphatidylinositol 3-kinase (PI3K) and serine-threonine protein kinase family (Akt) may also be involved in EGFR-mediated GCH [115].

The reproducibility of GCH and its molecular pathogenesis in human airway epithelial cells cultured under ALI conditions, which faithfully replicates the human respiratory pseudostratified epithelium, could represent a relevant tool to better delineate the phenotype and to test novel potential therapeutical strategies. For example, Tanabe et al. found that the macrolide antibiotic clarithromycin ameliorated mucus hypersecretion and decreased MUC5AC mRNA expression in a dose-dependent manner [116].

In this part of the thesis work, we characterized the effects of IL-13 on well-differentiated ALI cultures of human bronchial epithelial cells (MucilAir™), both from a healthy and a COPD donor, which provide *in vivo*-like structures accurately reproducing a functional mucociliary system and the secretion of mucus. In this system, we were able to reproduce the development of GCH and observed the inhibitory potential of a monoclonal antibody capable to block IL-13 binding to its receptor (IL-13 inhibitor).

Our findings indicated that human bronchial epithelial cells isolated from both healthy donors and donors with COPD produced a mix of pseudostratified and stratified highly-differentiated mucociliary epithelium with appropriate biophysical proprieties. Indeed, all TEER values remained above the minimal acceptable value of 100 $\Omega \cdot cm^2$ indicated by the producer and, despite COPD values were generally lower and fluctuated more, we could not detect any significant difference. This result is unexpected, since a defective epithelial barrier with decreased tissue resistance and decreased expression of tight junction proteins is a crucial driver of COPD. However, a higher number of experimental replicates and donors could allow to ascertain if the observed differences may reach statistical significance. With the same limitations, our experiments suggest that long-term exposure to IL-13 did not disrupt the epithelial barrier function, in accordance with previous data showing no effects of increasing concentrations of IL-13 on TEER, as compared to IL-4, which significantly disrupted epithelial function [117]. IL-13 inhibitor appeared to increase TEER values, especially in the COPD donor, but again no statistically significant differences could be observed in our reduced experimental setting.

Our morphological analysis confirmed the presence of the GCH phenotype characterized by epithelial cell proliferation and increased number of goblet cells and also that IL-13-driven goblet cell response is concentration-dependent. IL-13-treated epithelial cells also showed a reduction of FOXJ1 at the mRNA level and in IF staining in both donors, suggesting loss of cilia and impaired mucociliary functions. All these effects were counteracted in the presence of the IL-13 inhibitor, including the restoration of FOXJI and the reversion of MUC5AC expression, which correlated with decreased PAS-stained goblet cells.

Among the other mucin-pathway associated genes, IL-13 inhibitor also partially restored mRNA levels of MUC5B and CC16, two genes that are indispensable for airway defence. Previous studies reported that decreased circulating levels of MUC5B and CC16 positively correlate with COPD severity, increased mucin production, and decreased lumen fluid, which have harmful effects on airway health [107]. Thus, the restoration of their expression may be a significant readout of the efficacy of IL-13 blocking as a therapeutic strategy [110][118].

We believe that our experimental model may represent a useful tool to study the induction of the GCH phenotype by inhaled pathogens, chemicals, and cigarette smoke, and for assessing the efficacy of new drug candidates for treating respiratory diseases. Of course, this airway epithelium model lacks both resident and infiltrating immune cells (e.g. dendritic cells, macrophages, lymphocytes) and is devoid of the endothelial layer. This prevents its application to study the contributions of the immune system to processes related to the development and modulation of the GCH phenotype.

We also set the bases for implementing the ALI static model with MIVO technology, which was not done so far with human airway epithelial tissues, showing the importance of an optimized flow rate to maintain tissue integrity and achieve hyperplasia following IL-13 stimulation.

Overall, our results are in line with previous studies suggesting that IL-13 may induce a mucus hypersecretory phenotype via direct interaction with human airway epithelium. However, we could not found significant differences between healthy and COPD tissues, possibly because of the low number of donors available. More experiments are granted in this direction.

B. Modelling airway inflammation in ALI cultures

Lipopolysaccharide (LPS) is a major pathogenic mediator of local acute lung inflammation, inducing a phenotype that closely resembles a COPD-like acute disease [119]. Here, we aimed at assessing its capability to stimulate human airway epithelial cells at ALI. Two different human airway 3D ALI models were used: one developed by Epithelix Sarl (MucilAir™, already used in previous experiments) and a second by Mattek Corp (EpiAirway™). This latter differs from MucilAir™ in terms of: 1) diameter of Transwell insert, which is twice the diameter of the MucilAir™ insert, 2) number of seeded cells (10^6/insert as compared to $5X10^5$/insert), 3) culture medium volume/well (1 ml as compared to 0.7 ml). TEER measurement was used to assess epithelial barrier integrity and the release of TNFα was considered a readout of induction of an inflammatory response.

1. Results

1.1 ALI cultures respond weakly to high concentrations of LPS

ALI tissues from healthy donors were basolaterally exposed to increasing concentrations of LPS. We decided to extend our dose response curve to up to very high concentrations because epithelial tissues are known to be refractory and a strong variability among donors was observed by the same producer Epithelix Sarl [120]. Despite high, no LPS concentration compromised tissue barrier integrity at 24 hours of stimulation in any of the two models, as shown by TEER values remaining above the minimal acceptable value of 100 $\Omega \cdot cm^2$ (Figure 10).

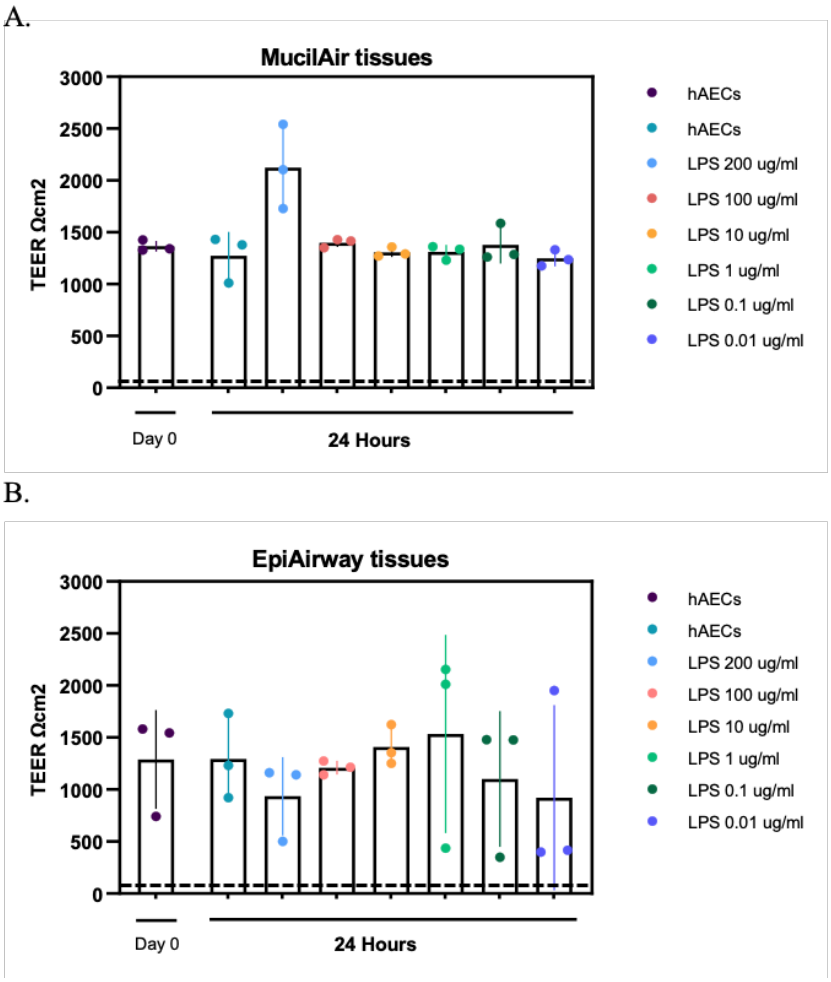

Figure 10. Assessment of epithelium barrier integrity in MucilAir (A) and EpiAirway tissues (B). ALI tissues were exposed to 200-100-10-1-0.1-0.01 ug/ml of LPS, via the basolateral compartment, for 24 hours. Each point was performed in triplicate in one ALI donor and TEER values are shown as the mean of the three. TEER was measured using a voltohmmeter and is represented as $\Omega \cdot cm^2$. All values remained above the threshold of 100 $\Omega \cdot cm^2$. No statistically significant differences could be detected.

The release of TNFα (Figure 11) confirmed the refractoriness of respiratory epithelial cells to respond to LPS. Indeed, in both systems very low levels of TNFα could be detected in the cell free supernatants and only with the highest LPS concentration. The absence of a dose response is not surprising since such low levels approximate to background signal in ELISA and are not measured reliably. In addition, EpiAirway tissue technical replicates seem to perform better as compared to MucilAir as shown by the statistical significance reached with the highest LPS concentration, possibly due to the largest working volumes and cell numbers.

A. B.

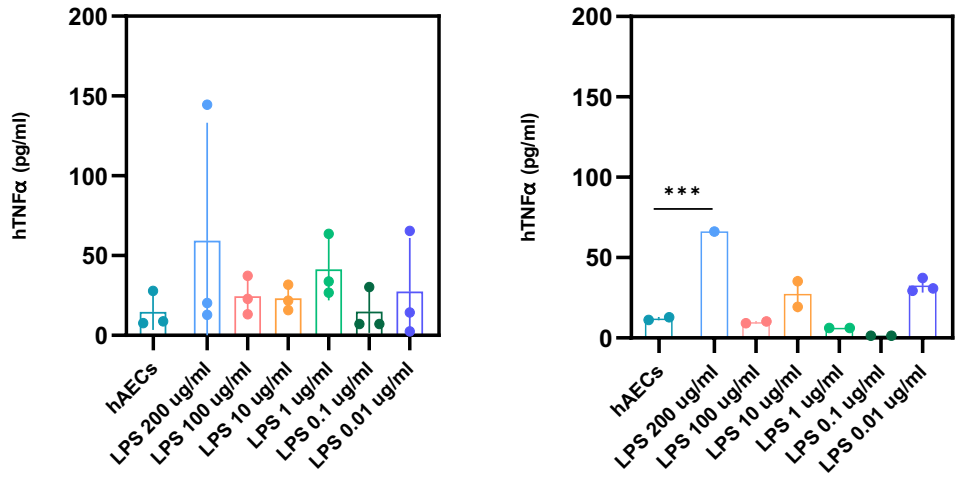

Figure 11. TNFα release after stimulation with an LPS concentration curve for MucilAir (A) and EpiAirway (B) tissue cultures. ALI tissues were exposed to 200-100-10-1-0.1-0.01 ug/ml of LPS, via the basolateral compartment, for 24 hours. The production of TNFα was evaluated by ELISA in cell-free supernatants. Statistical significance was calculated by one-way ANOVA: **** $p < 0,0001$, *** $p < 0,001$, ** $p < 0,01$ * $p < 0,05$.

1.2. Setting up of an epithelial/immune co-culture model in the ALI system

Given previous results, we reasoned that inflammation could be efficiently induced in our ALI model of airway epithelium in the presence of immune cells. Co-culturing cells in *in vitro* tissue models is widely used to study interactions between cell populations. In our setting, the presence of immune cells in the ALI model of human airway epithelium could allow to study not only the effects of inflammation, but also the relative contribution of this crucial component to cytokine production, epithelial thickening as well as targets of therapeutic strategies. However, the success of a co-culture system depends on multiple factors, which makes it a complex and sensitive task. Thus, we performed some experiments to determine appropriate conditions for airway and immune cell interaction by indirect contact. We choose to perform these experiments using peripheral blood mononuclear cells (PBMCs) which represent a rather complete immune cell population, but are also easy to obtain and to manage.

1.2.1 Defining the percentage of FBS tolerated by ALI cultures

We first performed a pilot study to assess the compatibility of MucilAir™ growth medium with PBMC medium over the course of a few days. MucilAir tissues are expanded in their custom, proprietary medium, provided by Epithelix and ready-to-use, serum free and supplemented with

growth factors (not known) and antibiotics (P/S). In contrast, the standard medium for PBMC isolation and culture is RPMI 1640, supplemented with 10% serum.

Thus, it was of critical importance understanding at what extent ALI culture could tolerate the addition of serum. Human airway epithelial cells from a healthy donor were cultures for 6 days combining custom ALI medium with 1% or 5% serum, with or without replacement every 2 days. Figure 12 shows the results of TEER measurement, with minimal differences in transepithelial resistance in all conditions. As in previous experiments, all measurements were above the minimal acceptable value of 100 $\Omega \cdot cm^2$ and no statistically significant differences could be detected. However, conditioned medium with 5% serum with replacement showed a constant decrease of TEER values in comparison with ALI medium alone and even conditioned medium with 1% serum, especially at day 6 (372 $\Omega \cdot cm^2$).

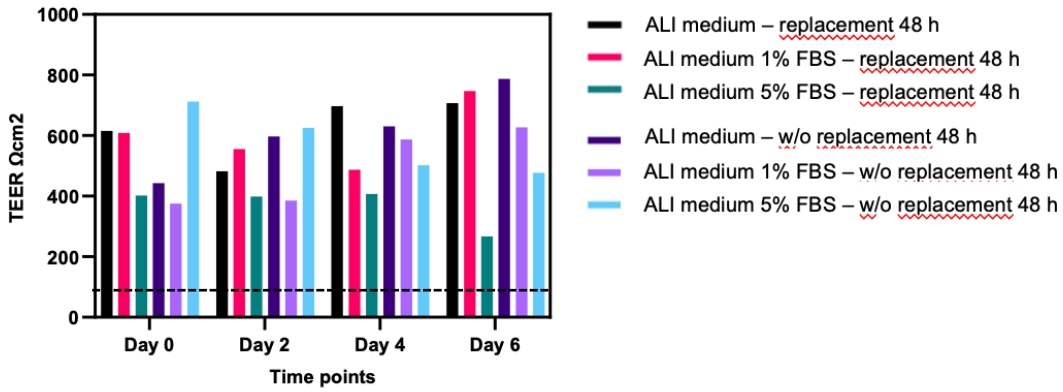

Figure 12. Measurements of transepithelial electrical resistance (TEER) affected by different conditioned medium. MucilAir tissues were exposed to two different growth media conditions (supplemented with 1-5% serum) over the course of 6 days, with or without refreshing every 2 days. Each point was performed in triplicate and TEER values are shown as the mean of the three. TEER was measured every 48 hours by using a voltohmmeter and is expressed as $\Omega \cdot cm^2$. All values remained above the threshold of 100 $\Omega \cdot cm^2$, indicating a substantial barrier integrity in all conditions. Despite fluctuations, no difference reached statistical significance.

To assess cell viability in the conditioned media we measured the release of LDH, a stable cytoplasmic enzyme rapidly released into cell culture supernatant when cell plasma membranes are damaged. Figure 13 showed a high percentage of cell viability, ranging from 93 to 98%, in all conditions. The lowest values were observed in cells cultured in conditioned media supplemented with 1-5% serum without replacement over the course of 6 days, despite the difference was not statistically significant.

Based on these experiments, we set out to adopt ALI medium 1% FBS (replaced every two days) as co-culture medium after testing its applicability to immune cell culturing.

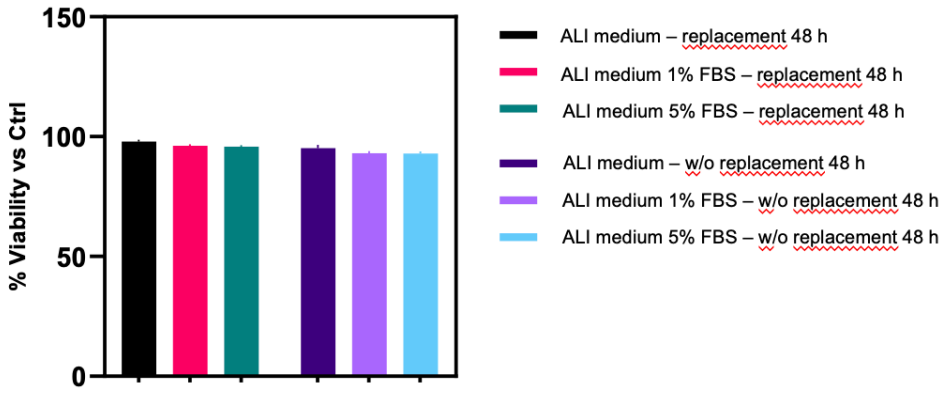

Figure 13. Percent viability of MucilAir tissues exposed to conditioned media. Cells at ALI conditions were exposed in triplicate to two different growth media conditions (supplemented with 1-5% serum) over the course of 6 days, with or without refreshing every 2 days. After 6 days, LDH release was investigated in the basolateral culture medium. LDH release is shown as percent viability as compared to the positive control of Triton-lysed cells. Data did not reach statistical significance.

1.2.2 Functional properties of cryopreserved PBMCs in co-culture medium

So far, little was known about immune cells compatibility with MucilAir culture medium. Based on previous results, we tested the performance of cryopreserved PBMC in proprietary ALI medium with 1% serum. PBMCs were thawed in conventional culture medium RPMI 10% FBS and left to recover 2 hours, then resuspended in ALI medium 1% FBS.

Figure 14 shows that ALI medium 1% FBS did not significantly impact cell viability after 24 hours of culture, a time frame adequate to investigate the induction of the immune response.

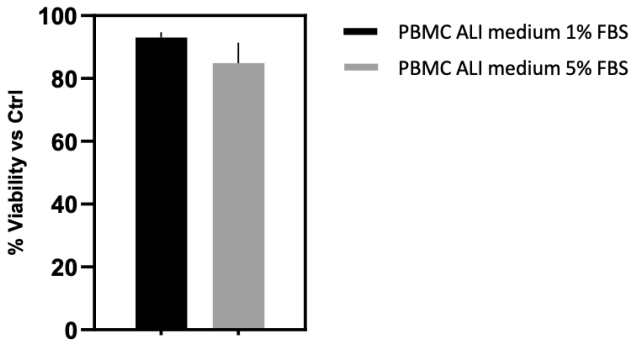

Figure 14. PBMC viability was assessed in terms of LDH release. After 24 hours of culture in the different media, LDH release was investigated in the basolateral culture medium in technical triplicates of one PBMC donor. LDH release is shown as percent viability compared to a positive control (Triton-lysed cells set to 100%). No statistically significant difference could be observed.

Functional properties of cryopreserved PBMC cultured in ALI medium 1% FBS were tested in comparison with PBMC cultured in standard conditions.

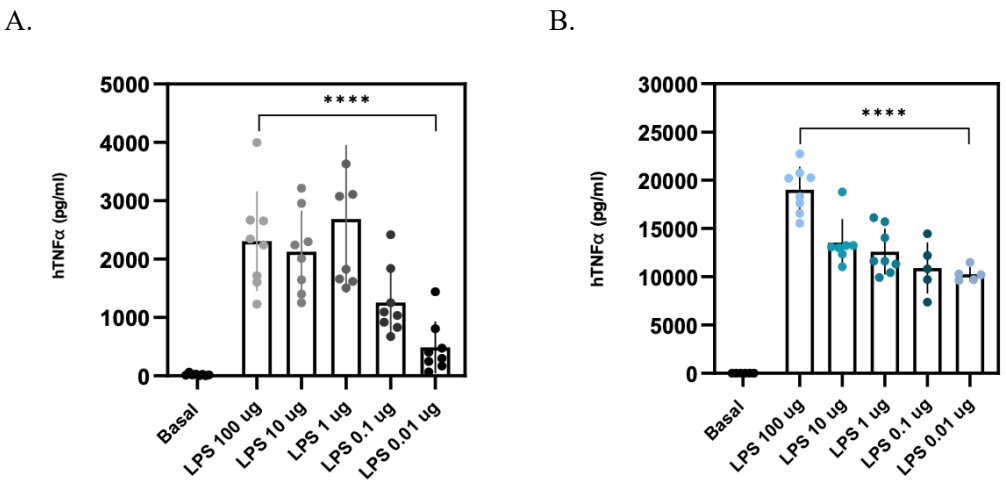

Figure 15. TNFα release after LPS titration of cryopreserved PBMCs (A) and fresh PBMCs (B). Cells were exposed to 100-10-1-0.1-0.01 ng/ml of LPS for 24 hours. The production of TNFα was evaluated in technical triplicates by ELISA in cell-free supernatants. Statistical significance was calculated by one-way ANOVA: **** $p < 0,0001$, *** $p < 0,001$, ** $p < 0,01$ * $p < 0,05$.

As expected (Figure 15. B), LPS induced a significant release of TNFα in a dose-dependent manner in fresh PBMCs. Cryopreserved PBMCs in ALI medium 1% FBS responded with lower but still significant activation (Figure 15. A), pointing out at their potential as immune cells for studying the induction of inflammation in ALI co-cultures, at least over a short time course.

1.2.3 The basolateral addition of PBMC does not alter the integrity of epithelial ALI cultures

In the next set of experiments, $1X10^5$ PBMCs were added basolaterally to each well of ALI cultures in order to characterize barrier integrity in the presence of resting immune cells. As a further comparison, we performed experiments in both 1% FBS and 5% FBS. Figure 16 shows that 5% FBS markedly decreased TEER values of both mono and co-cultures (TEER values 543 $\Omega \cdot cm^2$ and 521 $\Omega \cdot cm^2$, respectively, as compared to the serum-free cultures 1336 $\Omega \cdot cm^2$ and 994 $\Omega \cdot cm^2$), despite differences where not statistically significant and all values remained above 100 $\Omega \cdot cm^2$.

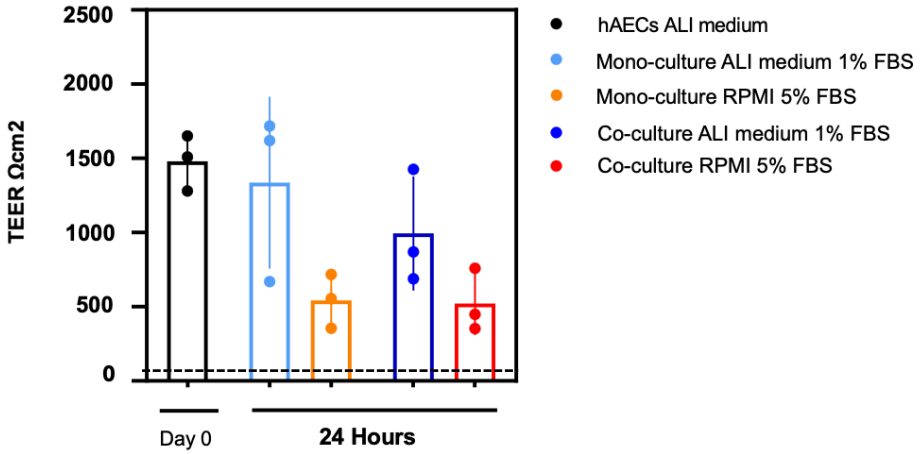

Figure 16. Transepithelial electrical resistance (TEER) measurements in mono- and co-culture in two different media conditions. MucilAir tissues were exposed to two different growth media (ALI medium and RPMI 5% serum) for 24 hours. Each point was performed in triplicate and represented as $\Omega \cdot cm^2$. Data did not reach statistical significance. In general, all values stayed above the threshold of 100 $\Omega \cdot cm^2$.

Cell viability at 24 hours was evaluated by measuring LDH release in the basolateral compartment. Figure 17 confirmed that co-culture in 1% FBS displayed slightly reduced, yet not statistically different viability in respect to mono-culture, while co-culture in 5% FBS showed a critical decrease in viability.

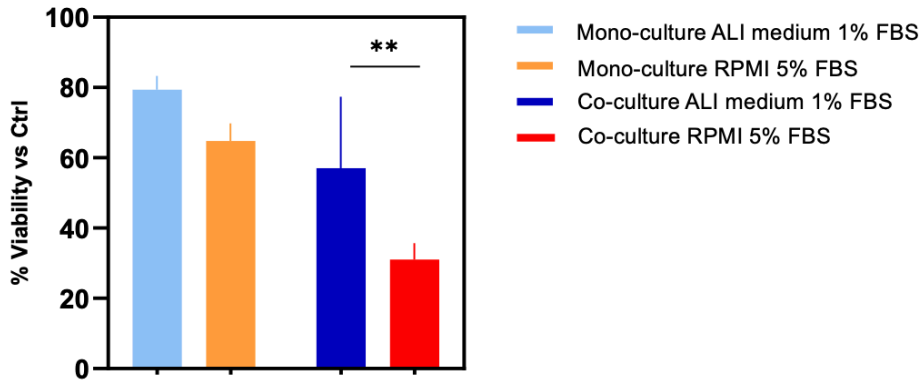

Figure 17. Percent viability of mono- and co-cultures in two different conditions at 24 hours of culture. LDH release was investigated in the basolateral culture medium in technical triplicates and shown as the mean of the three. LDH release is shown as percent viability compared to a positive control (Triton-lysed cells set to 100%). Statistical significance was calculated by one-way ANOVA: **** $p < 0,0001$, *** $p < 0,001$, ** $p < 0,01$ * $p < 0,05$.

1.3 LPS response in ALI epithelial/immune co-cultures

We set out to use our epithelial/immune ALI co-culture model to study the effect of immune-cell dependent inflammation on barrier integrity and epithelial activation in healthy and COPD samples. To this extent, we stimulated MucilAir tissues with LPS at 1 ug/ml which could efficiently activate PBMC while induce no or very weak activation in epithelial cells. Reasoning that epithelial inflammation was expected to depend largely on cytokines released by PBMCs, rather than on direct LPS stimulation, we included a later time point of 36 hours in addition to 24 hours. Barrier integrity was assessed by TEER and LDH evaluation, while activation was determined by cytokine production and release at both the mRNA and protein levels.

1.3.1 The presence of LPS-activated PBMCs does not alter barrier integrity of airway epithelial cells at ALI

Figure 18 shows that there were no significant differences observed in terms of reduced tissue barrier integrity at 24 hours in both healthy (Figure 18. A, left panel) and COPD donors (Figure 18. B, left panel). However, electrical resistance of the epithelium was significantly compromised in co-culture conditions with LPS after 36 hours of exposure (Figure 18. A, right panel). This decrease indicates that the presence of LPS, along with immune cells, impact on epithelial barrier function potentially disrupting the tight junctions that are crucial for maintaining barrier integrity. A similar trend could be observed in the COPD donor, where the lack of significance depends on the different behaviour of the two donors. More experiments are needed to ascertain if COPD tissues in this condition behave differently in respect to healthy ones. However, all values remained above the acceptable threshold of 100 $\Omega \cdot cm^2$, indicating that overall barrier integrity is not lost.

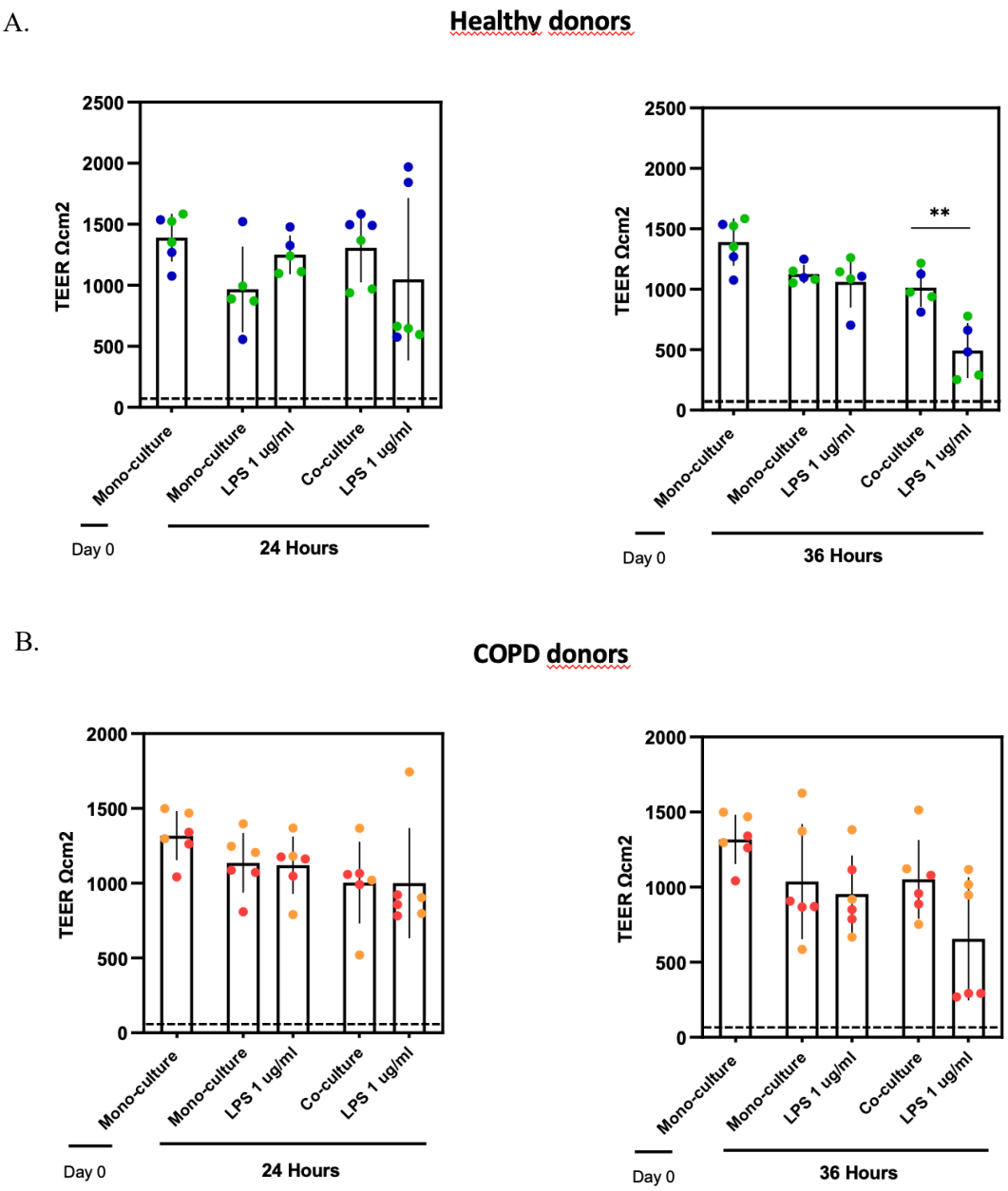

Figure 18. Measurement of transepithelial electrical resistance (TEER) across the epithelial layer at ALI in healthy (A) and COPD (B) tissues. Mono- and co-cultures of MucilAir tissues from two donors (identified by different colors) were exposed to 1 ug/ml of LPS via the basolateral compartment for 24 or 36 hours. For each donors, values were measured in triplicate wells and expressed as the mean +/-SE. TEER was measured by using a voltohmmeter and is represented as $\Omega \cdot cm^2$. Statistical significance was calculated by one-way ANOVA: **** $p < 0,0001$, *** $p < 0,001$, ** $p < 0,01$ * $p < 0,05$. All values remained above 100 $\Omega \cdot cm^2$.

Mono- and co-culture were then investigated for viability. The analysis of LDH release showed that there was no significant cell loss in either mono-culture and co-culture conditions at 24 and 36 hours, suggesting that the exposure to LPS did not grossly compromise cell survival.

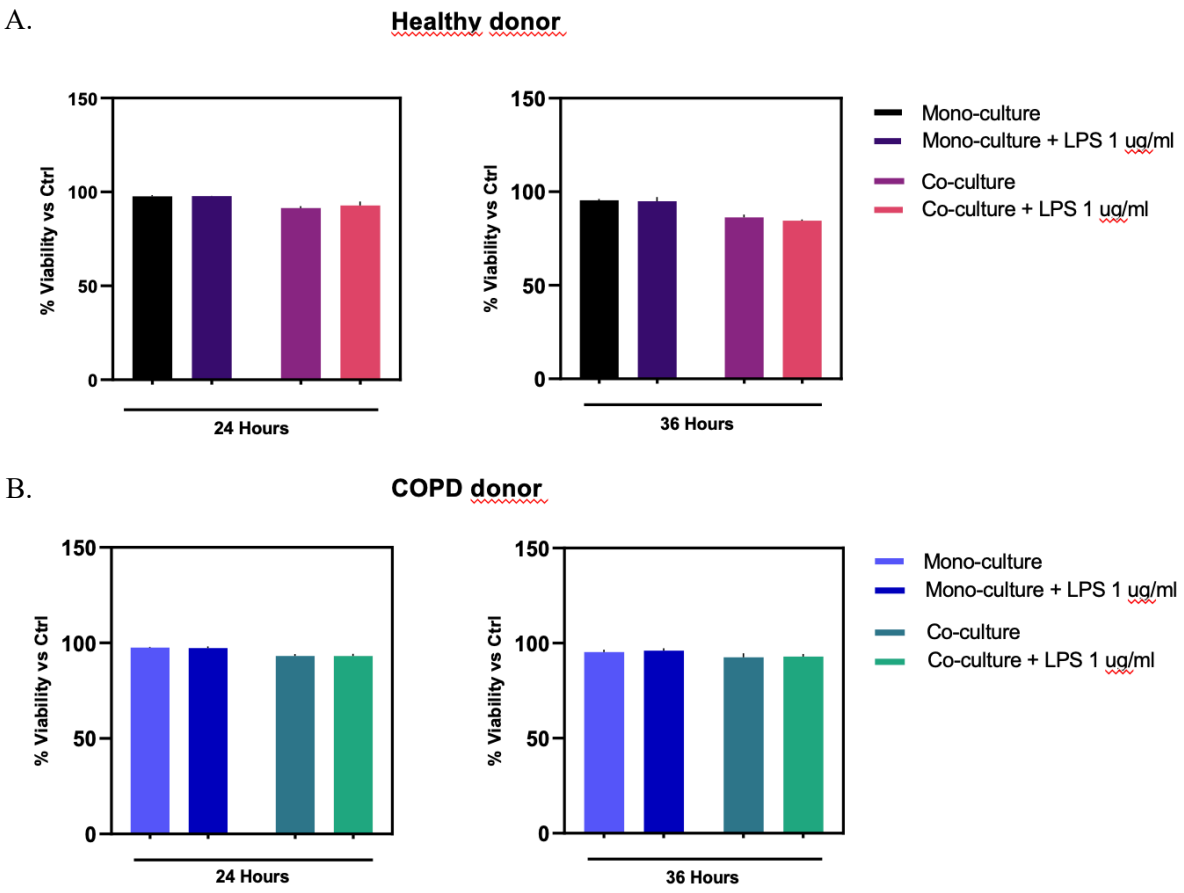

Figure 19. Evaluation of cell viability at 24 and 36 hours. Fresh supernatants from MucilAir tissues from healthy and COPD donors were harvested after stimulation with 1 ug/ml LPS at 24 hours and 36 hours. Cell viability was assessed by measuring the release of LDH. Data are expressed as mean ± SE.

1.3.2 The presence of LPS-activated PBMCs primes the transcription of selected inflammatory genes in airway epithelial cells at ALI

To assess if epithelial cells are activated following PBMC stimulation by LPS, so validating our model of immune-dependent inflammation, we collected airway epithelial cells for mRNA quantification devoid of PBMCs: indeed, these remain confined in the basolateral well compartment. In general, Figure 20 confirms our hypothesis by showing that airway cells co-cultured with PBMCs in the presence of LPS can upregulate the mRNA for inflammatory genes. This is observed for TNFα and CXCL8 in COPD samples at 24 hours, while healthy tissues appear to upregulate significantly IL-6 and CXCL8 at the later 36-hour time point. However, it is not possible to drive further conclusions concerning a potential difference in sensitivity or activation kinetic between healthy and COPD tissues because of the reduced sample size. Indeed, only two donors could be analysed for the two conditions, and some analysis could be performed with a single donor especially at 36 hours.

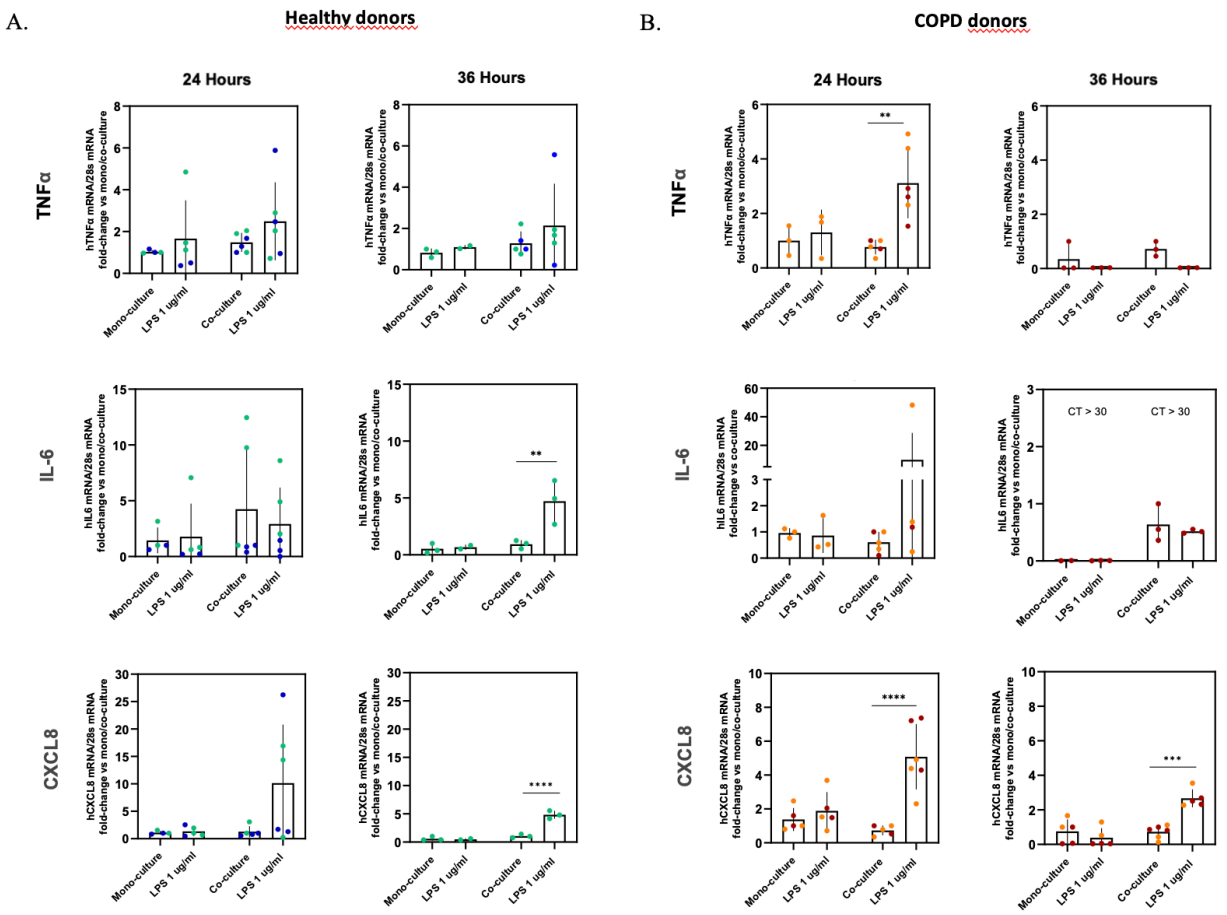

Figure 20. Quantitative analysis of TNFα, IL-6 and CXCL8 mRNA levels in epithelial cells following LPS stimulation in healthy (A) and COPD (B) donors. Mono- or co-culture of MucilAir tissues were stimulated with 1 ug/ml of LPS via the basolateral compartment for 24 or 36 hours. At the end of the stimulation, epithelial cells were harvested devoid of PBMCs and mRNA expression analysed by real-time PCR. Dots represent technical triplicates of the two healthy and COPD donors (identified by a different color) and are expressed as the mean+/-SE. Statistical significance was calculated by one-way ANOVA: **** $p < 0,0001$, *** $p < 0,001$, ** $p < 0,01$ * $p < 0,05$.

However, it is possible to point out at the reproducibility of CXCL8 induction, which may represent a good inflammatory marker in this model deserving further attention for its characterization in future experiments.

These results were confirmed at the protein level by measuring secreted cytokines in cell-free supernatants at 36 hours (Figure 21).

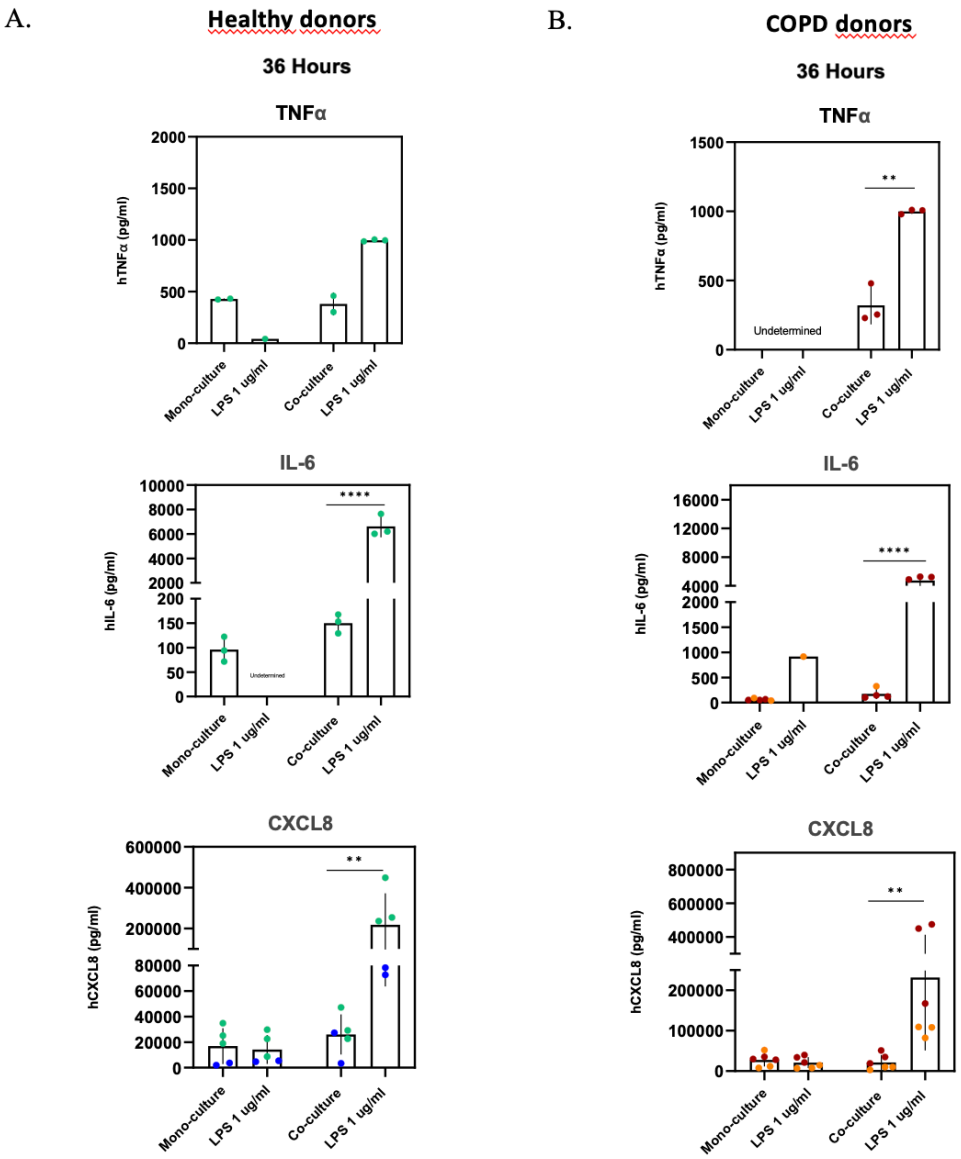

Figure 21. TNFα, IL-6 and CXCL8 release from ALI mono- and co-cultures at 36 hours. Fresh supernatants were collected from MucilAir cultures post-stimulation with 1 ug/ml of LPS. Dots represent technical triplicates of two donors for both conditions (identified by different colors) and expressed as mean+/-SE. Statistical significance was calculated by one-way ANOVA: **** $p < 0,0001$, *** $p < 0,001$, ** $p < 0,01$ * $p < 0,05$.

It must be noted, however, that in this case we detect cytokine secretion of both epithelial and immune cells, given that supernatants can freely diffuse between the compartments, which may explain apparent discrepancies with previous results.

2. Discussion

Obtaining an ALI co-culture model represents a significant advancement over traditional ALI mono-cultures and a step forward an in vitro model which more closely mirrors the respiratory environment and allows the study of the dynamics of cell-to-cell interactions in response to stimuli and treatments. However, existing literature is very limited in this regard. In our co-culture model combining 3D human airway MucilAir™ tissues and immune cells, we collected the proof of concept that the cross-talk between cells plays a crucial role in the initiation and perpetuation of the inflammatory response, a condition closely resembling COPD.

Given that 3D ALI models are conventionally cultured in serum-free medium, the initial challenge we faced was to develop an appropriate experimental setup that would support the simultaneous growth and functions of both epithelial cells and immune cells, which require medium supplemented with serum. To these end, we finally opted for the use of ALI conditioned medium with reduced serum levels, which supported immune cell viability and response over the required time frame, while minimizing potential adverse effects on epithelial barrier integrity.

As immune cells we decided to use PBMCs because previously employed in co-culture models for studying inflammation and because of their heterogeneity and representativity of different immune cell population [89]. By contrast, cryopreserved PBMCs represented a forced choice because of the limited availability of fresh patient-derived blood at Chiesi Farmaceutici R&D facility. However, we plan to refine our co-culture system by using purified immune cell populations such ad macrophages and dendritic cells, which are the most relevant sentinel cells involved in sensing inflammatory triggers and initiating the immune response. Of course, these cells are rare and often difficult to obtain in numbers adequate to the setting up of co-cultures and also display a marked sensitivity to medium requirements. However, previous work by our group demonstrated the feasibility of dendritic cell stimulation and manipulation in low serum conditions [121].

We show that mono-cultures of airway epithelial cells are very resistant to LPS, maintaining their barrier functions and scarcely inducing inflammatory genes even when stimulated with very high concentrations. It is well known that epithelial cells generally express lower levels of TLR4, the primary receptor for LPS, compared to immune cells [122] and activate downstream signaling pathways, such as NF-kB, more cautiously [123]. It was of great interest to find this refractoriness reverted in the presence of immune cells. Indeed, in co-cultures, epithelial cells increased the expression of inflammatory mediators even in the presence of much lower concentration of LPS. Since in our model airway and immune cells establish contact free interactions, we hypothesize that immune cells respond to LPS by producing inflammatory mediators which, in turn, prime epithelial

cells for inflammation by paracrine stimulation. Further work is granted to test this hypothesis for example by using blocking antibodies for different cytokines or cytokine receptors in co-cultures. In addition, it will be interesting to test the activation of co-cultures in response to inflammatory/microbial stimuli different from LPS.

As for what concerning the difference between healthy and COPD tissues, our results did not show any difference. However, the low number of available donors affected the reproducibility of some of our results and more subtle differences may emerge in future studies.

C. ALI cultures as a model to study the effects of anti-inflammatory drugs

In the final part of the thesis, we aimed at obtaining the proof of concept that our co-culture system could represent a tool to study the effects of anti-inflammatory drugs in a more physiological environment as compared to 2D culture of airway cells. To this extent, we used Tanimilast, a proprietary PDE4 inhibitor which immunomodulatory properties have been thoroughly investigated [30][67][121].

1. Results

1.1 Morphological analysis of inflamed healthy and COPD MucilAir tissues treated with Tanimilast

We analysed the morphological changes in MucilAir epithelial tissues from healthy and COPD donor following LPS stimulation and Tanimilast treatment, by using H&E (not shown) and PAS-AB (Figure 22) staining. Untreated paraffin-embedded mono-culture tissues from healthy donor (Figure 22.A upper left panel) exhibited a well-organized pseudostratified epithelium characterized by the presence of all the three main representative cellular types of the upper airway. By contrast, the co-culture tissue (Figure 22. A lower left panel) inserts at baseline already appeared thicker and exhibited milder goblet cell hyperplasia. However, the co-culture retained all the key feature observed in the untreated mono-culture, including the presence of a pseudostratified structure with cilia. Following LPS exposure, there was a notable increase in goblet cells size and number, indicative of goblet cell hyperplasia (Figure 22. A center panels). Interestingly, treatment restored the epithelial structure to a state resembling the untreated condition.

A.

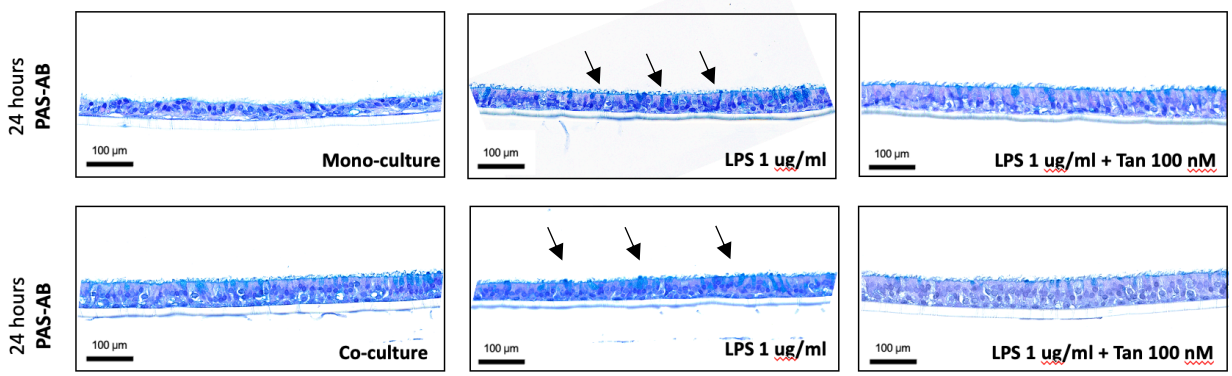

B.

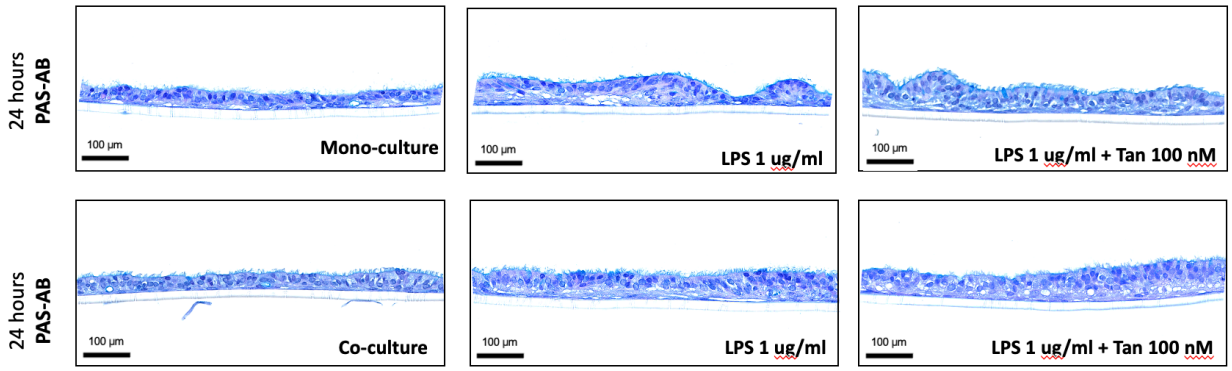

Figure 22. Images of Periodic Acid-Schiff (PAS)-Alcian blue staining of formalin-fixed paraffin-embedded sections of healthy (A) or COPD (B) mono- or co-cultures of MucilAir tissues (5 µm) grown with LPS (1 ug/ml) and Tanimilast (100 nM), for 24 hours. All cross-sectional images are oriented with the basolateral surface of the culture at the bottom of the image and the apical surface at the top of the image. Arrows show goblet cells with secretory granules. Scale bars = 100 µm.

In the COPD donor (Figure 22. B.), the effects of LPS stimulation appeared more pronounced, both in mono and co-culture, as compared to healthy donor. The epithelium became thicker and more irregular as compared to baseline conditions, but no signs of goblet hyperplasia could be detected. Treatment appeared not to yield any appreciable improvement as compared to LPS-conditions. More donors need to be analysed to ascertain if these observations reflect a property of COPD tissues or of this particular donor.

1.2 Modulation of cytokine release by Tanimilast in MucilAir™ tissues

The immunomodulatory effects of Tanimilast in LPS-stimulated mono- and co-cultures were investigated over a 24-hour period in healthy and COPD donor MucilAir™ tissues (Figure 23).

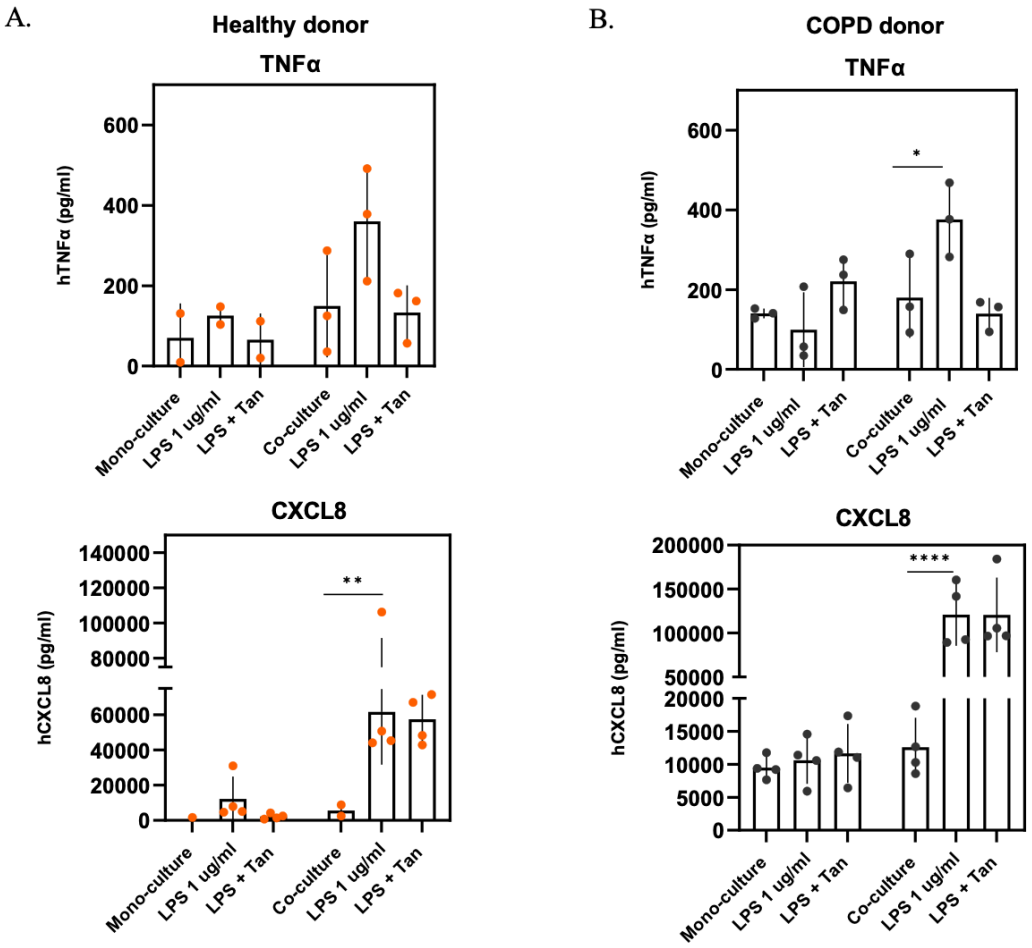

Figure 23. TNFα and CXCL8 release from healthy (A) and COPD (B) donors at 24 hours. Fresh supernatants were collected from mono- and co-cultures of MucilAir post-stimulation with 1 ug/ml of LPS, in the presence or absence of Tanimilast (100 nM). Dots represent technical replicates of one donor. Data are expressed as mean+/-SE. Statistical significance was calculated by one-way ANOVA: **** $p < 0{,}0001$, *** $p < 0{,}001$, ** $p < 0{,}01$ * $p < 0{,}05$.

As expected, both cytokines were upregulated in the LPS-stimulated co-culture. Tanimilast reverted the induction of TNFα, although the difference was not statistically significant, but could not block the induction of CXCL8.

1.3 Modulation of cytokine release by Tanimilast in EpiAirway™ tissues

The same experimental setup was reproduced in EpiAirway tissues from one healthy and four COPD donors (Figure 24). Consistent with previous observations, the mono-culture showed no significant response to LPS stimulation, while in the co-culture both cytokines were significantly induced. Tanimilast significantly reduced the release of TNFα, but not IL-6.

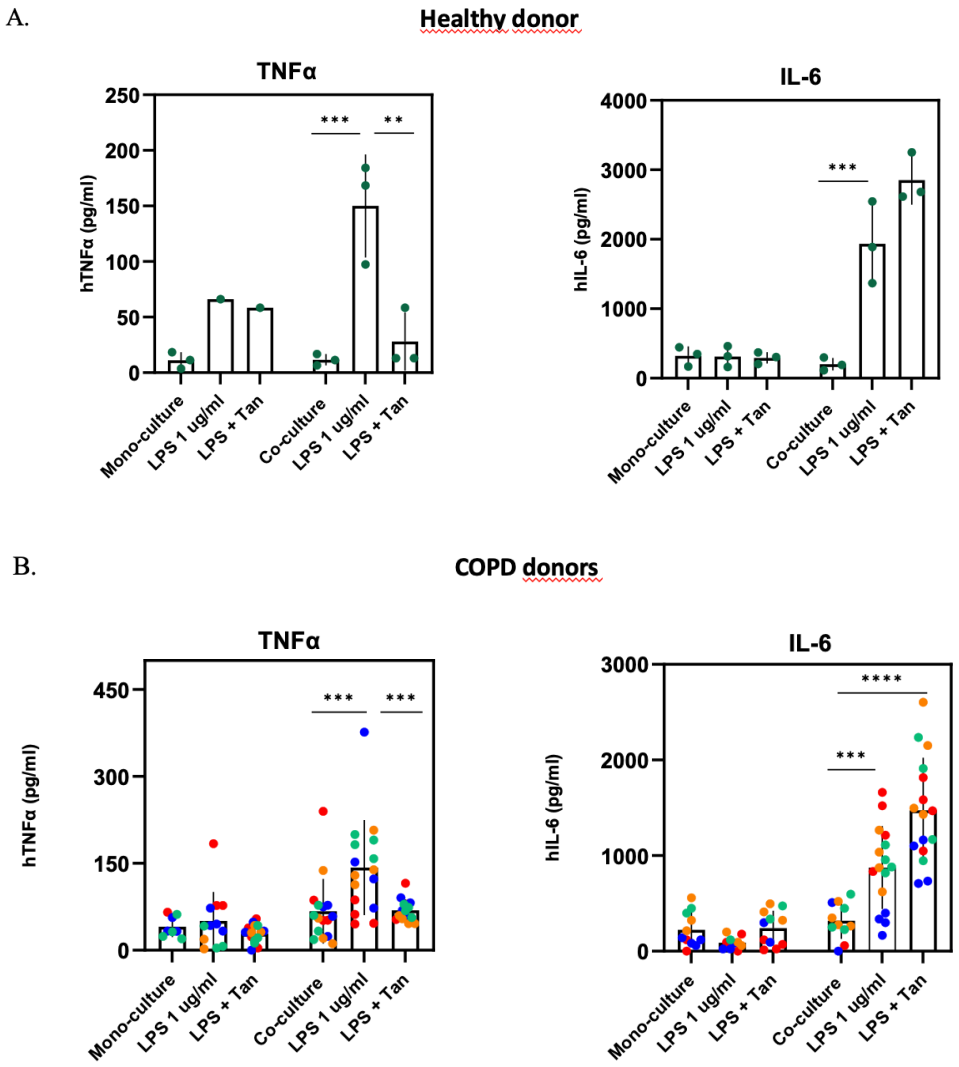

Figure 24. TNFα and IL-6 release from COPD donors in EpiAirway mono- and co-cultures. Fresh supernatants were collected from EpiAirway cultures post-stimulation with 1 ug/ml of LPS in the presence or absence Tanimilast (100 nM). Dots represents technical replicates in four different donors, identified by colours. Results are expressed as mean+/-SE. Statistical significance was calculated by one-way ANOVA: **** $p < 0,0001$, *** $p < 0,001$, ** $p < 0,01$ * $p < 0,05$.

These results, although preliminar, extend the feasibility of the co-culture model to the EpiAirway system.

2. Discussion

In this part of the thesis, we obtained preliminary evidence that our 3D co-culture systems, both from the MucilAir and the EpiAirway technologies, may represent a valuable tool to study the effects of anti-inflammatory drugs. Indeed, despite the reduced availability of donors, affecting the statistical significance and reproducibility of some results, we could demonstrate that Tanimilast can reduce the secretion of at least TNFα induced by LPS in co-cultures.

The inhibition of TNF-α secretion is a hallmark of several PDE4 inhibitors and was reported in different experimental settings: apremilast reduced the release of TNF-α in human LPS-stimulated PBMCs as well as in the murine air pouch model of inflammation [121], roflumilast in the LPS-stimulated murine macrophage cell line RAW264.7 [121], L826141 in heparinized whole human blood [121] and Tanimilast in human monocyte-derived dendritic cells [121]. Interestingly, IL-6 and CXCL8 were not inhibited by apremilast in LPS-stimulated human PBMCs [121], as well as IL-1α and IL-6 in the air pouch exudates [121], which is agreement with the lack of inhibition of IL-6 in MucilAir technology and of CXCL8 in EpiAirway tissues.

Chronic LPS exposure in vivo can induce goblet cell hyperplasia [124]. Here, we show for the first time that this effect can be induced in epithelial airway cells cultured at ALI and that Tanimilast may revert this effect, again underlining the relevance of our in vitro model. In addition, this novel role of PDE4 inhibition deserves further research to be confirmed and to address its molecular mechanisms.

We report that COPD tissues did not respond to LPS with goblet cell hyperplasia: this finding is obviously unexpected and potentially intriguing. However, the use of one single COPD donor does not allow to exclude a sample-specific behaviour or technical errors in sample manipulation. Again, further work is granted to shed light in this direction.

Last, but not least, we observed that the EpiAirway system, although less used in our study because of its cost and extended working volumes, shows a higher consistency of results among replicates and even among donors as compared to the Epithelix model, where inter-donor variability can be more pronounced. We hypothesize that this behaviour may at least partly depend on the increased working volume and tissue amount per well, which could make easier plate manipulation and subsequent sample examination. If confirmed, this increased consistency may render EpiAirway the model of choice for the future development of our co-culture models.

PART 1 CONCLUDING REMARKS

In the present part of the thesis, our work aimed at gaining proofs of concept that an epithelial/immune co-culture ALI model is feasible and applicable to the study of inflammation and anti-inflammatory drugs in in vitro settings. This is of crucial importance not only to reduce the number of in vivo experiments but also to allow more straightforward experiments, performed on human rather than on animal tissues, in which the complexity can be gradually increased. We are well aware that some of our findings remain preliminary, mostly because of the low number of tissues analysed, which in turn depends on a substantial low availability and slowliness in sample growth and preparation by the manufacturer. Nevertheless, our work represents a good starting point for future developments of this technique, paving the way to a more efficient, fast, and less expensive drug discovery to treat inflammatory diseases of the respiratory tract.

PART II

The overlap between COPD and asthma, commonly referred to as ACOS (Asthma-COPD Overlap Syndrome), presents a complex and often severe inflammatory profile [125]. This overlap condition combines various cardinal features of COPD (irreversible airflow limitation and neutrophilic/type-1/-17 inflammation) and of mild/moderate allergic asthma (reversible airflow limitation and eosinophilic/type-2 inflammation). Targeting alarmins in ACOS is increasingly recognized as an essential strategy due to their role as primary triggers of inflammation, bridging the pathological mechanisms found in both COPD and asthma [59]. In particular, TSLP has garnered significant attention in recent years for its ability in promoting the Th2-type response through upregulation of OX40L on dendritic cells, and through direct induction of IL-4 production in naïve $CD4^+$ T cell, even amidst a background of Th1- and Th-17 inflammation [106]. Dendritic cells (DCs) represent a specialized population of antigen presenting cells and their role in asthma pathology has been well recognized due to their capability to initiate and to maintain the allergen-triggered Th2 response in several *in vitro* and *in vivo* models [94]. TSLP-activated DCs potently prime naïve $CD4^+$ T cell towards an inflammatory T helper type 2 cell response [106].

The importance of inhibiting TSLP lies in the potential to halt the inflammatory cascade at an early stage, addressing the root of inflammation rather than its symptoms alone. Unlike therapies that act downstream, such as corticosteroids, PDE4 inhibitors could reduce the activation and recruitment of Th2 cells and other immune players. Tanimilast is an inhaled and selective PDE4 inhibitor, currently in advanced development (phase III) for the treatment of COPD that is poorly controlled by standard-of-care therapies, including glucocorticoids. However, its therapeutic potential in asthma is still under investigation.

RESULTS

Immunomodulatory effects of Tanimilast on TSLP-activated DCs

1. Results

1.1 TSLP does not induce moDCs activation

The effect of Tanimilast on TSLP-activated DC was first investigated on monocyte-derived dendritic cells (moDCs), an inflammatory subset of DCs shown to play critical part in ACOS. moDCs were previously used in several *in vitro* studies to investigate the immunomodulatory effects of PDE4i on DC functionality. Thus, we investigated whether TSLP could activate moDCs by measuring its capacity to induce moDC phenotypic maturation, characterized by the upregulation of costimulatory molecules CD80 and CD86.Immature moDCs were stimulated with TSLP or LPS (control stimulus) and DC activation was examined by analysing the induction of costimulatory molecules. Figure 1. A showed that, as expected, LPS upregulated membrane expression of both CD80 and CD86 but no induction was detected in TSLP-stimulated DC.

We subsequently examined the effect of TSLP on the capability of moDCs to activate naïve $CD4^+$ T-cells proliferation by performing an allogenic mixed lymphocyte reaction (MLR) assay. In accordance with the data about phenotypic maturation, LPS-treated moDC induced a strong T-cell proliferation while T-cells remained in a non-proliferative state when co-cultured with TSLP-stimulated moDCs. No T-cell proliferation was obtained by co-culture with immature moDC(Figure 1. B). Finally, using the same experimental approach, we analysed if TSLP-stimulated moDC can affect CD4+ T cell polarization. $CD4^+$ T cell polarization was evaluated in terms of cytokine production: IFNγ for Th-1 response and IL-13 for Th-2 response. As shown in Figure 1. C, TSLP-stimulated moDCs did not induce T-cell production of IFNγ or IL-13 cytokines, while, LPS-stimulated moDCs promoted the production of IFN-gamma, as expected.

Taken together, these findings suggested that TSLP could not activate moDCs and that this subset was not an appropriate model to investigate the effects of PDE4i on biological activities of DCs in response to TSLP.

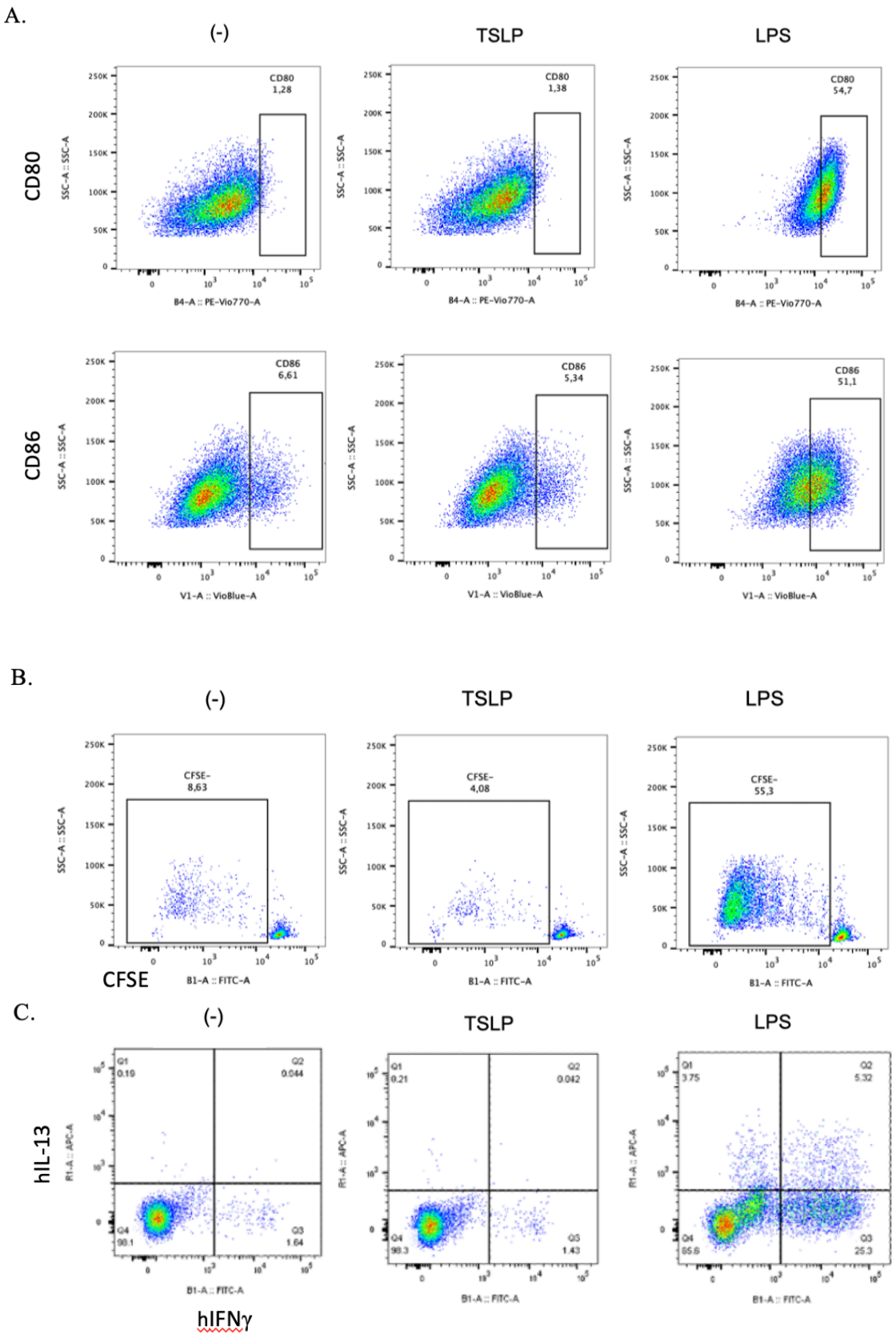
A.
(-)
TSLP
LPS
CD80
CD86
CD80 1,28
CD80 1,38
CD80 54,7
CD86 6,61
CD86 5,34
CD86 51,1
SSC-A :: SSC-A
B4-A :: PE-Vio770-A
V1-A :: VioBlue-A
B.
CFSE- 8,63
CFSE- 4,08
CFSE- 55,3
CFSE
B1-A :: FITC-A
C.
hIL-13
hIFNγ
R1-A :: APC-A
Q1 0.19
Q2 0.044
Q4 98.1
Q3 1.64
Q1 0.21
Q2 0.042
Q4 98.3
Q3 1.43
Q1 3.75
Q2 5.32
Q4 65.6
Q3 25.3

Figure 1. TSLP does not induce moDC activation. A: moDCs were stimulated for 24 hours with TSLP, LPS or vehicle (-) as indicated and the surface expression of CD80 and CD86 were evaluated by flow cytometry. B-C: Allogenic naïve T were stained with CFSE and then co-cultured with vehicle- (-), TSLP- or LPS-treated moDCs. After 6 days, T cell proliferation was assessed by measuring the loss of the dye CFSE using flow cytometry (B) and $CD4^+$ T cell polarization was evaluated by analysingIL-13 and IFNγ positive cells by intracellular staining (C). Representative dot plots from 3-4 different donors are shown.

1.2 TSLP-induced activation of mDCs

Several studies have demonstrated that TSLP can activate primary myeloid DC (mDC) (124). Therefore, we addressed TSLP ability to activate mDCs by analysing the phenotypic maturation profile, characterized by the upregulation of co-stimulatory molecule CD86 and the expression of Ox40L, a positive signal for Th2 differentiation. After 24 hours of treatment, CD86 membrane expression in mDCs was upregulated by TSLP. Interestingly, in this cell type (at difference with moDCs) also Tanimilast alone strongly increased the expression of CD86. The combination of the two stimuli further stimulated its expression, in line with previous results with moDCs activated by TLR ligands [121][125]. As expected, pretreatment with budesonide down-regulated CD86 expression induced by TSLP (Figure 2. A). In contrast, TSLP could not induce Ox40L in mDCs both at 24 and 48 hours of treatment. Tanimilast potently upregulated Ox40L both alone and, especially at 48 hours, in combination with TSLP (Figure 2. B).

A.

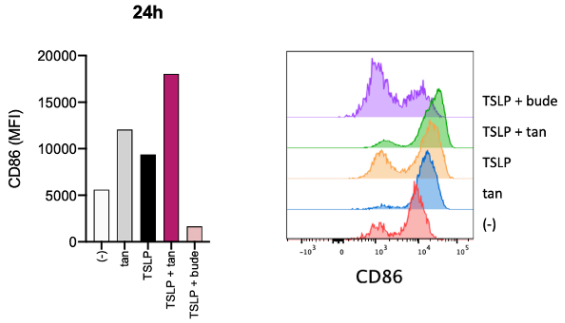

B.

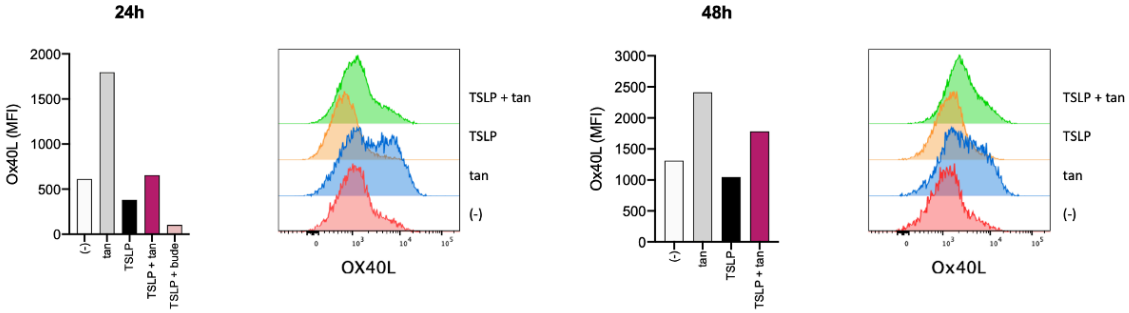

Figure 2. mDC phenotypic maturation profile. Effect of Tanimilast on mDC phenotypic maturation induced by TSLP (A, B) moDCs were pre-treated or not (-) with either Tanimilast (Tan) or budesonide (bude) (both at 10-7M) for 1 hour and subsequently stimulated or not with TSLP for the indicated time. The surface expression of the activating markers CD86 (A) and OX40L (B) were evaluated by FACS analysis. Data are expressed as representative cytofluorimetric profiles (right panels) and as the mean of the Median Fluorescence Intensity (MFI) from two independent donors (left panels).

1.3 Modulation of cytokine release in TSLP-stimulated mDCs

We also investigated the expression of the inflammatory C-C class chemokines 17 (CCL17) and 22 (CCL22) and of CXCL8 that have been detected in different lung pathologies associated to a Th2 profile [67][121]. Results in Figure 3. A show that TSLP induced the secretion of CCL17, CCL22 and CXCL8 by mDC, with no significant modulation by Tanimilast. Instead, budesonide, used as control, depressed cytokine production induced by TSLP (Figure 3. A, B). Figure 3 also suggest that the very variable net amount of secreted cytokine among different healthy donors may cause a high dispersion of the data and hamper statistical significance even if the observed phenomenon is strongly reproducible among different donors (Figure 3. A). Indeed, when data are normalized on maximal

cytokine secretion for each donor, intrinsic variability is removed and the statistical significance can be appreciated (Figure 3. B).

Overall, Tanimilast alone was shown to prompt the expression of the attracting Th2 effector cells CCL22 (MDC) and appeared to depress basal asthma-promoting mediator CXCL8.

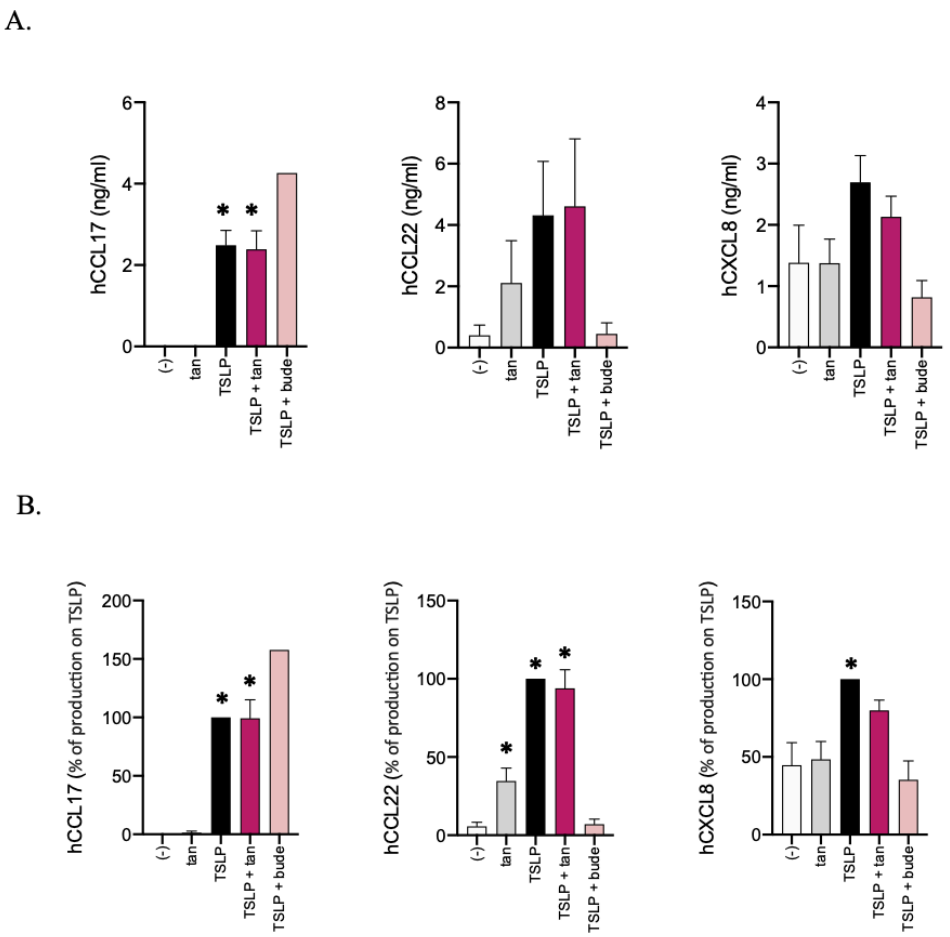

Figure 3. Cytokine profile in TSLP-stimulated mDCs. mDC were treated as indicated for 24h. Cytokine production was evaluated by ELISA and reported ng/ml (A) or as % of production on TSLP (B) Results are expressed as the mean±SEM (n=5-7).

1.4 Tanimilast does not affect $CD4^+$ T cell proliferation induced by TSLP-activated mDCs

The effect of Tanimilast on the ability of TSLP-activated mDCs to induce $CD4^+$ T-cell proliferation was evaluated by MLR experiments. (Figure 4). Co-culture of TSLP-activated mDC with allogenic CD4+ T cells promoted T cell proliferation, especially at DC:T ratio 1:20 and 1:40. mDC pretreatment with Tanimilast did not affect the ability of TSLP-activated mDC to induce $CD4^+$ T cell proliferation,

which was completely inhibited when TSLP-activated mDC were pre-treated with budesonide. Tanimilast alone did not induce T cell-proliferation.

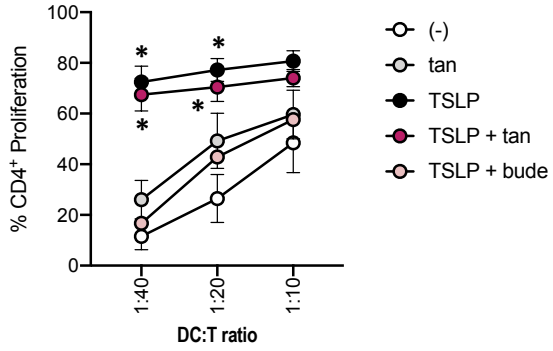

Figure 4. Tanimilast did not affect $CD4^+$ T cell proliferation induced by TSLP-activated mDCs. mDCs were stimulated with TSLP in the presence or absence of Tanimilast or budesonide. After 24h, TSLP-treated mDCs were co-cultured with CFSE-stained allogenic $CD4^+$ T cells for 6 days at the indicated DC:T ratio. Alloreactive T cell proliferation was assessed by measuring CFSE dye loss by flow cytometry. Results are expressed as the mean±SEM of the percentage of proliferated $CD4^+$ T cell (n=4).

1.5 Effects of Tanimilast on Th2 polarization induced by TSLP-activated mDCs

Next, we examined the effects of Tanimilast on the ability of TSLP-activated mDCs to promote T-cell polarization, as assessed in terms of IL-13 and IFNγ intracellular accumulation. TSLP-activated mDCs promoted an increase in the $IL\text{-}13^+$ population, indicating a Th2 polarization. Pretreatment with Tanimilast did not reduce, but rather increased the percentage of IL-13-expressing T-cells as shown by the statistical significance at lower DC:T ratios. Budesonide did not modify the percentage of $IL\text{-}13^+$ cells, however statistics could not be performed because of the limited number of available samples in this experimental condition (Figure 5. A, B). The $IFN\gamma^+$ population was unaffected even at lower ratios (Figure 5. A, C).

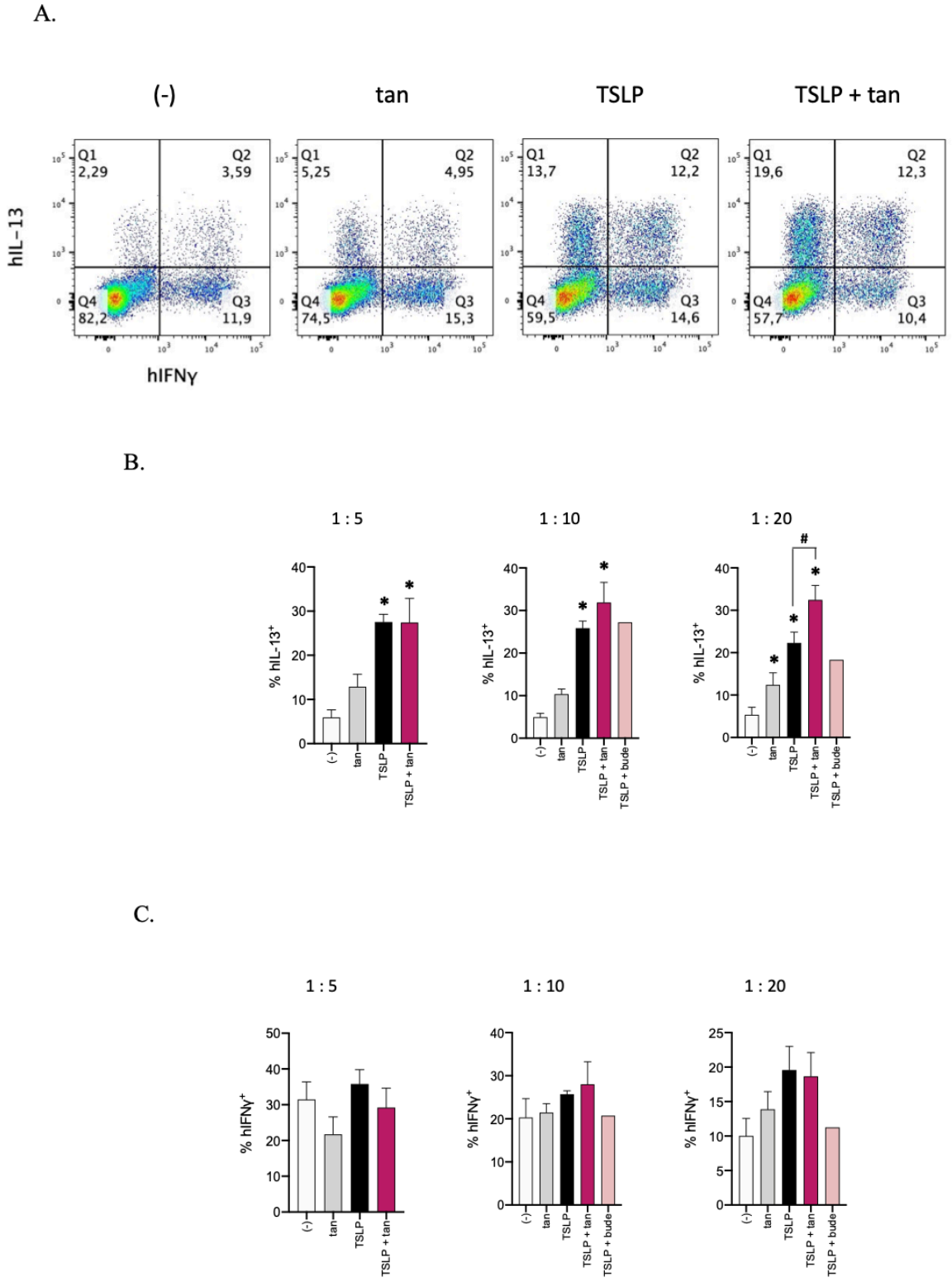

Figure 5. Tanimilast did not affect the Th2 polarization induced by TSLP-activated mDCs IL-13 and IFNγ production was evaluated by intracellular staining after 6 days of mDC-T cell co-culture at the indicated DC:T ratio. (A) Dot plot from one representative experiment. (B)Percentage of IL-13-producing T cells. (C) Percentage of IFNγ-producing T cells. Cumulative results are expressed as the mean±SEM (n=5/2).

1.6 Effects of Tanimilast on the production of TNFα and IL-10 by Th2 effector cells

We next explored if Tanimilast may affect the Th2 polarization induced by TSLP, by skewing Th2 cells towards a regulatory and anti-inflammatory phenotype, allowing to categorize them as "regulatory Th2" according to what proposed by Ito and colleagues [106]. To this aim, we used the same experimental approach, and analyzed the CD4+T cell production of TNFα and IL-10, which can indicate an inflammatory vs immunomodulatory Th2 phenotype, respectively. Pretreatment with Tanimilast did not modify the ability of TSLP-activated mDC to promote TNF-alpha production by T cells (Figure 6. A, B). In accordance with the potent inhibitory effect of budesonide on mDC activation and T cell proliferation, pretreatment with budesonide led to a reduction in this percentage, although statistical significance for this sample could not be assessed due to the limited number of available replicates (Figure 6. A, B). Importantly, in this experimental setting, we could not detect the intracellular accumulation of IL-10. Thus, we decided to repeat this set of experiments by a different approach, i.e. the detection of secreted TNFα and IL-10 by sandwich Elisa on the co-culture supernatants.

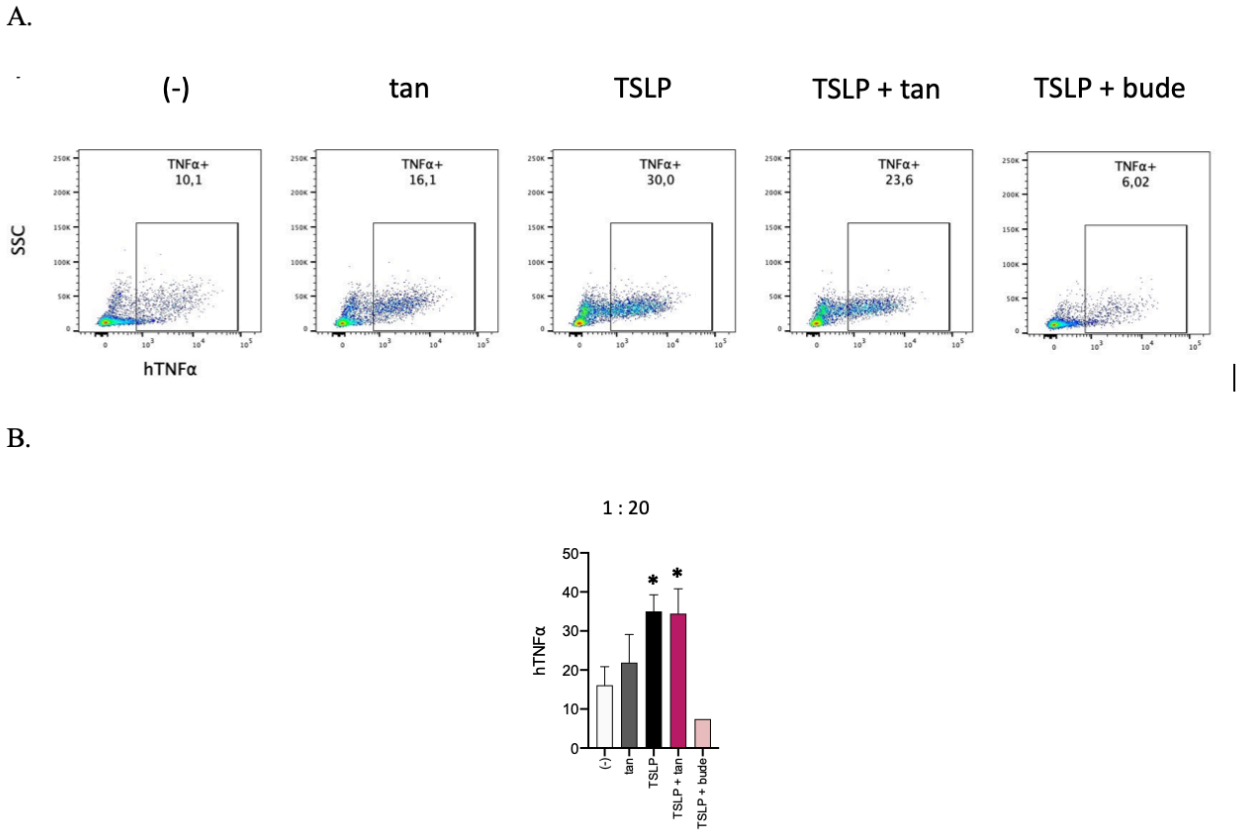

Figure 6. Tanimilast did not affect the ability of TSLP-activated mDC to induce TNFα production by Th2 cells. TNFα production was evaluated by intracellular staining and flow cytometry analysis after 6 days of mDC/T-cell co-culture at

the indicated DC:T ratio. (A) Dot plot from one representative experiment. (B) Percentage of TNFα-producing T cells expressed as the mean±SEM (n=7/3).

The analysis of total cytokine production during MLR by sandwich Elisa was chosen as an alternative approach to intracellular staining not only because it offers higher resolution to detect even minimal amounts of cytokines produced asynchronously by small percentages of cells (which may explain the failure to detect intracellular IL-10), but also to gain a fuller insight into TNFα production. The Elisa technique allows for the capture of TNFα production cumulatively over time, as opposed to intracellular staining, which provides a snapshot of cells producing a particular cytokine at a single point in time. However, Elisa results confirmed that Tanimilast did not significantly down-regulate the release of TNFα by Th2 cells stimulated by TSLP-activated mDCs (Figure 7. A). Considering that IL-10 is a cytokine that is released at relatively late time points, experiments were repeated at a later time point. On Day 6 of co-culture the cells were stimulated for 24 hours with PMA/Ionomycin with the aim of better capturing IL-10 release. Results show that, as expected, Th2 cells stimulated by TSLP-activated mDCs significantly downregulate IL-10 production and that pretreatment with tanimilast is not able to rescue IL-10 secretion by Th2 cells (Figure 6. B). Despite budesonide cannot be considered a real control because its effects in these experimental conditions have not been characterized, it makes sense that it reverted TNFα release. In contrast, the biological significance of the reduction in IL-10 secretion following pre-treatment with budesonide remains to be addressed.

A.

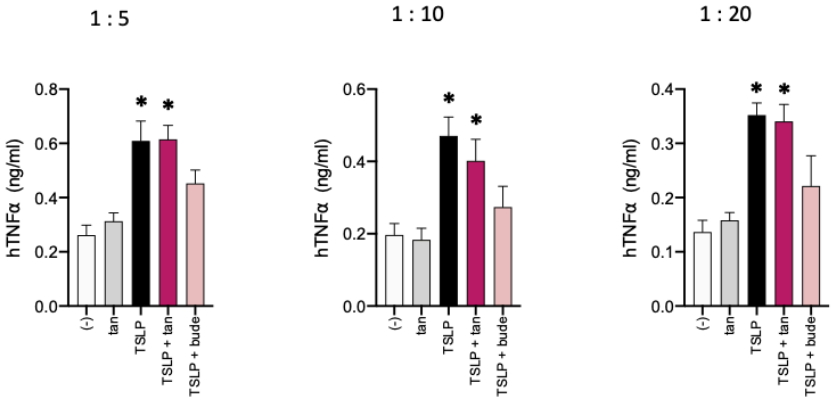

B.

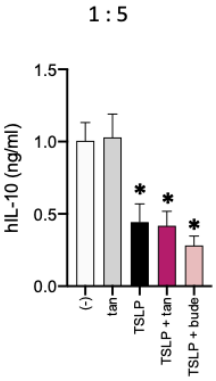

Figure 7. Tanimilast did not affect TNFα and IL-10 secretion in MLR supernatants. Cytokine secretion was evaluated by ELISA. TNFα (A) production was analysed after 6 days of mDC/T-cell co-culture at DC:T ratio 1:5, 1:10 and 1:20 as indicated. IL-10 (B) secretion was measured after 6 days of mDC/T-cell co-culture at DC:T ratio 1:5 with PMA/Ionomycin re-stimulation. At higher DC:T ratios IL-10 could not be detected. Results are expressed as the mean±SEM (n=4/3)

2. Discussion

The pivotal role of TSLP in inflammatory responses has been extensively studied. It is known that TLSP controls allergic Th2 responses through the induction of distinct activation programs in DCs [126]. We initially conducted experiments to assess whether TSLP was able to activate moDCs, which have been extensively used in previous studies [30][66][67][121]. Given the role of TSLP in modulating immune responses, we hypothesized that it could potently induce the activation of moDCs, which are crucial in initiating and perpetuating immune responses. However, our results indicated that TSLP did not activate moDCs as we expected. Despite the known ability of TSLP to drive the maturation of DCs to promote T-cell differentiation, we did not observe any significant phenotypic changes in moDCs following TSLP stimulation, as compared to LPS. There was no upregulation of the activation markers CD80 and CD86, nor was there any detectable increase in T-cell proliferation and cytokine production. These findings led us to reconsider the use of moDCs in subsequent experiments, as they may not be the ideal model for studying TSLP effects. Based on data in the literature demonstrating that TSLP potently activated mDCs to upregulate major histocompatibility classes I and II and costimulatory molecules CD40, CD80, CD83 and CD86 [106], we decided to investigate the immunomodulatory effects of Tanimilast on mDCs stimulated with TSLP to eventually provide evidence for its potential use in the management of airway respiratory diseases via the modulation of DC functions. Importantly, TSLP has been shown to induce activation of these cells, promoting the secretion of pro-inflammatory cytokines and enhancing their capacity to prime T cells towards a Th2-polarized immune response. Thus, we demonstrated that mDCs are responsive to TSLP, as shown by the induction of CCL17, CCL22 and CXCL8 expression, and the upregulation, although mild, of the costimulatory molecule CD86. Our findings also suggest that Tanimilast enhanced the activity of TSLP by potentiating CD86 expression. By contrast, budesonide downregulated CD86 and restored basal levels of CCL22 and CXCL8.

By performing MLR experiments, we revealed that TSLP-activated mDCs induced T-cell proliferation, which was not affected by Tanimilast pretreatment, and that it was completely inhibited by mDC pretreatment with budesonide. Hence, our results indicated that TSLP-activated mDCs in the presence of the PDE4 inhibitor fully retained the capability to stimulate T-cell proliferation as compared to the glucocorticoid. Notably, TSLP-activated mDCs promoted Th2 polarization in terms of increased IL-13^{+} cells. Pretreatment with Tanimilast did not reduce this percentage, nor did it affect the polarization of IFNγ-producing cells thus demonstrating its capacity to maintain Th2 response. This finding confirmed previous data demonstrating that Tanimilast in LPS-stimulated moDCs skewed T-cells towards a Th2 phenotype without affecting T-cell proliferation, but enhancing the

development of T-cells producing IL-13, while budesonide significantly reduced the percentage of proliferating cells [67].

Tanimilast ability to induce OX40L expression on mDC prompted us to investigate if Tanimilast could skew Th2 cells toward a regulatory phenotype characterized by a reduced production of TNF-alpha and an increased production of IL-10 [106].

Our data showed that Tanimilast could not decrease TNFα expression, nor restore IL-10 basal levels suggesting that Tanimilast is not able to modulate the TSLP-driven Th2 response towards a regulatory phenotype.

A great challenge in our study has been the very variable behavior of freshly-isolated primary mDCs. Indeed, these cells displayed ample donor-to-donor variation in baseline activation status, leading to fluctuations between individual results and sometimes even contrasting results. Further complicating the model, MLR experiments require a combination of these primary cells with freshly isolated T-cells from different donors, thus amplifying donor-related variation. Indeed, we observed that some mDCs basally induced the production of IFNγ by T-cells, a condition that physiologically reduces the percentage of Th2 cells, while others were neutral at steady state. Another serious limitation of our study was represented by the low amount of mDCs isolated from each blood donation, which was approximately around 2 million cells as compared to the tens of millions of moDCs used in our previous experiments, that unfortunately failed to respond to TSLP. This low number of available mDCs limited the number of conditions that could be included in each experiment and further limited intracellular staining as conditions for staining vary for different cytokines, thus requiring a higher number of cells.

The data presented here demonstrated the ability of Tanimilast to maintain or even potentiate the Th2-skewing induced by mDCs activated by TSLP, despite donor-to-donor variability amplified by experimental limitations based on the use of primary mDCs rather than mDCs differentiated *in vitro* from monocytes. Expanding the donor pool would allow for a more comprehensive analysis of Tanimilast effects and help to minimize the variability observed between individual responses by enhancing the robustness and generalizability of our findings. By limiting the impact of inter-donor variability, we could strengthen the overall reproducibility of the data, thereby providing a clearer understanding of the immunomodulatory potential of Tanimilast in the context of TSLP stimulation and its therapeutic value in both COPD and asthma.

BIBLIOGRAPHY

1. Christenson, S. A., Smith, B. M., Bafadhel, M., & Putcha, N. (2022). Chronic obstructive pulmonary disease. In *The Lancet* (Vol. 399, Issue 10342, pp. 2227–2242). Elsevier B.V. https://doi.org/10.1016/S0140-6736(22)00470-6

2. Boers, E., Barrett, M., Su, J. G., Benjafield, A. v., Sinha, S., Kaye, L., Zar, H. J., Vuong, V., Tellez, D., Gondalia, R., Rice, M. B., Nunez, C. M., Wedzicha, J. A., & Malhotra, A. (2023). Global Burden of Chronic Obstructive Pulmonary Disease Through 2050. *JAMA Network Open*, *6*(12), E2346598. https://doi.org/10.1001/jamanetworkopen.2023.46598

3. Lin, C. H., Cheng, S. L., Chen, C. Z., Chen, C. H., Lin, S. H., & Wang, H. C. (2023). Current Progress of COPD Early Detection: Key Points and Novel Strategies. In *International Journal of COPD* (Vol. 18, pp. 1511–1524). Dove Medical Press Ltd. https://doi.org/10.2147/COPD.S413969

4. Barnes, P. J. (2019). Inflammatory endotypes in COPD. In *Allergy: European Journal of Allergy and Clinical Immunology* (Vol. 74, Issue 7, pp. 1249–1256). Blackwell Publishing Ltd. https://doi.org/10.1111/all.13760

5. Szalontai, K., Gémes, N., Furák, J., Varga, T., Neuperger, P., Balog, J., Puskás, L. G., & Szebeni, G. J. (2021). Chronic obstructive pulmonary disease: Epidemiology, biomarkers, and paving the way to lung cancer. In *Journal of Clinical Medicine* (Vol. 10, Issue 13). MDPI. https://doi.org/10.3390/jcm10132889

6. Rodrigues, S. de O., da Cunha, C. M. C., Soares, G. M. V., Silva, P. L., Silva, A. R., & Gonçalves-De-albuquerque, C. F. (2021). Mechanisms, pathophysiology and currently proposed treatments of chronic obstructive pulmonary disease. In *Pharmaceuticals* (Vol. 14, Issue 10). MDPI. https://doi.org/10.3390/ph14100979

7. Kim, V., Oros, M., Durra, H., Kelsen, S., Aksoy, M., Cornwell, W. D., Rogers, T. J., & Criner, G. J. (2015). Chronic bronchitis and current smoking are associated with more goblet cells in moderate to severe COPD and smokers without airflow obstruction. *PLoS ONE*, *10*(2). https://doi.org/10.1371/journal.pone.0116108

8. Li, C. L., & Liu, S. F. (2024). Exploring Molecular Mechanisms and Biomarkers in COPD: An Overview of Current Advancements and Perspectives. In *International Journal of Molecular Sciences* (Vol. 25, Issue 13). Multidisciplinary Digital Publishing Institute (MDPI). https://doi.org/10.3390/ijms25137347

9. Guo, P., Li, R., Piao, T. H., Wang, C. L., Wu, X. L., & Cai, H. Y. (2022). Pathological Mechanism and Targeted Drugs of COPD. In *International Journal of COPD* (Vol. 17, pp. 1565–1575). Dove Medical Press Ltd. https://doi.org/10.2147/COPD.S366126

10. D'Armiento JM, Goldklang MP, Hardigan AA, et al. Increased matrix metalloproteinase (MMPs) levels do not predict disease severity or progression in emphysema. PLoS One. 2013;8(2):e56352.

11. O'Donnell, C., Newbold, P., White, P., Thong, B., Stone, H., & Stockley, R. A. (2010). 3-chlorotyrosine in sputum of COPD patients: Relationship with airway inflammation. *COPD: Journal of Chronic Obstructive Pulmonary Disease*, *7*(6), 411–417. https://doi.org/10.3109/15412555.2010.528086

12. Finicelli, M., Digilio, F. A., Galderisi, U., & Peluso, G. (2022). The Emerging Role of Macrophages in Chronic Obstructive Pulmonary Disease: The Potential Impact of Oxidative Stress and Extracellular Vesicle on Macrophage Polarization and Function. In *Antioxidants* (Vol. 11, Issue 3). MDPI. https://doi.org/10.3390/antiox11030464

13. Nurwidya, F., Damayanti, T., & Yunus, F. (2016). The role of innate and adaptive immune cells in the immunopathogenesis of chronic obstructive pulmonary disease. In *Tuberculosis and Respiratory Diseases* (Vol. 79, Issue 1, pp. 5–13). Korean National Tuberculosis Association. https://doi.org/10.4046/trd.2016.79.1.5

14. Alfahad, A. J., Alzaydi, M. M., Aldossary, A. M., Alshehri, A. A., Almughem, F. A., Zaidan, N. M., & Tawfik, E. A. (2021). Current views in chronic obstructive pulmonary disease pathogenesis and management. In *Saudi Pharmaceutical Journal* (Vol. 29, Issue 12, pp. 1361–1373). Elsevier B.V. https://doi.org/10.1016/j.jsps.2021.10.008

15. Christenson, S. A., Smith, B. M., Bafadhel, M., & Putcha, N. (2022). Chronic obstructive pulmonary disease. In *The Lancet* (Vol. 399, Issue 10342, pp. 2227–2242). Elsevier B.V. https://doi.org/10.1016/S0140-6736(22)00470-6

16. Calderon, A. A., Dimond, C., Choy, D. F., Pappu, R., Grimbaldeston, M. A., Mohan, D., & Chung, K. F. (2023). Targeting interleukin-33 and thymic stromal lymphopoietin pathways for novel pulmonary therapeutics in asthma and COPD. In *European Respiratory Review* (Vol. 32, Issue 167). European Respiratory Society. https://doi.org/10.1183/16000617.0144-2022

17. Kleiveland, C., & Kleiveland, C. (2015). Peripheral blood mononuclear cells. In *The Impact of Food Bioactives on Health: In Vitro and Ex Vivo Models* (pp. 161–167). Springer International Publishing. https://doi.org/10.1007/978-3-319-16104-4_15

18. P.J. Delves, S.J.Martin, D.R.Burton, I.M.Roitt (2017). *Roitt_s Essential Immunology Thirteenth Edition*

19. Qu, X., Dang, X., Wang, W., Li, Y., Xu, D., Shang, D., & Chang, Y. (2018). Long noncoding RNAs and mRNA regulation in peripheral blood mononuclear cells of patients with chronic obstructive pulmonary disease. *Mediators of Inflammation*, *2018*. https://doi.org/10.1155/2018/7501851

20. Sophia Keddache, Caroline Laheurte, Laura Boullerot, Lucie Laurent, Jean-Charles Dalphin, Olivier Adotevi, Thibaud Soumagne. Inflammatory and immunological profile in COPD secondary to organic dust exposure, Clinical Immunology, Volume 229, 2021, 108798, ISSN 1521-6616. https://doi.org/10.1016/j.clim.2021.108798.

21. Krakauer, T. (2002). Stimulant-dependent modulation of cytokines and chemokines by airway epithelial cells: Cross talk between pulmonary epithelial and peripheral blood mononuclear cells.

Clinical and Diagnostic Laboratory Immunology, *9*(1), 126–131. https://doi.org/10.1128/CDLI.9.1.126-131.2002

22. Pniewska, E., Sokolowska, M., Kupryÿ-Lipińska, I., Kacprzak, D., Kuna, P., & Pawliczak, R. (2014). Exacerbating factors induce different gene expression profiles in peripheral blood mononuclear cells from asthmatics, patients with chronic obstructive pulmonary disease and healthy subjects. *International Archives of Allergy and Immunology*, *165*(4), 229–243. https://doi.org/10.1159/000370067

23. Tan, D. B. A., Fernandez, S., Price, P., French, M. A., Thompson, P. J., & Moodley, Y. P. (2014). Impaired function of regulatory T-cells in patients with chronic obstructive pulmonary disease (COPD). *Immunobiology*, *219*(12), 975–979. https://doi.org/10.1016/j.imbio.2014.07.005

24. Liu, K. (2016). Dendritic Cells. In *Encyclopedia of Cell Biology* (Vol. 3, pp. 741–749). Elsevier Inc. https://doi.org/10.1016/B978-0-12-394447-4.30111-0

25. Zanna, M. Y., Yasmin, A. R., Omar, A. R., Arshad, S. S., Mariatulqabtiah, A. R., Nur-Fazila, S. H., & Mahiza, M. I. N. (2021). Review of dendritic cells, their role in clinical immunology, and distribution in various animal species. In *International Journal of Molecular Sciences* (Vol. 22, Issue 15). MDPI. https://doi.org/10.3390/ijms22158044

26. Del Cacho, E., Gallego, M., López-Bernard, F., Sánchez-Acedo, C., & Lillehoj, H. S. (2008). Isolation of chicken follicular dendritic cells. *Journal of Immunological Methods*, *334*(1–2), 59–69. https://doi.org/10.1016/j.jim.2008.02.001

27. Collin, M., & Bigley, V. (2018). Human dendritic cell subsets: an update. In *Immunology* (Vol. 154, Issue 1, pp. 3–20). Blackwell Publishing Ltd. https://doi.org/10.1111/imm.12888

28. Musumeci, A., Lutz, K., Winheim, E., & Krug, A. B. (2019). What makes a PDC: Recent advances in understanding plasmacytoid DC development and heterogeneity. In *Frontiers in Immunology* (Vol. 10, Issue MAY). Frontiers Media S.A. https://doi.org/10.3389/fimmu.2019.01222

29. Böttcher JP, Reis e Sousa C. The Role of Type 1 Conventional Dendritic Cells in Cancer Immunity. Trends Cancer. 2018 Nov;4(11):784-792. doi: 10.1016/j.trecan.2018.09.001. Epub 2018 Sep 29. PMID: 30352680; PMCID: PMC6207145.

30. Nguyen, H. O., Tiberio, L., Facchinetti, F., Ripari, G., Violi, V., Villetti, G., Salvi, V., & Bosisio, D. (2023). Modulation of Human Dendritic Cell Functions by Phosphodiesterase-4 Inhibitors: Potential Relevance for the Treatment of Respiratory Diseases. In *Pharmaceutics* (Vol. 15, Issue 9). Multidisciplinary Digital Publishing Institute (MDPI). https://doi.org/10.3390/pharmaceutics15092254

31. Al-Ashmawy GMZ. Dendritic Cell Subsets, Maturation and Function. Dendritic Cells [Internet]. 2018 Nov 7 [cited 2020 Jan 14]; Available from: https://www.intechopen.com/books/dendritic-cells/dendritic-cell-subsets-maturation-and-function

32. Ness, S., Lin, S., & Gordon, J. R. (2021). Regulatory Dendritic Cells, T Cell Tolerance, and Dendritic Cell Therapy for Immunologic Disease. In *Frontiers in Immunology* (Vol. 12). Frontiers Media S.A. https://doi.org/10.3389/fimmu.2021.633436

33. Mantia-Smaldone GM, Chu CS. A Review of Dendritic Cell Therapy for Cancer: Progress and Challenges. BioDrugs. 2013 Oct 1;27(5):453–68.

34. Peter J. Delves, Seamus J. Martin, Dennis R. Burton, Ivan M. Roitt. Roitt's Essential Immunology, 13th edition. January 2017. ISBN: 978-1-118-41577-1

35. Volchenkov, R., Nygaard, V., Sener, Z., & Skålhegg, B. S. (2017). Th17 polarization under hypoxia results in increased IL-10 production in a pathogen-independent manner. *Frontiers in Immunology*, *8*(JUN). https://doi.org/10.3389/fimmu.2017.00698

36. Stoll, P., Ulrich, M., Bratke, K., Garbe, K., Virchow, J. C., & Lommatzsch, M. (2015). Imbalance of dendritic cell co-stimulation in COPD. *Respiratory Research*, *16*(1). https://doi.org/10.1186/s12931-015-0174-x

37. Demedts, I. K., Bracke, K. R., van Pottelberge, G., Testelmans, D., Verleden, G. M., Vermassen, F. E., Joos, G. F., & Brusselle, G. G. (2007). Accumulation of dendritic cells and increased CCL20 levels in the airways of patients with chronic obstructive pulmonary disease. *American Journal of Respiratory and Critical Care Medicine*, *175*(10), 998–1005. https://doi.org/10.1164/rccm.200608-1113OC

38. Van Pottelberge, G. R., Bracke, K. R., Joos, G. F., & Brusselle, G. G. (2009). The role of dendritic cells in the pathogenesis of copd: Liaison officers in the front line. *COPD: Journal of Chronic Obstructive Pulmonary Disease*, *6*(4), 284–290. https://doi.org/10.1080/15412550903049124

39. Galgani, M., Fabozzi, I., Perna, F., Bruzzese, D., Bellofiore, B., Calabrese, C., Vatrella, A., Galati, D., Matarese, G., Sanduzzi, A., & Bocchino, M. (2010). Imbalance of circulating dendritic cell subsets in chronic obstructive pulmonary disease. *Clinical Immunology*, *137*(1), 102–110. https://doi.org/10.1016/j.clim.2010.06.010

40. Bratke, K., Klug, M., Bier, A., Julius, P., Kuepper, M., Virchow, J. C., & Lommatzsch, M. (2008). Function-associated surface molecules on airway dendritic cells in cigarette smokers. *American Journal of Respiratory Cell and Molecular Biology*, *38*(6), 655–660. https://doi.org/10.1165/rcmb.2007-0400OC

41. Tsoumakidou, M., Demedts, I. K., Brusselle, G. G., & Jeffery, P. K. (2008). Dendritic cells in chronic obstructive pulmonary disease: New players in an old game. In *American Journal of Respiratory and Critical Care Medicine* (Vol. 177, Issue 11, pp. 1180–1186). https://doi.org/10.1164/rccm.200711-1727PP

42. Levy, J., & M Zhou, D. (2015). Cyclic Adenosine Monophosphate Signalling in Inflammatory Skin Disease. *Journal of Clinical & Experimental Dermatology Research*, *07*(01). https://doi.org/10.4172/2155-9554.1000326

43. Yan, K., Gao, L. N., Cui, Y. L., Zhang, Y., & Zhou, X. (2016). The cyclic AMP signaling pathway: Exploring targets for successful drug discovery (review). *Molecular Medicine Reports*, *13*(5), 3715–3723. https://doi.org/10.3892/mmr.2016.5005

44. Nourian, Y. H., Salimian, J., Ahmadi, A., Salehi, Z., Karimi, M., Emamvirdizadeh, A., Azimzadeh Jamalkandi, S., & Ghanei, M. (2023). cAMP-PDE signaling in COPD: Review of cellular, molecular and clinical features. In *Biochemistry and Biophysics Reports* (Vol. 34). Elsevier B.V. https://doi.org/10.1016/j.bbrep.2023.101438

45. Zuo, H., Cattani-Cavalieri, I., Musheshe, N., Nikolaev, V. O., & Schmidt, M. (2019). Phosphodiesterases as therapeutic targets for respiratory diseases. *Pharmacology and Therapeutics*, *197*, 225–242. https://doi.org/10.1016/j.pharmthera.2019.02.002

46. Omori, K., & Kotera, J. (2007). Overview of PDEs and their regulation. In *Circulation Research* (Vol. 100, Issue 3, pp. 309–327). https://doi.org/10.1161/01.RES.0000256354.95791.f1

47. Maurice DH, Palmer D, Tilley DG, Dunkerley HA, Netherton SJ, Raymond DR, Elbatarny HS, Jimmo SL. Cyclic nucleotide phosphodiesterase activity, expression, and targeting in cells of the cardiovascular system. Mol Pharmacol. 2003 Sep;64(3):533-46. doi: 10.1124/mol.64.3.533. PMID: 12920188.

48. Fan, T., Wang, W., Wang, Y., Zeng, M., Liu, Y., Zhu, S., & Yang, L. (2024). PDE4 inhibitors: potential protective effects in inflammation and vascular diseases. In *Frontiers in Pharmacology* (Vol. 15). Frontiers Media SA. https://doi.org/10.3389/fphar.2024.1407871

49. Li, H., Zuo, J., & Tang, W. (2018). Phosphodiesterase-4 inhibitors for the treatment of inflammatory diseases. In *Frontiers in Pharmacology* (Vol. 9, Issue OCT). Frontiers Media S.A. https://doi.org/10.3389/fphar.2018.01048

50. Kumar, N., Goldminz, A. M., Kim, N., & Gottlieb, A. B. (2013). Phosphodiesterase 4-targeted treatments for autoimmune diseases. In *BMC Medicine* (Vol. 11, Issue 1). https://doi.org/10.1186/1741-7015-11-96

51. Spadaccini, M., D'Alessio, S., Peyrin-Biroulet, L., & Danese, S. (2017). PDE4 inhibition and inflammatory bowel disease: A novel therapeutic avenue. In *International Journal of Molecular Sciences* (Vol. 18, Issue 6). MDPI AG. https://doi.org/10.3390/ijms18061276

52. Kwak HJ, Song JS, Heo JY, Yang SD, Nam JK, Cheon HG (2005). Roflumilast inhibits lipopolysaccharide-induced inflammatory mediators via suppression of NF-kB, P38 MAP kinase and JNK activation. In *J Pharmacol Exp Ther*; 315(3):1188-1195

53. Peter, D., Jin, S. L. C., Conti, M., Hatzelmann, A., & Zitt, C. (2007). Differential Expression and Function of Phosphodiesterase 4 (PDE4) Subtypes in Human Primary CD4+ T Cells: Predominant Role of PDE4D. *The Journal of Immunology*, *178*(8), 4820–4831. https://doi.org/10.4049/jimmunol.178.8.4820

54. Heystek, H. C., Thierry, A. C., Soulard, P., & Moulon, C. (2003). Phosphodiesterase 4 inhibitors reduce human dendritic cell inflammatory cytokine production and Th 1-polarizing capacity. In *International Immunology* (Vol. 15, Issue 7, pp. 827–835). Oxford University Press. https://doi.org/10.1093/intimm/dxg079

55. Bopp, T., Dehzad, N., Reuter, S., Klein, M., Ullrich, N., Stassen, M., Schild, H., Buhl, R., Schmitt, E., & Taube, C. (2009). Inhibition of cAMP Degradation Improves Regulatory T Cell-Mediated Suppression. *The Journal of Immunology*, *182*(7), 4017–4024. https://doi.org/10.4049/jimmunol.0803310

56. Edwards, M. R., Facchinetti, F., Civelli, M., Villetti, G., & Johnston, S. L. (2016). Anti-inflammatory effects of the novel inhaled phosphodiesterase type 4 inhibitor CHF6001 on virus-inducible cytokines. *Pharmacology Research and Perspectives*, *4*(1). https://doi.org/10.1002/prp2.202

57. Kawamatawong, T. (2021). Phosphodiesterase-4 Inhibitors for Non-COPD Respiratory Diseases. In *Frontiers in Pharmacology* (Vol. 12). Frontiers Media S.A. https://doi.org/10.3389/fphar.2021.518345

58. Rhee, C. K., & Kim, D. K. (2020). Role of phosphodiesterase-4 inhibitors in chronic obstructive pulmonary disease. In *Korean Journal of Internal Medicine* (Vol. 35, Issue 2, pp. 276–283). Korean Association of Internal Medicine. https://doi.org/10.3904/kjim.2020.035

59. Rabe, K. F., Watz, H., Baraldo, S., Pedersen, F., Biondini, D., Bagul, N., et al. (2018). Anti-inflammatory effects of roflumilast in chronic obstructive pulmonary disease (ROBERT): a 16-week, randomised, placebo-controlled trial. Lancet Respir. Med. 6 (11), 827–836. doi:10.1016/s2213-2600(18)30331-x

60. Gamble, E., Grootendorst, D. C., Brightling, C. E., Troy, S., Qiu, Y., Zhu, J., Parker, D., Matin, D., Majumdar, S., Vignola, A. M., Kroegel, C., Morell, F., Hansel, T. T., Rennard, S. I., Compton, C., Amit, O., Tat, T., Edelson, J., Pavord, I. D., … Jeffery, P. K. (2003). Antiinflammatory Effects of the Phosphodiesterase-4 Inhibitor Cilomilast (Ariflo) in Chronic Obstructive Pulmonary Disease. *American Journal of Respiratory and Critical Care Medicine*, *168*(8), 976–982. https://doi.org/10.1164/rccm.200212-1490OC

61. Matera, M. G., Ora, J., Cavalli, F., Rogliani, P., & Cazzola, M. (2021). New avenues for phosphodiesterase inhibitors in asthma. *Journal of Experimental Pharmacology*, *13*, 291–302. https://doi.org/10.2147/JEP.S242961

62. Luo, J., Yang, L., Yang, J., Yang, D., Liu, B. C., Liu, D., Liang, B. M., & Liu, C. T. (2018). Efficacy and safety of phosphodiesterase 4 inhibitors in patients with asthma: A systematic review and meta-analysis. In *Respirology* (Vol. 23, Issue 5, pp. 467–477). Blackwell Publishing. https://doi.org/10.1111/resp.13276

63. Gauvreau, G. M., Boulet, L. P., Schmid-Wirlitsch, C., Côté, J., Duong, M. L., Killian, K. J., Milot, J., Deschesnes, F., Strinich, T., Watson, R. M., Bredenbröker, D., & O'Byrne, P. M. (2011). Roflumilast attenuates allergen-induced inflammation in mild asthmatic subjects. *Respiratory Research*, *12*. https://doi.org/10.1186/1465-9921-12-140

64. Facchinetti, F., Civelli, M., Singh, D., Papi, A., Emirova, A., & Govoni, M. (2021). Tanimilast, A Novel Inhaled Pde4 Inhibitor for the Treatment of Asthma and Chronic Obstructive Pulmonary Disease. In *Frontiers in Pharmacology* (Vol. 12). Frontiers Media S.A. https://doi.org/10.3389/fphar.2021.740803

65. Singh, D., Emirova, A., Francisco, C., Santoro, D., Govoni, M., & Nandeuil, M. A. (2020). Efficacy and safety of CHF6001, a novel inhaled PDE4 inhibitor in COPD: The PIONEER study. *Respiratory Research*, *21*(1). https://doi.org/10.1186/s12931-020-01512-y

66. Schioppa, T., Nguyen, H. O., Salvi, V., Maugeri, N., Facchinetti, F., Villetti, G., Civelli, M., Gaudenzi, C., Passari, M., Sozio, F., Barbazza, I., Tamassia, N., Cassatella, M. A., del Prete, A., Bosisio, D., & Tiberio, L. (2022). The PDE4 Inhibitor Tanimilast Restrains the Tissue-Damaging Properties of Human Neutrophils. *International Journal of Molecular Sciences*, *23*(9). https://doi.org/10.3390/ijms23094982

67. Nguyen, H. O., Salvi, V., Tiberio, L., Facchinetti, F., Govoni, M., Villetti, G., Civelli, M., Barbazza, I., Gaudenzi, C., Passari, M., Schioppa, T., Sozio, F., del Prete, A., Sozzani, S., & Bosisio, D. (2022). The PDE4 inhibitor Tanimilast shows distinct immunomodulatory properties associated with a type 2 endotype and CD141 upregulation. *Journal of Translational Medicine*, *20*(1). https://doi.org/10.1186/s12967-022-03402-x

68. Cazzola, M., Ora, J., Cavalli, F., Rogliani, P., & Matera, M. G. (2021). An overview of the safety and efficacy of monoclonal antibodies for the chronic obstructive pulmonary disease. In *Biologics: Targets and Therapy* (Vol. 15, pp. 363–374). Dove Medical Press Ltd. https://doi.org/10.2147/BTT.S295409

69. Ryman, J. T., & Meibohm, B. (2017). Pharmacokinetics of monoclonal antibodies. *CPT: Pharmacometrics and Systems Pharmacology*, *6*(9), 576–588. https://doi.org/10.1002/psp4.12224

70. Matera, M. G., Calzetta, L., Rogliani, P., & Cazzola, M. (2019). Monoclonal antibodies for severe asthma: Pharmacokinetic profiles. In *Respiratory Medicine* (Vol. 153, pp. 3–13). W.B. Saunders Ltd. https://doi.org/10.1016/j.rmed.2019.05.005

71. Tang, Y., Cain, P., Anguiano, V., Shih, J. J., Chai, Q., & Feng, Y. (2021). Impact of IgG subclass on molecular properties of monoclonal antibodies. *MAbs*, *13*(1). https://doi.org/10.1080/19420862.2021.1993768

72. Lyly, A., Laulajainen-Hongisto, A., Gevaert, P., Kauppi, P., & Toppila-Salmi, S. (2020). Monoclonal antibodies and airway diseases. *International Journal of Molecular Sciences*, *21*(24), 1–21. https://doi.org/10.3390/ijms21249477

73. Plichta, J., Kuna, P., & Panek, M. (2023). Biologic drugs in the treatment of chronic inflammatory pulmonary diseases: recent developments and future perspectives. In *Frontiers in Immunology* (Vol. 14). Frontiers Media S.A. https://doi.org/10.3389/fimmu.2023.1207641

74. McCann, M. R., Kosloski, M. P., Xu, C., Davis, J. D., & Kamal, M. A. (2024). Dupilumab: Mechanism of action, clinical, and translational science. *Clinical and Translational Science*, *17*(8). https://doi.org/10.1111/cts.13899

75. Matsunaga, K., Katoh, N., Fujieda, S., Izuhara, K., & Oishi, K. (2020). Dupilumab: Basic aspects and applications to allergic diseases. In *Allergology International* (Vol. 69, Issue 2, pp. 187–196). Japanese Society of Allergology. https://doi.org/10.1016/j.alit.2020.01.002

76. Tajiri, T., Suzuki, M., Nishiyama, H., Ozawa, Y., Kurokawa, R., Takeda, N., Ito, K., Fukumitsu, K., Kanemitsu, Y., Mori, Y., Fukuda, S., Uemura, T., Ohkubo, H., Takemura, M., Maeno, K., Ito, Y., Oguri, T., Izuhara, K., & Niimi, A. (2024). Efficacy of dupilumab for airway hypersecretion and airway wall thickening in patients with moderate-to-severe asthma: A prospective, observational study. *Allergology International*, *73*(3), 406–415. https://doi.org/10.1016/j.alit.2024.02.002

77. Bhatt, S. P., Rabe, K. F., Hanania, N. A., Vogelmeier, C. F., Cole, J., Bafadhel, M., Christenson, S. A., Papi, A., Singh, D., Laws, E., Mannent, L. P., Patel, N., Staudinger, H. W., Yancopoulos, G. D., Mortensen, E. R., Akinlade, B., Maloney, J., Lu, X., Bauer, D., … Abdulai, R. M. (2023). Dupilumab for COPD with Type 2 Inflammation Indicated by Eosinophil Counts. *New England Journal of Medicine*, *389*(3), 205–214. https://doi.org/10.1056/nejmoa2303951

78. Cacciamali, A., Villa, R., & Dotti, S. (2022). 3D Cell Cultures: Evolution of an Ancient Tool for New Applications. In *Frontiers in Physiology* (Vol. 13). Frontiers Media S.A. https://doi.org/10.3389/fphys.2022.836480

79. Bloise, N., Giannaccari, M., Guagliano, G., Peluso, E., Restivo, E., Strada, S., Volpini, C., Petrini, P., & Visai, L. (2024). Growing Role of 3D In Vitro Cell Cultures in the Study of Cellular and Molecular Mechanisms: Short Focus on Breast Cancer, Endometriosis, Liver and Infectious Diseases. In *Cells* (Vol. 13, Issue 12). Multidisciplinary Digital Publishing Institute (MDPI). https://doi.org/10.3390/cells13121054

80. Lee, S. Y., Koo, I. S., Hwang, H. J., & Lee, D. W. (2023). In Vitro three-dimensional (3D) cell culture tools for spheroid and organoid models. In *SLAS Discovery* (Vol. 28, Issue 4, pp. 119–137). Society for Laboratory Automation and Screening (SLAS). https://doi.org/10.1016/j.slasd.2023.03.006

81. Gunti, S., Hoke, A. T. K., Vu, K. P., & London, N. R. (2021). Organoid and spheroid tumor models: Techniques and applications. In *Cancers* (Vol. 13, Issue 4, pp. 1–18). MDPI AG. https://doi.org/10.3390/cancers13040874

82. Carvalho, V., Bañobre-López, M., Minas, G., Teixeira, S. F. C. F., Lima, R., & Rodrigues, R. O. (2022). The integration of spheroids and organoids into organ-on-a-chip platforms for tumour research: A review. In *Bioprinting* (Vol. 27). Elsevier B.V. https://doi.org/10.1016/j.bprint.2022.e00224

83. Dellaquila, A., Thomée, E. K., McMillan, A. H., & Lesher-Pérez, S. C. (2019). Lung-on-a-chip platforms for modeling disease pathogenesis. In Organ-on-a-chip: Engineered Microenvironments for Safety and Efficacy Testing (pp. 133–180). Elsevier. https://doi.org/10.1016/B978-0-12-817202-5.00004-8

84. Upadhyay, S., & Palmberg, L. (2018). Air-liquid interface: Relevant in vitro models for investigating air pollutant-induced pulmonary toxicity. In *Toxicological Sciences* (Vol. 164, Issue 1, pp. 21–30). Oxford University Press. https://doi.org/10.1093/toxsci/kfy053

85. Baldassi, D., Gabold, B., & Merkel, O. M. (2021). Air−Liquid Interface Cultures of the Healthy and Diseased Human Respiratory Tract: Promises, Challenges, and Future Directions. In *Advanced NanoBiomed Research* (Vol. 1, Issue 6). John Wiley and Sons Inc. https://doi.org/10.1002/anbr.202000111

86. Schamberger, A. C., Staab-Weijnitz, C. A., Mise-Racek, N., & Eickelberg, O. (2015). Cigarette smoke alters primary human bronchial epithelial cell differentiation at the air-liquid interface. *Scientific Reports*, *5*. https://doi.org/10.1038/srep08163

87. Gindele, J. A., Kiechle, T., Benediktus, K., Birk, G., Brendel, M., Heinemann, F., Wohnhaas, C. T., LeBlanc, M., Zhang, H., Strulovici-Barel, Y., Crystal, R. G., Thomas, M. J., Stierstorfer, B., Quast, K., & Schymeinsky, J. (2020). Intermittent exposure to whole cigarette smoke alters the differentiation of primary small airway epithelial cells in the air-liquid interface culture. *Scientific Reports*, *10*(1). https://doi.org/10.1038/s41598-020-63345-5

88. Ji, J., Hedelin, A., Malmlöf, M., Kessler, V., Seisenbaeva, G., Gerde, P., & Palmberg, L. (2017). Development of combining of human bronchial mucosa models with XposeALI® for exposure of air pollution nanoparticles. *PLoS ONE*, *12*(1). https://doi.org/10.1371/journal.pone.0170428

89. Luukkainen, A., Puan, K. J., Yusof, N., Lee, B., Tan, K. sen, Liu, J., Yan, Y., Toppila-Salmi, S., Renkonen, R., Chow, V. T., Rotzschke, O., & Wang, D. Y. (2018). A Co-culture Model of PBMC and Stem Cell Derived Human Nasal Epithelium Reveals Rapid Activation of NK and Innate T Cells Upon Influenza A Virus Infection of the Nasal Epithelium. *Frontiers in Immunology*, *9*. https://doi.org/10.3389/fimmu.2018.02514

90. Ladjemi, M. Z., Lecocq, M., Weynand, B., Bowen, H., Gould, H. J., van Snick, J., Detry, B., & Pilette, C. (2015). Increased IgA production by B-cells in COPD via lung epithelial interleukin-6 and TACI pathways. *European Respiratory Journal*, *45*(4), 980–993. https://doi.org/10.1183/09031936.00063914

91. Gras, D., Martinez-Anton, A., Bourdin, A., Garulli, C., de Senneville, L., Vachier, I., Vitte, J., & Chanez, P. (2017). Human bronchial epithelium orchestrates dendritic cell activation in severe asthma. *European Respiratory Journal*, *49*(3), 1602399. https://doi.org/10.1183/13993003.02399-2016ï

92. Osei, E. T., Noordhoek, J. A., Hackett, T. L., Spanjer, A. I. R., Postma, D. S., Timens, W., Brandsma, C. A., & Heijink, I. H. (2016). Interleukin-1α drives the dysfunctional cross-talk of the airway epithelium and lung fibroblasts in COPD. *European Respiratory Journal*, *48*(2), 359–369. https://doi.org/10.1183/13993003.01911-2015

93. Rothen-Rutishauser, B. M., Kiama, S. C., & Gehr, P. (2005). A three-dimensional cellular model of the human respiratory tract to study the interaction with particles. *American Journal of*

Respiratory Cell and Molecular Biology, *32*(4), 281–289. https://doi.org/10.1165/rcmb.2004-0187OC

94. Paplinska-Goryca, M., Misiukiewicz-Stepien, P., Nejman-Gryz, P., Proboszcz, M., Mlacki, M., Gorska, K., & Krenke, R. (2020). Epithelial-macrophage-dendritic cell interactions impact alarmins expression in asthma and COPD. *Clinical Immunology*, *215*. https://doi.org/10.1016/j.clim.2020.108421

95. Huang, X., Huang, Z., Gao, W., Gao, W., He, R., Li, Y., Crawford, R., Zhou, Y., Xiao, L., & Xiao, Y. (2022). Current Advances in 3D Dynamic Cell Culture Systems. In *Gels* (Vol. 8, Issue 12). MDPI. https://doi.org/10.3390/gels8120829

96. Schneider, M. R., Oelgeschlaeger, M., Burgdorf, T., van Meer, P., Theunissen, P., Kienhuis, A. S., Piersma, A. H., & Vandebriel, R. J. (2021). Applicability of organ-on-chip systems in toxicology and pharmacology. In Critical Reviews in Toxicology (Vol. 51, Issue 6, pp. 540–554). Taylor and Francis Ltd. https://doi.org/10.1080/10408444.2021.1953439

97. Benam, K., Villenave, R., Lucchesi, C. *et al.* Small airway-on-a-chip enables analysis of human lung inflammation and drug responses *in vitro*. *Nat Methods* **13**, 151–157 (2016). https://doi.org/10.1038/nmeth.3697

98. Marrella, A., Varani, G., Aiello, M., Vaccari, I., Vitale, C., Mojzisek, M., et al. (2021). 3D fluid-dynamic ovarian cancer model resembling systemic drug administration for efficacy assay. ALTEX-Alternatives Anim. Exp. 38, 82–94.doi:10.14573/altex.2003131

99. Marzagalli, M., Pelizzoni, G., Fedi, A., Vitale, C., Fontana, F., Bruno, S., Poggi, A., Dondero, A., Aiello, M., Castriconi, R., Bottino, C., & Scaglione, S. (2022). A multi-organ-on-chip to recapitulate the infiltration and the cytotoxic activity of circulating NK cells in 3D matrix-based tumor model. Frontiers in Bioengineering and Biotechnology, 10. https://doi.org/10.3389/fbioe.2022.945149

100. Fedi, A., Vitale, C., Fato, M., & Scaglione, S. (2023). A Human Ovarian Tumor & Liver Organ-on-Chip for Simultaneous and More Predictive Toxo-Efficacy Assays. Bioengineering, 10(2). https://doi.org/10.3390/bioengineering10020270

101. Fedi, A., Vitale, C., Ponschin, G., Ayehunie, S., Fato, M., & Scaglione, S. (2021). In vitro models replicating the human intestinal epithelium for absorption and metabolism studies: A systematic review. In Journal of Controlled Release (Vol. 335, pp. 247–268). Elsevier B.V. https://doi.org/10.1016/j.jconrel.2021.05.028

102. Bhowmick, R., Gappa-Fahlenkamp, H. Cells and Culture Systems Used to Model the Small Airway Epithelium. Lung 194, 419–428 (2016). https://doi.org/10.1007/s00408-016-9875-2

103. Miller, A. J., & Spence, J. R. (2017). In vitro models to study human lung development, disease and homeostasis. In Physiology (Vol. 32, Issue 3, pp. 246–260). American Physiological Society. https://doi.org/10.1152/physiol.00041.2016

104. Kitajima, M., Lee, H. C., Nakayama, T., & Ziegler, S. F. (2011). TSLP enhances the function of helper type 2 cells. *European Journal of Immunology*, *41*(7), 1862–1871. https://doi.org/10.1002/eji.201041195

105. Lee, H. Y., Lee, H. Y., Hur, J., Kang, H. S., Choi, J. Y., Rhee, C. K., Kang, J. Y., Kim, Y. K., & Lee, S. Y. (2020). Blockade of thymic stromal lymphopoietin and CRTH2 attenuates airway inflammation in a murine model of allergic asthma. *Korean Journal of Internal Medicine*, *35*(3), 619–629. https://doi.org/10.3904/kjim.2018.248

106. Ito, T., Wang, Y. H., Duramad, O., Hori, T., Delespesse, G. J., Watanabe, N., Qin, F. X. F., Yao, Z., Cao, W., & Liu, Y. J. (2005). TSLP-activated dendritic cells induce an inflammatory T helper type 2 cell response through OX40 ligand. *Journal of Experimental Medicine*, *202*(9), 1213–1223. https://doi.org/10.1084/jem.20051135

107. Bolmarcich, J., Wilbert, S., Jackson, G. R., Oldach, J., Bachelor, M., Kenney, T., Wright, C. D., & Hayden, P. J. (2018). In Vitro human airway models for study of goblet cell hyperplasia and mucus production: Effects of Th2 cytokines, double-stranded RNA, and tobacco smoke. *Applied In Vitro Toxicology*, *4*(4), 332–346. https://doi.org/10.1089/aivt.2017.0001

108. Park, K. S., Korfhagen, T. R., Bruno, M. D., Kitzmiller, J. A., Wan, H., Wert, S. E., Khurana Hershey, G. K., Chen, G., & Whitsett, J. A. (2007). SPDEF regulates goblet cell hyperplasia in the airway epithelium. *Journal of Clinical Investigation*, *117*(4), 978–988. https://doi.org/10.1172/JCI29176

109. Laucho-Contreras, M. E., Polverino, F., Tesfaigzi, Y., Pilon, A., Celli, B. R., & Owen, C. A. (2016). Club Cell Protein 16 (CC16) Augmentation: A Potential Disease-modifying Approach for Chronic Obstructive Pulmonary Disease (COPD). In Expert Opinion on Therapeutic Targets (Vol. 20, Issue 7, pp. 869–883). Taylor and Francis Ltd. https://doi.org/10.1517/14728222.2016.1139084

110. Huang, X., Guan, W., Xiang, B., Wang, W., Xie, Y., & Zheng, J. (2022). MUC5B regulates goblet cell differentiation and reduces inflammation in a murine COPD model. *Respiratory Research*, *23*(1). https://doi.org/10.1186/s12931-021-01920-8

111. Kondo, M., Tamaoki, J., Takeyama, K., Isono, K., Kawatani, K., Izumo, T.-H., & Nagai, A. (n.d.). *Elimination of IL-13 Reverses Established Goblet Cell Metaplasia into Ciliated Epithelia in Airway Epithelial Cell Culture*. www.jsaweb.jp

112. Jabbar, F., Kim, Y. S., & Lee, S. H. (2022). Biological Influence of Pulmonary Disease Conditions Induced by Particulate Matter on Microfluidic Lung Chips. *Biochip Journal*, *16*(3), 305–316. https://doi.org/10.1007/s13206-022-00068-x

113. Yu, H., Li, Q., Kolosov, V. P., Perelman, J. M., & Zhou, X. (2011). Interleukin-13 induces mucin 5AC production involving STAT6/SPDEF in human airway epithelial cells. Cell Communication and Adhesion, 17(4–6), 83–92. https://doi.org/10.3109/15419061.2010.551682

114. Yanling Qin, Youfan Jiang, Awais Shafiq Sheikh, Shanshan Shen, Jing Liu, Depeng Jiang (2016). Interleukin-13 stimulates MUC5AC expression via a STAT6-TMEM16A-ERK1/2

pathway in human airway epithelial cells. International Immunopharmacology,Volume 40, Pages 106-114, ISSN 1567-5769, https://doi.org/10.1016/j.intimp.2016.08.033.

115. Tyner, J. W., Kim, E. Y., Ide, K., Pelletier, M. R., Roswit, W. T., Morton, J. D., Battaile, J. T., Patel, A. C., Patterson, G. A., Castro, M., Spoor, M. S., You, Y., Brody, S. L., & Holtzman, M. J. (2006). Blocking airway mucous cell metaplasia by inhibiting EGFR antiapoptosis and IL-13 transdifferentiation signals. *Journal of Clinical Investigation*, *116*(2), 309–321. https://doi.org/10.1172/JCI25167

116. Tanabe, T., Kanoh, S., Tsushima, K., Yamazaki, Y., Kubo, K., & Rubin, B. K. (2011). Clarithromycin inhibits interleukin-13-induced goblet cell hyperplasia in human airway cells. *American Journal of Respiratory Cell and Molecular Biology*, *45*(5), 1075–1083. https://doi.org/10.1165/rcmb.2010-0327OC

117. Gavett SH, O'Hearn DJ, Karp CL, Patel EA, Schofield BH, Finkelman FD, and Wills-Karp M. Interleukin-4 receptor blockade prevents airway responses induced by antigen challenge in mice. Am J Physiol Lung Cell Mol Physiol 272: L253-L261, 1997.

118. Almuntashiri, S., Zhu, Y., Han, Y., Wang, X., Somanath, P. R., & Zhang, D. (2020). Club cell secreted protein CC16: Potential applications in prognosis and therapy for pulmonary diseases. In *Journal of Clinical Medicine* (Vol. 9, Issue 12, pp. 1–16). MDPI. https://doi.org/10.3390/jcm9124039

119. Liu, X., Yin, S., Chen, Y., Wu, Y., Zheng, W., Dong, H., Bai, Y., Qin, Y., Li, J., Feng, S., & Zhao, P. (2018). LPS-induced proinflammatory cytokine expression in human airway epithelial cells and macrophages via NF-κB, STAT3 or AP-1 activation. *Molecular Medicine Reports*, *17*(4), 5484–5491. https://doi.org/10.3892/mmr.2018.8542

120. Sharma, M., Stucki, A. O., Verstraelen, S., Stedeford, T. J., Jacobs, A., Maes, F., Poelmans, D., van Laer, J., Remy, S., Frijns, E., Allen, D. G., & Clippinger, A. J. (2023). Human cell-based in vitro systems to assess respiratory toxicity: A case study using silanes. *Toxicological Sciences*, *195*(2), 213–230. https://doi.org/10.1093/toxsci/kfad074

121. Gianello, V., Salvi, V., Parola, C., Moretto, N., Facchinetti, F., Civelli, M., Villetti, G., Bosisio, D., & Sozzani, S. (2019). The PDE4 inhibitor CHF6001 modulates pro-inflammatory cytokines, chemokines and Th1- and Th17-polarizing cytokines in human dendritic cells. Biochemical Pharmacology, 163, 371–380. https://doi.org/10.1016/j.bcp.2019.03.006

122. Bäckhed, F., & Hornef, M. (2003). Toll-like receptor 4-mediated signaling by epithelial surfaces: Necessity or threat? In *Microbes and Infection* (Vol. 5, Issue 11, pp. 951–959). Elsevier Masson SAS. https://doi.org/10.1016/S1286-4579(03)00189-8

123. Sheller, J. R., Polosukhin, V. v., Mitchell, D., Cheng, D. S., Peebles, R. S., & Blackwell, T. S. (2009). Nuclear factor kappa B induction in airway epithelium increases lung inflammation in allergen-challenged mice. *Experimental Lung Research*, *35*(10), 883–895. https://doi.org/10.3109/01902140903019710

124. Toward, T. J., & Broadley, K. J. (2002). Goblet cell hyperplasia, airway function, and leukocyte infiltration after chronic lipopolysaccharide exposure in conscious guinea pigs: Effects of rolipram and dexamethasone. *Journal of Pharmacology and Experimental Therapeutics*, *302*(2), 814–821. https://doi.org/10.1124/jpet.102.033951

125. Tu, X., Donovan, C., Kim, R. Y., Wark, P. A. B., Horvat, J. C., & Hansbro, P. M. (2021). Asthma-COPD overlap: Current understanding and the utility of experimental models. *European Respiratory Review*, *30*(159). https://doi.org/10.1183/16000617.0185-2019

126. Nguyen, H. O., Schioppa, T., Tiberio, L., Facchinetti, F., Villetti, G., Civelli, M., del Prete, A., Sozio, F., Gaudenzi, C., Passari, M., Barbazza, I., Sozzani, S., Salvi, V., & Bosisio, D. (2022). The PDE4 Inhibitor Tanimilast Blunts Proinflammatory Dendritic Cell Activation by SARS-CoV-2 ssRNAs. *Frontiers in Immunology*, *12*. https://doi.org/10.3389/fimmu.2021.797390

127. Melum, G. R., Farkas, L., Scheel, C., van Dieren, B., Gran, E., Liu, Y. J., Johansen, F. E., Jahnsen, F. L., & Baekkevold, E. S. (2014). A thymic stromal lymphopoietin-responsive dendritic cell subset mediates allergic responses in the upper airway mucosa. *The Journal of Allergy and Clinical Immunology*, *134*(3), 613-621.e7. https://doi.org/10.1016/j.jaci.2014.05.010

PARTICIPATION TO CONGRESS

1. LIVe 2024, Nice, 20-21 June 2024. *Oral presentation*

2. SIICA International PhD Retreat 2024, Otranto, 20-22 May 2024. *Oral presentation*

3. The SIICA School of Immunology 2024. Online meeting, 26/2 – 1/03/2024. *Auditor*

4. Organ Modeling & 3D Cell Culture, London, 18-19 March 2024. *Oral presentation*

PUBLICATIONS

"Modulation of Human Dendritic Cell Functions by Phosphodiesterase-4 Inhibitors: Potential Relevance for the Treatment of Respiratory Diseases" H.O.Nguyen, L.Tiberio, F.Facchinetti, G. Ripari, V. Violi, G. Villetti, V. Salvi and D. Bosisio, Pharmaceutics 2023 Aug 31;15(9):2254. doi: 10.3390/pharmaceutics15092254.

https://www.mdpi.com/1999-4923/15/9/2254

Pharmaceutics Impact Factor 2022: 5.4

ACKNOWLEDGMENTS

First and foremost, I am extremely grateful to my supervisor, Prof. Annalisa Del Prete for her continuous support and patience during my PhD study. I would also like to thank Dr. Gessica Marchini, head of Advanced In Vitro Model (AIM) facility of Chiesi Farmaceutici, for her great advice and technical support during all my industry period. Her immense knowledge and plentiful experience have encouraged me in all the time of my academic research and daily life.

I would like to thank all the members of the Department of Experimental Pharmacology and Translational Science in Corporate Pre-Clinical R&D of Chiesi Farmaceutici, especially Dr. Fabrizio Facchinetti and Dr. Gino Villetti, and all the members in the Lab of Immunology, especially my thanks to Prof. Daniela Bosisio and Prof. Laura Tiberio.

Finally, I would like to express my gratitude to Alessia, my life partner, who has given me strength to reach this important milestone, and to you, grandma, my constant supporter who, wherever you are, I know you will be proud of your “little girl”.